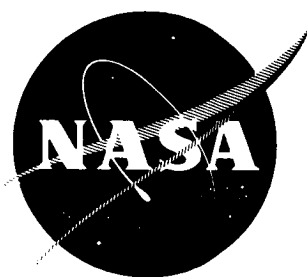


**N 7 4 1 0 8 6 1**

**NASA CR-121279**

**CASE FILE  
COPY**



**THE PREDICTION OF NONLINEAR THREE-  
DIMENSIONAL COMBUSTION INSTABILITY IN LIQUID  
ROCKETS WITH CONVENTIONAL NOZZLES**

by

**E. A. Powell and B. T. Zinn**

**GEORGIA INSTITUTE OF TECHNOLOGY**

prepared for

**NATIONAL AERONAUTICS AND SPACE ADMINISTRATION**

**NASA Lewis Research Center  
Grant NGL 11-002-083  
Richard J. Priem, Project Manager**

NOTICE

This report was prepared as an account of Government-sponsored work. Neither the United States, nor the National Aeronautics and Space Administration (NASA), nor any person acting on behalf of NASA:

- A.) Makes any warranty or representation, expressed or implied, with respect to the accuracy, completeness, or usefulness of the information contained in this report, or that the use of any information, apparatus, method, or process disclosed in this report may not infringe privately-owned rights; or
- B.) Assumes any liabilities with respect to the use of, or for damages resulting from the use of, any information, apparatus, method or process disclosed in this report.

As used above, "person acting on behalf of NASA" includes any employee or contractor of NASA, or employee of such contractor, to the extent that such employee or contractor of NASA or employee of such contractor prepares, disseminates, or provides access to any information pursuant to his employment or contract with NASA, or his employment with such contractor.

Requests for copies of this report should be referred to

National Aeronautics and Space Administration  
Scientific and Technical Information Facility  
P. O. Box 33  
College Park, Md. 20740

## FOREWORD

The research described herein, which was conducted at Georgia Institute of Technology, was supported by NASA Grant No. NGL-11-002-083. The work was done under the management of the NASA Project Manager, Dr. Richard J. Priem, Chemical Rockets Division, NASA-Lewis Research Center.

## ABSTRACT

An analytical technique is developed to solve nonlinear three-dimensional, transverse and axial combustion instability problems associated with liquid-propellant rocket motors. The Method of Weighted Residuals is used to determine the nonlinear stability characteristics of a cylindrical combustor with uniform injection of propellants at one end and a conventional DeLaval nozzle at the other end. Crocco's pressure sensitive time-lag model is used to describe the unsteady combustion process. The developed model predicts the transient behavior and nonlinear wave shapes as well as limit-cycle amplitudes and frequencies typical of unstable motor operation. The limit-cycle amplitude increases with increasing sensitivity of the combustion process to pressure oscillations. For transverse instabilities, calculated pressure waveforms exhibit sharp peaks and shallow minima, and the frequency of oscillation is within a few percent of the pure acoustic mode frequency. For axial instabilities, the theory predicts a steep-fronted wave moving back and forth along the combustor.

## TABLE OF CONTENTS

	Page
SUMMARY . . . . .	1
INTRODUCTION . . . . .	2
SYMBOLS . . . . .	3
ANALYSIS . . . . .	6
Development of the Wave Equation . . . . .	6
Method of Solution . . . . .	8
RESULTS AND DISCUSSION . . . . .	14
Linear Solutions . . . . .	14
Nonlinear Solutions . . . . .	17
Transverse Mode Solutions . . . . .	17
Longitudinal Mode Solutions . . . . .	25
CONCLUDING REMARKS . . . . .	30
APPENDIX A - MOMENTUM INTERCHANGE BETWEEN LIQUID AND GAS PHASES . . . . .	32
Analysis . . . . .	32
Linear Stability Limits . . . . .	34
Nonlinear Solutions . . . . .	34
APPENDIX B - USE OF COMPLEX VARIABLES IN THE SOLUTION OF NONLINEAR DIFFERENTIAL EQUATIONS . . . . .	38
APPENDIX C - PROGRAM COEFFS3D: A USER'S MANUAL . . . . .	41
Statement of the Problem . . . . .	41
Structure of the Numerical Calculations . . . . .	43
Input Data . . . . .	45
Complex Linear Coefficients . . . . .	49
Axial Acoustic Eigenvalues . . . . .	49
Steady State Mach Number Distribution . . . . .	51
Orthogonality of Transverse Eigenfunctions . . . . .	53
Axial Integrals . . . . .	53

TABLE OF CONTENTS (CONTINUED)

	Page
Complex Nonlinear Coefficients . . . . .	54
Azimuthal Integrals . . . . .	54
Radial Integrals . . . . .	56
Axial Integrals . . . . .	57
Coefficients for Equivalent Real System . . . . .	59
Output . . . . .	62
Printed Output . . . . .	62
Drum Storage . . . . .	63
Card Output . . . . .	67
FORTRAN Listing . . . . .	71
 APPENDIX D - PROGRAM LCYC3D: A USER'S MANUAL . . . . .	 96
General Description . . . . .	96
Program Structure . . . . .	96
Input Data . . . . .	99
Coefficients in Series for $\Phi_t$ , $\Phi_\theta$ , and $\Phi_z$ . . . . .	106
Initial Amplitudes . . . . .	107
Integration of the Differential Equations . . . . .	109
Pressure and Axial Velocity Perturbations . . . . .	111
Maximum and Minimum Values . . . . .	112
Calculation of Limit-Cycle Amplitude . . . . .	112
Output . . . . .	113
Printed Output . . . . .	113
Plotted Output . . . . .	114
Sample Output . . . . .	114
FORTRAN Listing . . . . .	124
 APPENDIX E - USER'S MANUAL FOR THE LINEAR STABILITY PROGRAMS: LINSOL AND LSTB3D . . . . .	  150
General Description . . . . .	150
Linear Analysis . . . . .	150
Program LINSOL . . . . .	152

TABLE OF CONTENTS (CONTINUED)

	Page
Program Structure . . . . .	152
Input . . . . .	152
Calculation of $C_1$ , $C_2$ , and $C_3$ . . . . .	155
Iterative Solution for $\Lambda$ and $\omega$ . . . . .	155
Output . . . . .	156
Sample Input and Output . . . . .	156
Program LSTB3D . . . . .	156
Program Structure . . . . .	156
Input . . . . .	159
Calculation of $C_1$ , $C_2$ , and $C_3$ . . . . .	159
Iterative Solution for $n$ and $\omega$ . . . . .	160
Output . . . . .	160
Sample Input and Output . . . . .	160
FORTTRAN Listings . . . . .	162
REFERENCES . . . . .	171

## LIST OF ILLUSTRATIONS

Figure	Page
1. Combustor Configuration and Coordinate System . . . . .	9
2. Nonlinear Pressure Waveforms for the 1T Mode . . . . .	18
3. Nozzle Boundary Condition for Nonlinear 1T Mode Solutions for Quasi-Steady Nozzles . . . . .	20
4. Limit-Cycle Amplitudes for the 1T Mode . . . . .	21
5. Effect of Nozzle Phase Shift, $\phi$ , on Nozzle Waveforms for Spinning 1T Modes . . . . .	23
6. Effect of Nozzle Phase Shift on Limit-Cycle Amplitudes for the Standing 1T Mode . . . . .	24
7. Nozzle Boundary Condition for Nonlinear 1T Mode Solutions . . .	26
8. Comparison of Nonlinear 1L Mode Solutions for Quasi-Steady Nozzles . . . . .	27
9. Longitudinal Mode Waveforms for Quasi-Steady Nozzles . . . . .	28
10. Longitudinal Mode Waveforms for Nozzles with Complex Admittances . . . . .	29
A-1. Effect of Droplet Momentum Source on Linear Stability Limits for the 1L Mode . . . . .	35
A-2. Effect of Droplet Momentum Source on Limit-Cycle Amplitude. . .	36
C-1. Flow Chart for Program COEFFS3D . . . . .	44
C-2. Steady-State Mach Number Distribution . . . . .	52
D-1. Flow Chart for Program LCYC3D . . . . .	97
D-2. Sample Pressure Plot . . . . .	122
D-3. Sample Amplitude Plot . . . . .	123
E-1. Flow Chart for Program LINSOL . . . . .	153
E-2. Flow Chart for Program LSTB3D . . . . .	158



## LIST OF TABLES

Table	Page
1. Correspondence Between Eq. (6) and (9) for a Three-Mode Series . . . . .	11
2. 1T Mode Linear Solutions (Numerical). . . . .	15
3. 1L Mode Linear Solutions (Numerical). . . . .	16
C-1. Sample Input (COEFFS3D) . . . . .	48
C-2. Sample Printed Output (COEFFS3D), Page 1 . . . . .	64
C-3. Sample Printed Output (COEFFS3D), Page 2 . . . . .	65
C-4. Sample Printed Output (COEFFS3D), Page 5 . . . . .	66
C-5. Sample Card Output (COEFFS3D) . . . . .	69
D-1. Numbering of Plots . . . . .	103
D-2. Sample Input (LCYC3D) . . . . .	106
D-3. Chamber Locations for Pressure Calculations . . . . .	107
D-4. Sample Output (LCYC3D), Section 1 . . . . .	115
D-5. Sample Output (LCYC3D), Section 2 . . . . .	117
D-6. Sample Output (LCYC3D), Section 3 . . . . .	118
D-7. Sample Output (LCYC3D), Section 4 . . . . .	119
D-8. Sample Output (LCYC3D), Section 5 . . . . .	121
E-1. Sample Input for LINSOL . . . . .	157
E-2. Sample Output for LINSOL . . . . .	157
E-3. Sample Input for LSTB3D . . . . .	160
E-4. Sample Output for LSTB3D . . . . .	161

## SUMMARY

An approximate analytical technique has been developed for the solution of nonlinear three-dimensional, transverse and axial combustion instability problems that are frequently observed in liquid-propellant rocket motors. This theory is an extension and generalization of previous analyses, which could analyze either transverse or axial instabilities in liquid combustors with quasi-steady nozzles, to the practical situations of three-dimensional instabilities in combustors with conventional DeLaval nozzles. Unlike the quasi-steady nozzle, the presence of a conventional nozzle imposes restrictions upon the behavior of both the amplitudes and phases of the oscillations at the nozzle entrance plane. The Method of Weighted Residuals is used to determine the nonlinear stability characteristics of a cylindrical combustor with uniform injection of propellants at one end and a conventional nozzle at the other end. Crocco's pressure sensitive time-lag model is used to describe the unsteady combustion process. The developed model can predict the transient behavior and nonlinear wave shapes as well as limit-cycle amplitudes and frequencies typical of unstable motor operation. These results establish the relationship that exists between the resulting instability (i.e., waveform, final amplitude and final frequency), the combustion parameters (i.e., interaction index,  $n$ , and time-lag,  $\bar{\tau}$ ), and the chamber Mach number and length-to-diameter ratio. Results indicate that the limit-cycle amplitude increases with increasing sensitivity of the combustion process to pressure oscillations. For transverse instabilities, calculated pressure waveforms exhibit sharp peaks and shallow minima, and the frequency of oscillation is always within a few percent of the frequency of one of the chamber's acoustic modes. For axial instabilities, the theory predicts the presence of a steep-fronted wave moving back and forth along the combustor. In both cases calculations of pressure and velocity perturbations at the nozzle entrance plane show that the approximation to the nozzle boundary condition is very good. The theory described in this report represents the final stage in the development of a unified nonlinear theory for the solution of general three-dimensional, transverse and axial combustion instability problems.

## INTRODUCTION

Observation of the behavior of unstable rocket motors indicates that combustion instability can be divided into two categories; that is, linear and nonlinear instabilities. Linear instabilities are spontaneous in nature, and they are usually an outgrowth of the random combustion and flow fluctuations present in the system. On the other hand, nonlinearly unstable motors require the introduction of a finite amplitude disturbance to produce (or trigger) combustion instability. In either case the instability, after a transient period, reaches a limiting maximum amplitude (i.e., limit-cycle amplitude) at which it oscillates with a given frequency that is usually close to the frequency of one of the chamber's acoustic modes. Pressure measurements taken during test firings of unstable motors indicate that the limit-cycle waveforms of transverse instabilities are non-sinusoidal; that is, they exhibit sharp peaks and flattened minima.<sup>1</sup> On the other hand, experimental observations of axial instabilities indicate the presence of shock-like steep-fronted waves in the chamber.<sup>2</sup> These results indicate that nonlinearities need to be considered in the theoretical treatment of combustion instability.

Any analytical treatment of combustion instability should be capable of solving nonlinear multi-dimensional combustion instability problems without exceeding memory core limitations of current computers and without requiring excessive computation time. To be of practical use, such a solution technique should be conceptually simple and easily adaptable for use by industry. This report describes the development and use of such a numerical solution technique.

Work on this problem has been in progress during the past several years, and due to its complexity, the problem had to be tackled in stages. In earlier investigations by these authors theories describing the nonlinear behavior of longitudinal<sup>3,4</sup> and transverse<sup>5,6</sup> instabilities in liquid combustors with quasi-steady nozzles were developed. These theories, which were based upon the application of the Method of Weighted Residuals (MWR), successfully

predicted the transient behavior, nonlinear waveforms, and limit-cycle amplitudes of longitudinal and transverse instabilities in unstable liquid rockets. This report is concerned with the development of a generalized nonlinear theory that will be capable of analyzing three-dimensional, transverse and axial instabilities in the more practical situations where the combustors are attached to conventional nozzles. Obviously, this generalized theory will encompass the above-mentioned investigations as special cases. Contrary to the quasi-steady nozzle case, the presence of a conventional nozzle imposes both amplitude and phase boundary conditions that must be satisfied by the solutions of the problem at the nozzle entrance plane. The generalized theory presented herein also provides a better description of the unsteady flow field in the vicinity of the nozzle entrance plane.

The application of the theory presented herein will be demonstrated by considering the nonlinear stability of a liquid-propellant rocket combustor with uniform injection of propellants at one end and a conventional nozzle at the other end. Crocco's pressure sensitive time lag model<sup>7</sup> is used to describe the unsteady combustion process. In the sections to follow, the development of the wave equation for the analysis of nonlinear combustion instability in liquid rockets will be briefly described, the solution of this nonlinear wave equation will be outlined, and typical results will be presented and discussed. User's Manuals and program listings for the computer programs used to solve these problems are included as appendices to this report.

#### SYMBOLS

$A_{lmn}(t), B_{lmn}(t)$	time-dependent amplitudes in series given by Eq. (6)
$A_p(t)$	time-dependent amplitudes in series given by Eq. (9)
$B(\phi)$	boundary residual
$b_{lmn}$	complex axial acoustic eigenvalue
$c^*$	velocity of sound, ft/sec

$C_0, C_1, C_2, C_3$	coefficients of linear terms in Eqs.(12)
$D_1, D_2, D_3, D_4$	coefficients of nonlinear terms in Eqs. (12)
$E(\tilde{\Phi})$	residual of Eq. (10)
$i$	imaginary unit, $\sqrt{-1}$
$J_m$	Bessel function of the first kind, order $m$
$l, m$	axial and tangential mode numbers, respectively
$n$	pressure interaction index
$p$	dimensionless pressure, $\gamma p^* / \rho_0^* c_0^{*2}$
$r$	dimensionless radial coordinate, $r^* / R_c^*$
$R_c^*$	chamber radius, ft
$R_p(r)$	radial acoustic eigenfunction in Eq. (9)
$S_{mn}$	dimensionless transverse mode frequency
$t$	dimensionless time, $\frac{t^*}{(R_c^*/c_0^*)}$
$u$	dimensionless axial velocity, $u^* / c_0^*$
$\vec{v}$	dimensionless velocity vector, $\vec{v}^* / c_0^*$
$W'_m$	unsteady combustion mass source
$Y$	complex nozzle admittance

$z$	dimensionless axial coordinate, $z^*/R_c^*$
$Z_{\ell mn}(z), Z_p(z)$	axial acoustic eigenfunctions
$\gamma$	ratio of specific heats
$e$	ordering parameter
$\theta$	azimuthal coordinate
$\Theta_p(\theta)$	tangential acoustic eigenfunction in Eq. (9)
$\rho$	dimensionless density, $\rho^*/\rho_o^*$
$\tau$	dimensionless pressure sensitive time lag, $\frac{\tau^*}{(R_c^*/c_o^*)}$
$\phi$	velocity potential
Subscripts:	
$e$	evaluated at the nozzle entrance
$n$	radial mode number
$r, t, z, \theta$	partial differentiation with respect to $r, t, z,$ or $\theta$ respectively
$r, i$	real and imaginary parts of a complex quantity, respectively
$o$	stagnation quantity
Superscripts:	
$'$	perturbation quantity, differentiation with respect to argument

- steady state quantity
- \* dimensional quantity, complex conjugate
- ~ approximate solution

## ANALYSIS

### Development of the Wave Equation

To keep the problem as simple as possible, yet still physically meaningful, the following assumptions are made. The gas phase in the combustor is assumed to consist of a single constituent which is thermally and calorically perfect. Transport phenomena, such as diffusion, viscosity, and heat conduction are neglected. The momentum interchange between the liquid and gas phases is neglected (see Appendix A for a discussion of this assumption), and the specific stagnation enthalpy of the unburned propellant is assumed constant throughout the chamber. The presence of burning propellant drops is represented by a distribution of unsteady mass sources<sup>7</sup> and it is also assumed that the Mach number of the combustor's mean flow is small and that the waves have moderate amplitudes.

As a result of the last two assumptions, the governing conservation equations may be combined and the unsteady flow in the combustor can be described by a single nonlinear wave equation. The derivation of this equation appears in Refs. 8 and 9, where it was assumed that each perturbation quantity and the mean flow Mach number were of  $O(\epsilon)$ , where  $\epsilon$  is an ordering parameter that is a measure of the wave amplitude. After neglecting all terms of  $O(\epsilon^3)$  or higher and combining equations, one obtains the following nonlinear partial differential equation that describes the behavior of the velocity potential,  $\phi$ , of the combustor disturbance:

$$\nabla^2 \phi - \phi_{tt} = 2\vec{V} \cdot \nabla \phi_t + \gamma(\nabla \cdot \vec{V})\phi_t + 2\nabla \phi \cdot \nabla \phi_t + (\gamma - 1)\phi_t \nabla^2 \phi + W'_m \quad (1)$$

Equation (1) is the desired wave equation, and it is similar to the inhomogeneous wave equation solved by Maslen and Moore<sup>10</sup> in a related study on nonlinear acoustics. This equation accounts for the following effects: (1) the

effect of a steady state flow on the wave motion (viz., the first two terms on the right-hand side), (2) the coupling between the gas dynamical oscillations and the unsteady combustion process (viz., the last term on the right-hand side), and (3) the second order nonlinearities of the gas dynamical processes (viz., the third and fourth terms on the right-hand side).

In addition to satisfying Eq. (1), the desired solutions must satisfy rigid wall boundary conditions at the injector end of the chamber and at the chamber walls, while a nozzle admittance condition must be satisfied at the nozzle entrance. These boundary conditions are given (in a cylindrical coordinate system) by:

$$\begin{aligned}\bar{\phi}_r &= 0 \text{ at } r = 1 \\ \bar{\phi}_z &= 0 \text{ at } z = 0 \\ B(\bar{\phi}) &= \bar{\phi}_z + \gamma Y \bar{\phi}_t = 0 \text{ at } z = z_e\end{aligned}\quad (2)$$

The nozzle admittance,  $Y$ , is a complex number defined by

$$Y = Y_r + iY_i = (u'/p')_{z = z_e} \quad (3)$$

where  $u'$  is the dimensionless axial velocity perturbation and  $p'$  is the dimensionless pressure perturbation.

It should be pointed out that due to the absence of an appropriate nonlinear nozzle admittance boundary condition, the solutions of the problem are required to satisfy a linear nozzle admittance. Although inconsistent with the nonlinear wave equation, the linear nozzle admittance condition is used herein with the hope that the solution techniques developed herein will also be applicable when nonlinear nozzle admittance conditions become available. Also, the relative importance of nozzle nonlinearities is not known at the moment and it is quite possible that the linear nozzle boundary condition used herein adequately describes the flow conditions at the nozzle entrance.

The unsteady combustion process is represented by mass sources distributed throughout the volume of the chamber, and the response of the mass sources to pressure oscillations is assumed to be described by Crocco's pressure sensitive time-lag hypothesis.<sup>7</sup> The mass source perturbation,  $W'_m$ , is then given by:<sup>5,8</sup>



$$W'_m = -\gamma n \frac{d\bar{u}}{dz} \left[ \bar{\phi}_t(r, \theta, z, t) - \bar{\phi}_t(r, \theta, z, t - \bar{\tau}) \right] \quad (4)$$

where  $n$  is the pressure "interaction index" that describes the sensitivity of the combustion process to pressure oscillations, and  $\bar{\tau}$ , commonly referred to as the sensitive time-lag, is the part of the total combustion time-lag during which the combustion process is sensitive to pressure oscillations. The unsteady combustion response described by Eq. (4) is linear and the comments made above regarding the use of a linear nozzle admittance boundary condition are also applicable to this case.

Substituting Eq. (4) into Eq. (1) and expressing the resulting equation in a cylindrical coordinate system yields the following wave equation:

$$\begin{aligned} & \bar{\phi}_{rr} + \frac{1}{r} \bar{\phi}_r + \frac{1}{r^2} \bar{\phi}_{\theta\theta} + \bar{\phi}_{zz} - \bar{\phi}_{tt} \\ & - 2\bar{\phi}_r \bar{\phi}_{rt} - \frac{2}{r} \bar{\phi}_\theta \bar{\phi}_{\theta t} - 2\bar{\phi}_z \bar{\phi}_{zt} \\ & - (\gamma - 1) \bar{\phi}_t \left( \bar{\phi}_{rr} + \frac{1}{r} \bar{\phi}_r + \frac{1}{r^2} \bar{\phi}_{\theta\theta} + \bar{\phi}_{zz} \right) \\ & - 2\bar{u} \bar{\phi}_{zt} - \gamma \bar{\phi}_t \frac{d\bar{u}}{dz} \\ & + \gamma n \frac{d\bar{u}}{dz} \left[ \bar{\phi}_t(r, \theta, z, t) - \bar{\phi}_t(r, \theta, z, t - \bar{\tau}) \right] = 0 \end{aligned} \quad (5)$$

The combustor and nozzle geometries considered in this study, as well as the cylindrical coordinate system used in writing Eq. (5), are shown in Fig. 1.

### Method of Solution

Since Eq. (5) has no known closed-form mathematical solution, it is necessary to resort to the use of either exact numerical solution techniques or approximate analytical techniques. For multi-dimensional problems, the exact numerical solution techniques generally exceed the computer storage capacities, therefore an approximate solution technique is used herein. The experience of previous investigators in the fields of structural stability and aeroelasticity indicates that an approximate solution technique known as the Method of Weighted Residuals<sup>11, 12</sup> may be effective in the solution of this nonlinear wave equation.

In order to employ the Method of Weighted Residuals in the solution on Eq. (5), it is first necessary to express the velocity potential,  $\bar{\phi}$ , as an

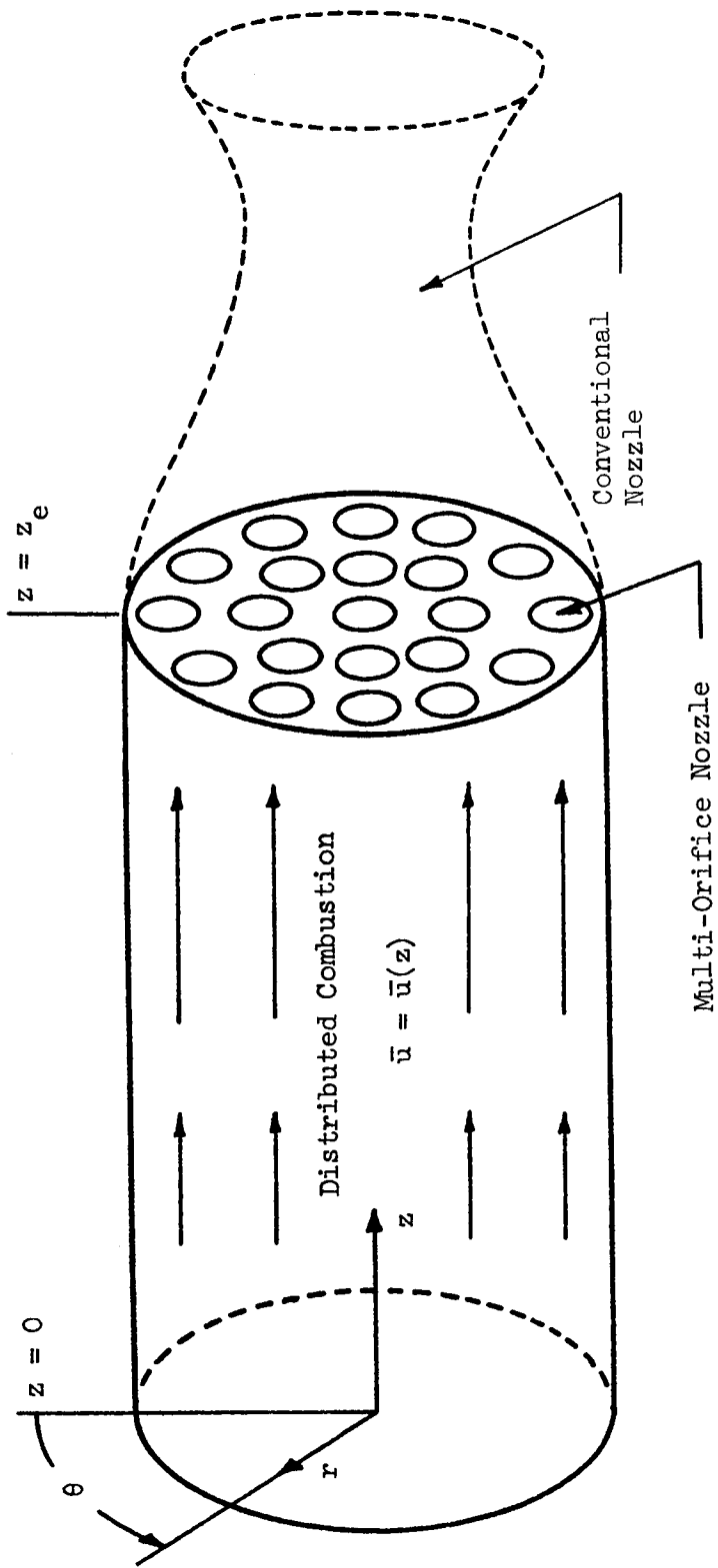


Figure 1. Combustor Configuration and Coordinate System.

approximating series expansion,  $\tilde{\phi}$ . The question naturally arises as to what form of series expansion should be used. Inasmuch as the experimentally observed pressure oscillations during combustion instability usually resemble the natural acoustic modes of the chamber, the velocity potential,  $\phi$ , is expanded in terms of the natural acoustic modes of the chamber with unknown time-dependent amplitudes.

In previous analyses<sup>3,6</sup> of related problems the approximate solutions were expressed in terms of the acoustic modes for a cylindrical chamber with solid wall boundary conditions at both the injector and the nozzle ends. Consequently, the approximation of the flow conditions at the nozzle entrance was poor. In the present analysis a better approximation to the flow at the nozzle entrance is obtained by expanding the velocity potential in terms of the acoustic eigenfunctions for a chamber with a solid wall boundary condition at the injector end and a nozzle admittance condition at the other end. This removes both the two-dimensionality and the quasi-steady nozzle restrictions imposed upon the previous investigations.

The velocity potential,  $\phi$ , is therefore approximated by the following series expansion:

$$\tilde{\phi} = \sum_l \sum_m \sum_n \left\{ A_{lmn}(t) \sin m\theta + B_{lmn}(t) \cos m\theta \right\} Z_{lmn}(z) J_m(S_{mn} r) \quad (6)$$

where the A's and B's are unknown complex functions of time, and the Z's are the complex axial acoustic eigenfunctions. The complex form of the axial acoustic eigenfunctions is given by

$$Z_{lmn}(z) = \cosh(ib_{lmn} z) \quad (7)$$

where the  $b_{lmn}$  are the axial acoustic eigenvalues which must satisfy the following transcendental equation:

$$b_{lmn}^2 \sin^2(b_{lmn} z_e) + \gamma^2 Y^2 (S_{mn}^2 + b_{lmn}^2) \cos^2(b_{lmn} z_e) = 0 \quad (8)$$

Equations (7) and (8) are obtained by linearizing Eq. (5) and solving the resulting equation for the case of no mean flow or combustion (i.e., the acoustic case) subject to the boundary conditions specified in Eq. (2). Each term in the above expansion exactly satisfies the solid wall boundary conditions at the injector end (i.e., at  $z = 0$ ) and at the chamber wall (i.e., at

$r = 1$ ); however, due to the unknown time dependence of Eq. (6) the nozzle admittance condition imposed at  $z = z_e$  is not exactly satisfied by the individual terms. Including both the  $\sin m\theta$  and  $\cos m\theta$  terms in the expansion for  $\tilde{\Phi}$  allows for the possibility of either spinning or standing wave solutions.

In order to simplify the algebra involved in the application of the Method of Weighted Residuals, the development of the associated computer program, and the presentation of the results; the expansion of the velocity potential is written as a single summation as follows:

$$\tilde{\Phi} = \sum_{p=1}^N A_p(t) Z_p(z) \Theta_p(\theta) R_p(r) \quad (9)$$

where the  $A_p$ 's are the unknown time-dependent amplitudes. In order to use Eq. (9) a correspondence must be established between the index,  $p$ , in Eq. (9) and the mode-numbers  $l$ ,  $m$ , and  $n$  in Eq. (6). Such a correspondence is given in Table 1 for a three mode series consisting of the spinning first tangential (1T) mode ( $l = 0$ ,  $m = 1$ ,  $n = 1$ ), the spinning second tangential (2T) mode ( $l = 0$ ,  $m = 2$ ,  $n = 1$ ), and the first radial (1R) mode ( $l = 0$ ,  $m = 0$ ,  $n = 1$ ).

Table 1  
Correspondence Between Eq. (6) and (9) for a Three-Mode Series

$p$	Mode	$l(p)$	$m(p)$	$n(p)$	$A_p$	$\Theta_p$
1	1T	0	1	1	$A_{011}(t)$	$\sin \theta$
2	1T	0	1	1	$B_{011}(t)$	$\cos \theta$
3	2T	0	2	1	$A_{021}(t)$	$\sin 2\theta$
4	2T	0	2	1	$B_{021}(t)$	$\cos 2\theta$
5	1R	0	0	1	$B_{001}(t)$	1

Before proceeding with the analysis, the wave equation (i.e., Eq. (1)) must be modified for use with the assumed complex solution given by Equation (9). This modification is necessary because only the real part of the assumed solution is physically meaningful. It can easily be shown that if  $\Phi = \varphi + i\psi$  is a solution to Eq. (1), the real part,  $\varphi$ , is not a solution to Eq. (1).

This failure of  $\varphi$  to satisfy Eq. (1) is due to the presence of the nonlinear terms in this equation. It can also be shown, however, that a modified wave equation can be constructed for which the real part of its solution satisfies the original wave equation (i.e., Eq. (1)). This modified wave equation is given by:

$$\begin{aligned}
E(\Phi) = & \nabla^2 \Phi - \Phi_{tt} - 2\bar{V} \cdot \nabla \Phi_t - \gamma(\nabla \cdot \bar{V}) \Phi_t - W'_m \\
& - \frac{1-i}{2} \left[ \nabla \Phi \cdot \nabla \Phi_t + \nabla \Phi^* \cdot \nabla \Phi_t^* \right] - \frac{1+i}{2} \left[ \nabla \Phi \cdot \nabla \Phi_t^* + \nabla \Phi^* \cdot \nabla \Phi_t \right] \\
& - \frac{\gamma-1}{4} \left\{ (1-i) \left[ \Phi_t \nabla^2 \Phi + \Phi_t^* \nabla^2 \Phi^* \right] \right. \\
& \left. + (1+i) \left[ \Phi_t \nabla^2 \Phi^* + \Phi_t^* \nabla^2 \Phi \right] \right\} = 0 \tag{10}
\end{aligned}$$

where  $\Phi^*$  is the complex conjugate of  $\Phi$ . The derivation of this equation is discussed in Appendix B. Thus, the Method of Weighted Residuals will be used to obtain approximate solutions to Eq. (10) (i.e.,  $\tilde{\Phi} = \tilde{\varphi} + i\tilde{\psi}$ ) from which the real part,  $\tilde{\varphi}$ , will be taken as the approximate solution of Eq. (1).

In order to obtain a solution, the unknown time-dependent mode-amplitudes (i.e.,  $A_p(t)$ ) are determined by the following mathematical procedure. The assumed series expansion,  $\tilde{\Phi}$ , (i.e., Eq. (9)) is substituted into the wave equation (i.e., Eq. (10)) to form the equation residual,  $E(\tilde{\Phi})$ . Similarly, substituting the series expansion into the nozzle boundary condition (i.e., the last of Eq. (2)) yields the boundary residual,  $B(\tilde{\Phi})$ . In the event that these residuals are both identically zero, the solution is an exact solution. The residuals  $E(\tilde{\Phi})$  and  $B(\tilde{\Phi})$  represent the errors incurred by using the approximate solution,  $\tilde{\Phi}$ .

According to the modified version of the Method of Weighted Residuals, developed by the authors in Refs. 5 and 8, the residuals  $E(\tilde{\Phi})$  and  $B(\tilde{\Phi})$  must satisfy the following orthogonality conditions:

$$\begin{aligned}
& \int_0^{z_e} \int_0^{2\pi} \int_0^1 E(\tilde{\Phi}) Z_j^*(z) \Theta_j(\theta) R_j(r) r dr d\theta dz \\
& - \int_0^{2\pi} \int_0^1 B(\tilde{\Phi}) Z_j^*(z_e) \Theta_j(\theta) R_j(r) r dr d\theta = 0 \tag{11}
\end{aligned}$$

where in the present study the complex conjugate of the axial eigenfunction,  $Z_j^*$ , is used in the weighting functions. The chosen weighting functions must correspond to the terms that appear in the assumed series solution; that is, Eq. (9).

Evaluating the spatial integrals in Eq. (11) yields the following system of  $N$  complex ordinary differential equations to be solved for the unknown complex amplitude functions,  $A_p(t)$ :

$$\sum_{p=1}^N \left\{ C_0(j,p) \frac{d^2 A_p}{dt^2} + C_1(j,p) A_p(t) + [C_2(j,p) - nC_3(j,p)] \frac{dA_p}{dt} + nC_3(j,p) \frac{d[A_p(t - \bar{\tau})]}{dt} \right\} + \sum_{p=1}^N \sum_{q=1}^N \left\{ D_1(j,p,q) A_p \frac{dA_q}{dt} + D_2(j,p,q) A_p \frac{dA_q^*}{dt} + D_3(j,p,q) A_p^* \frac{dA_q}{dt} + D_4(j,p,q) A_p^* \frac{dA_q^*}{dt} \right\} = 0 \quad (12)$$

$$j = 1, 2, \dots, N$$

The coefficients appearing in the above equations are determined by evaluating the various integrals of hyperbolic, trigonometric, and Bessel functions that arise from the spatial integrations indicated in Eq. (11). A user's manual for the computer program COEFFS3D used to calculate these coefficients is given in Appendix C.

The time-dependent behavior of an engine following the introduction of a disturbance is determined by specifying the form of the initial disturbance and then following the subsequent behavior of the individual modes by numerically integrating Eqs. (12). Once the time-dependence of the individual modes is known, the velocity potential,  $\tilde{\Phi}$ , is calculated from Eq. (9). The pressure perturbation at any location within the chamber is related to the real part of  $\tilde{\Phi}$  (i.e.,  $\tilde{\varphi}$ ) by the following second-order momentum equation (see Refs. 5 and 8):

$$\tilde{p}' = -\gamma[\tilde{\varphi}_t + \bar{u}(z)\tilde{\varphi}_z + \frac{1}{2}(\tilde{\varphi}_r^2 + \frac{1}{r^2}\tilde{\varphi}_\theta^2 + \tilde{\varphi}_z^2) - \frac{1}{2}\tilde{\varphi}_t^2] \quad (13)$$

A user's manual for the computer program, LCYC3D, which obtains numerical solutions of Eqs. (12) and (13) is given in Appendix D.

In summary, the theory presented in this section represents a two-stage simplification of the original problem. In the first stage the problem has been reduced to the solution of a single nonlinear, partial differential equation (i.e., Eq. (1)). In the second stage the solution was expanded in a series of acoustic modes with time-dependent coefficients and the Method of Weighted Residuals was used to replace the solution of the nonlinear partial differential equation with the solution of a system of nonlinear, ordinary differential equations (i.e., Eq. (12)). Typical numerical solutions of these equations will be presented and discussed in the following section.

## RESULTS AND DISCUSSION

The generalized three-dimensional theory introduced in the previous section has been used to obtain both linear and nonlinear data for pure transverse modes and pure longitudinal modes for rocket motors with conventional nozzles. Nonlinear data for the first tangential (1T) mode and the first longitudinal (1L) mode has also been obtained for combustors with quasi-steady nozzles for comparison with the results of the previous two-dimensional theories.

### Linear Solutions

Before proceeding with the nonlinear analysis, it was desired to obtain numerical solutions of the linearized equations (i.e., Eqs. (12) with  $D_1 = D_2 = D_3 = D_4 = 0$ ) in order to determine how closely the approximate solutions satisfied the nozzle boundary condition. The linear solution is also needed for comparison with the corresponding nonlinear results. The linear solutions were obtained by assuming a one-mode series expansion consisting only of the mode under consideration. Due to the presence of the retarded variables (i.e.,  $d[A_p(t - \bar{\tau})]/dt$ ) in Eqs. (12), it is necessary to specify the initial amplitudes over the interval  $-\bar{\tau} \leq t \leq 0$ . In this study the initial values were chosen such that the nozzle boundary condition was exactly satisfied during this initial time period. Solutions were obtained for values of  $n$  and  $\bar{\tau}$  on the neutral stability limit (see Appendix E for the determination of neutral stability limits) for various conventional nozzle configurations. The nozzle admittance was expressed in the form,  $Y = Ae^{i\varphi}$ , where  $A$  is the amplitude fac-

tor and  $\varphi$  is the phase shift. The pressure perturbation,  $p'$ , and the axial velocity perturbation,  $u'$ , at the nozzle entrance were calculated numerically for several values of the nozzle phase shift,  $\varphi$ . These calculated values were then used to compute the ratios  $(u'/p')_{z=z_e}$ , which were then compared with the specified nozzle admittance values. These results are shown in Tables (2) and (3) where  $A_n$  and  $\varphi_n$  are the computed values of the amplitude factor and phase shift, respectively. These results show that the approximation to the nozzle boundary condition is very good for both the 1T and 1L modes; that is, the maximum error in the amplitude ratio is about 5% and the maximum error in phase is approximately 0.5 degree. These results are in contrast with previous theoretical investigations where the representation of the unsteady flow conditions in the vicinity of the nozzle entrance was very poor.

Table 2. 1T Mode Linear Solutions (Numerical).

A = 0.02			Error at Nozzle	
$\varphi$ (Degrees)	$\bar{\tau}$	n	$\frac{A_n - A}{A}$	$\varphi_n - \varphi$ (Degrees)
0	1.2	0.66416	-.029	0.4
0	1.7	0.55001	.003	0.4
0	2.2	0.64710	.034	0.4
45	1.2	0.66137	-.031	0.5
45	1.7	0.54490	.001	0.5
45	2.2	0.63665	.032	0.5
90	1.2	0.62507	-.031	0.3
90	1.7	0.51252	-.001	0.3
90	2.2	0.59758	.028	0.3
135	1.2	0.57746	-.031	-0.1
135	1.7	0.47274	-.004	-0.1
135	2.2	0.55353	.023	-0.1
180	1.2	0.54825	-.030	-0.4
180	1.7	0.45003	-.004	-0.4
180	2.2	0.53121	.022	-0.4
225	1.2	0.55357	-.030	-0.4
225	1.7	0.45677	-.003	-0.4
225	2.2	0.54292	.024	-0.5



270	1.2	0.58854	-.029	-0.3
270	1.7	0.48787	.001	-0.3
270	2.2	0.58090	.028	-0.3
315	1.2	0.63362	-.029	0.1
315	1.7	0.52602	.003	0.1
315	2.2	0.62368	.032	0.1

Table 3. 1L Mode Linear Solutions (Numerical).

A = 0.02			Error at Nozzle	
$\phi$ (Degrees)	$\bar{\tau}$	n	$\frac{A_n - A}{A}$	$\phi_n - \phi$ (Degrees)
0	0.6	1.44680	-0.048	0.4
0	1.0	1.01686	0.002	0.4
0	1.4	1.37491	0.049	0.4
45	0.6	1.42414	-0.048	0.5
45	1.0	0.99216	0.001	0.5
45	1.4	1.32746	0.047	0.5
90	0.6	1.33681	-0.046	0.3
90	1.0	0.92275	-0.001	0.3
90	1.4	1.23131	0.042	0.3
135	0.6	1.23678	-0.044	-0.1
135	1.0	0.85007	-0.002	-0.1
135	1.4	1.14229	0.038	-0.1
180	0.6	1.18443	-0.043	-0.4
180	1.0	0.81682	-0.003	-0.4
180	1.4	1.11190	0.036	-0.4
225	0.6	1.20963	-0.043	-0.5
225	1.0	0.84176	-0.001	-0.5
225	1.4	1.15854	0.039	-0.5
270	0.6	1.29571	-0.044	-0.3
270	1.0	0.91003	0.001	-0.3
270	1.4	1.25539	0.044	-0.3
315	0.6	1.39320	-0.046	0.1
315	1.0	0.98248	0.003	0.1
315	1.4	1.34523	0.049	0.1

## Nonlinear Solutions

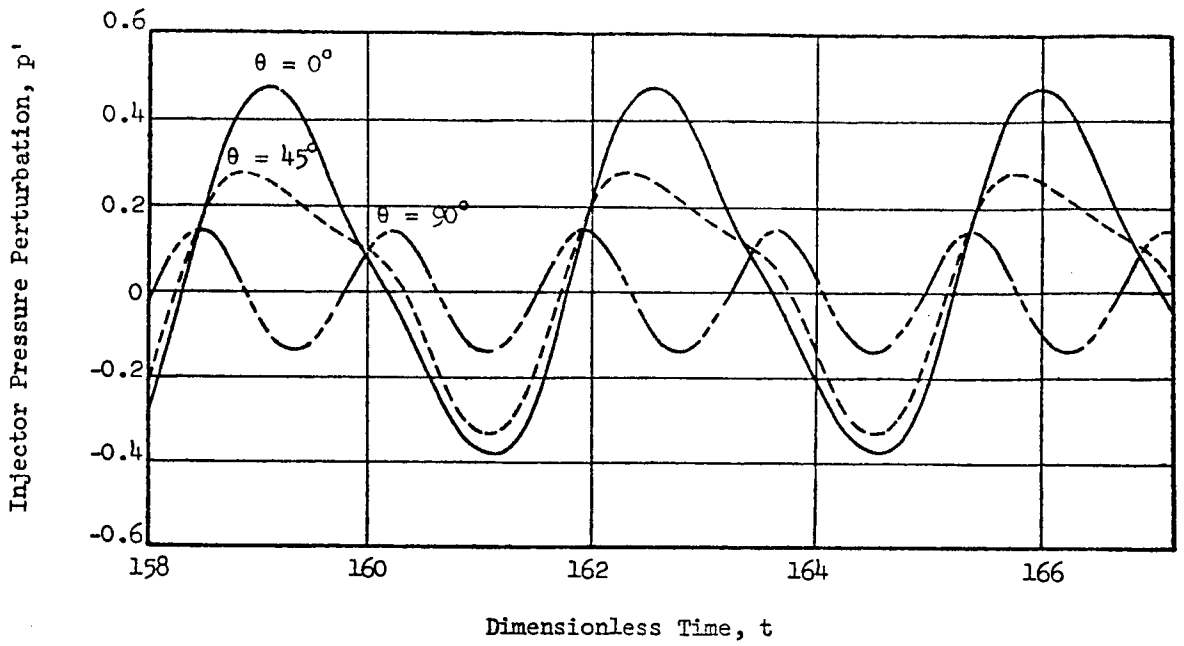
Nonlinear solutions have been computed for both the 1T mode and the 1L mode. For the 1T mode calculations a three mode series expansion consisting of the 1T, 2T (second tangential), and 1R (first radial) modes was used. These are the same modes that were included in the series expansion used in the previous two-dimensional transverse instability studies.<sup>5,6</sup> In these studies it was shown that convergence was obtained with this three mode series; that is, the addition of higher transverse modes (i.e., 3T, 4T, etc.) to the basic series had little effect on the solution. The 1L mode computations were made using a series consisting of the first five longitudinal modes (i.e., 1L, 2L, 3L, 4L, and 5L). It has been shown by Lores and Zinn<sup>3,4</sup> that convergence is obtained with this five-mode series.

Transverse Mode Solutions. Nonlinear solutions have been computed for rocket combustors with quasi-steady nozzles (i.e., real admittances) and also for nozzles with complex admittances. The quasi-steady nozzle solutions were generated for comparison with the results of the previous two-dimensional theory.<sup>5</sup> For this case the nozzle admittance is given by:<sup>13</sup>

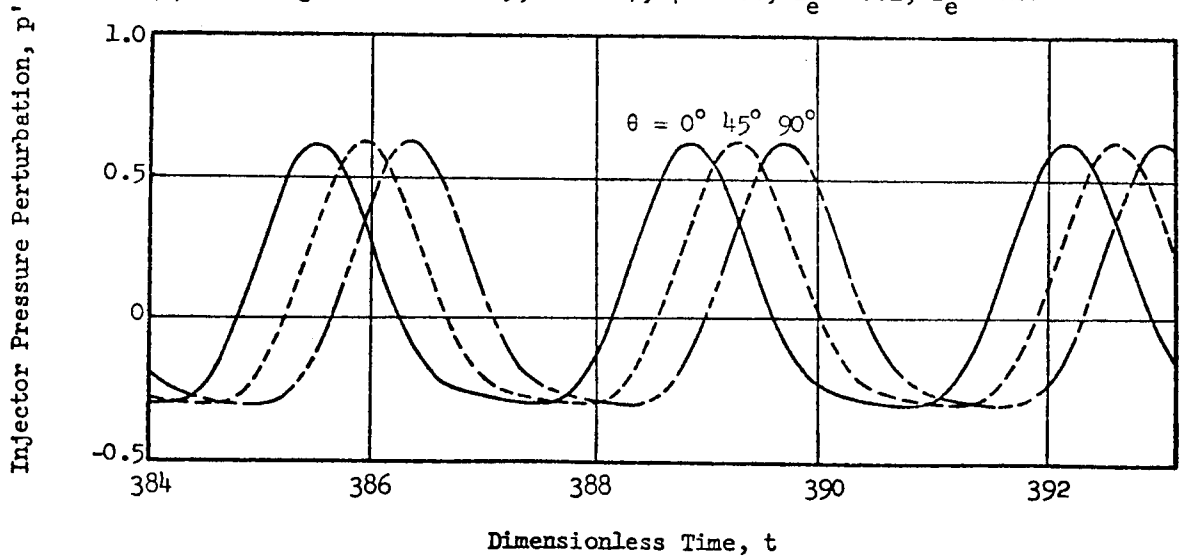
$$Y_r = \frac{\gamma - 1}{2\gamma} \bar{u}_e$$
$$Y_i = 0 \quad (14)$$

For nozzles with complex admittances the admittance was expressed in the form,  $Y = Ae^{i\varphi}$ . For both cases limit-cycle amplitudes and waveforms have been computed for both standing and spinning first tangential instability. This required three series terms to describe standing instability and five series terms to describe spinning instability. Typical computation times on a Univac 1108 computer to reach a limit-cycle were one minute for a standing wave and two minutes for a spinning wave.

Wall pressure waveforms ( $r = 1$ ) were computed at the injector face ( $z = 0$ ) and at the nozzle entrance ( $z = z_e$ ) for three azimuthal locations,  $\theta = 0^\circ$ ,  $\theta = 45^\circ$ , and  $\theta = 90^\circ$ . The initial conditions for standing waves were chosen such that a pressure anti-node occurred at  $\theta = 0^\circ$ . Injector pressure waveforms for both standing and spinning instability are shown in Fig. 2 for combustors with quasi-steady nozzles. These waveforms exhibit sharp peaks



(a) Standing Wave:  $n = 0.65$ ,  $\bar{\tau} = 1.7$ ,  $\gamma = 1.2$ ,  $\bar{u}_e = 0.2$ ,  $z_e = 1.0$



(b) Spinning Wave:  $n = 0.58$ ,  $\bar{\tau} = 1.7$ ,  $\gamma = 1.2$ ,  $\bar{u}_e = 0.2$ ,  $z_e = 1.0$

Figure 2. Nonlinear Pressure Waveforms for the 1T Mode.

and shallow minima; they are nearly identical in shape to those calculated using the previous two-dimensional theory.<sup>5,6</sup> Comparison of injector and nozzle pressure waveforms ( $\theta = 0^\circ$ ) shows that there is very little variation in pressure with axial position. These waveforms are in qualitative agreement with the results of pressure measurements taken during test firings of unstable rocket motors.<sup>1</sup>

To check the accuracy of the approximation of the nozzle boundary condition, wall pressure and axial velocity waveforms were calculated at the nozzle entrance. The error at the nozzle boundary ( $z = z_e$ ) is shown for nonlinear standing and spinning 1T mode instabilities in Fig. 3. Here the axial velocity perturbation,  $u'$ , and the product of the quasi-steady nozzle admittance and the pressure perturbation,  $Y_r p'$  are plotted as a function of time. The latter quantity is the axial velocity perturbation that would be obtained at the nozzle entrance if the nozzle boundary condition were exactly satisfied (i.e., the nozzle admittance condition requires that  $u' = Y_r p'$  at  $z = z_e$ ). Most of the discrepancy between the two curves is due to a slight phase shift between pressure and velocity and the second harmonic distortion of the pressure waveform resulting from the nonlinearities of the system. The nozzle boundary condition is satisfied in an average sense, however, for the ratio of the velocity amplitude (peak-to-peak) to pressure amplitude (peak-to-peak) is very close to the required value,  $Y_r$ .

In another study, limit-cycle amplitudes were calculated as a function of  $n$  and  $\bar{\tau}$  for standing 1T mode instability. Values of  $n$  in the linearly unstable region were chosen for below resonant ( $\bar{\tau} = 1.9$ ), resonant ( $\bar{\tau} = 1.706$ ), and above resonant ( $\bar{\tau} = 1.5$ ) conditions. The resulting amplitudes are compared with those obtained with the two-dimensional theory in Fig. 4. This figure shows that the three-dimensional theory predicts a slightly higher limit-cycle amplitude than the two-dimensional theory for chambers with quasi-steady nozzles.

Figure 4 also shows that the three-dimensional theory, like the previous two-dimensional one, cannot predict triggering of 1T mode instability by the introduction of finite amplitude disturbances. This result was expected since it was shown in Refs. 6 and 8 that the second order (i.e.,  $O(\epsilon^2)$ ) theory can predict triggering only for pure radial modes ( $m = 0, n = 1, 2 \dots$ ). Such triggering limits for the 1R mode are discussed in Ref. 9. It has also been

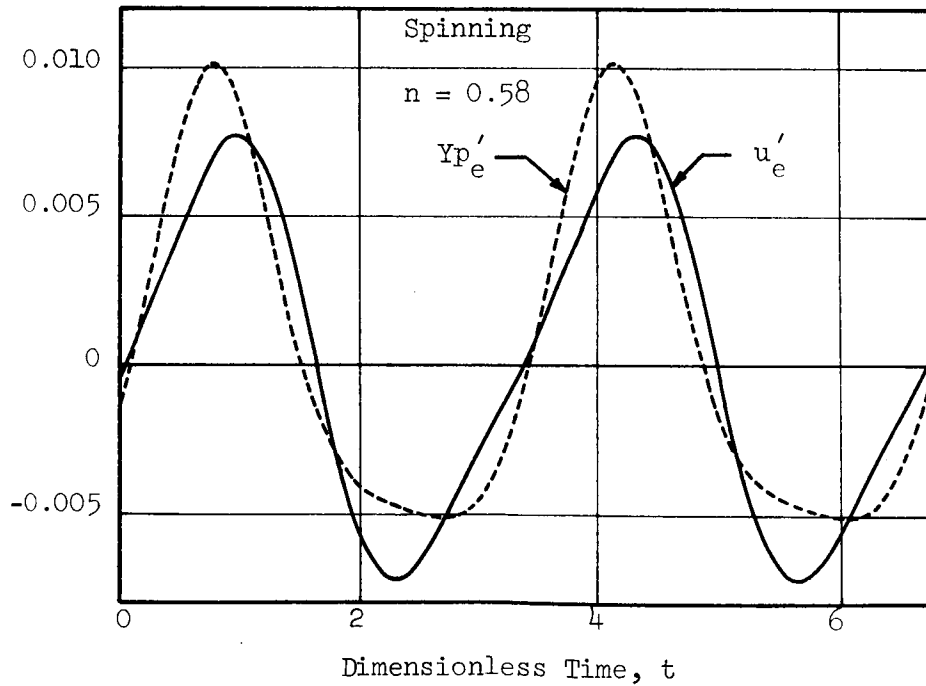
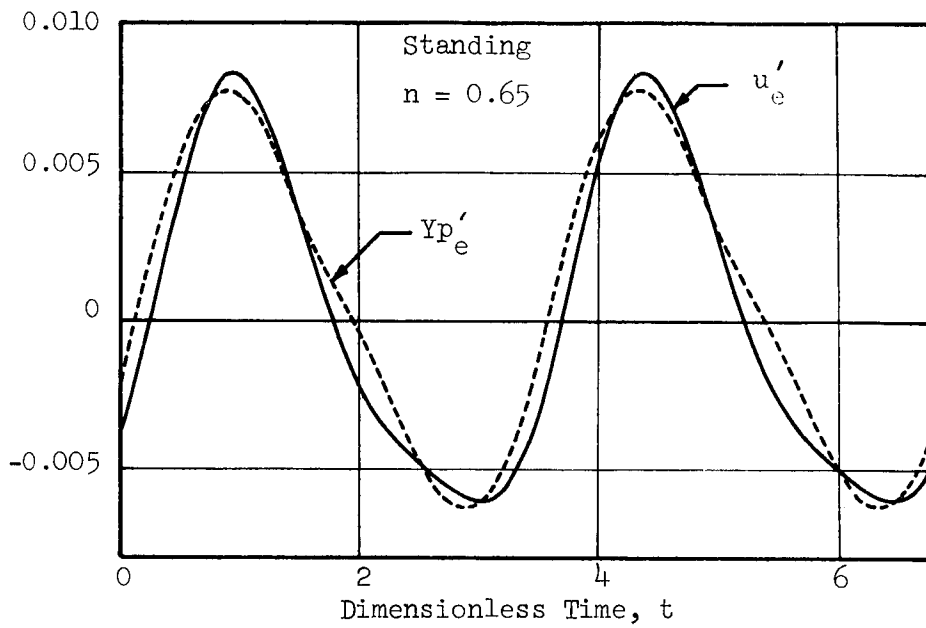


Figure 3. Nozzle Boundary Condition for Nonlinear 1T Mode Solutions for Quasi-Steady Nozzles.

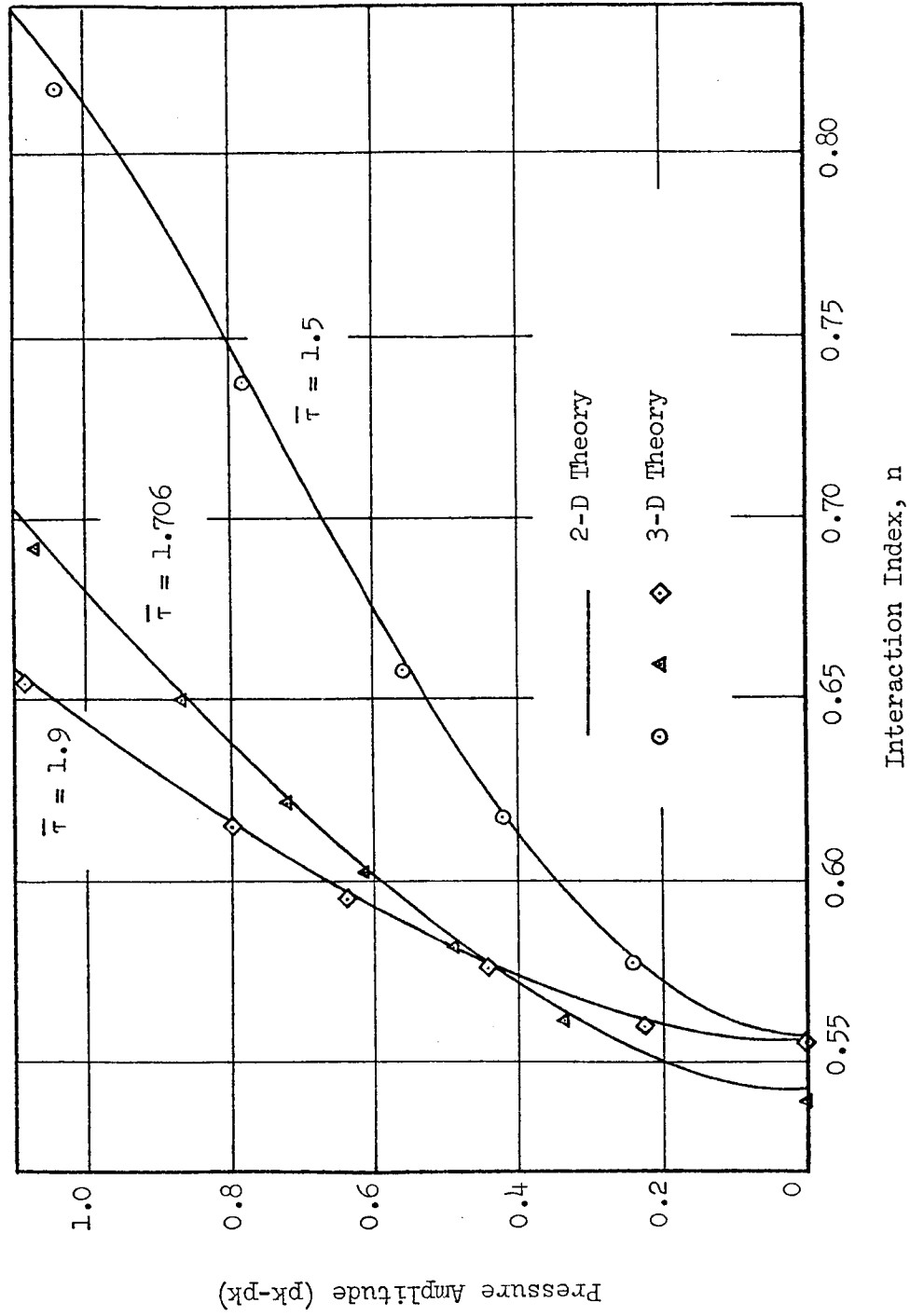


Figure 4. Limit-Cycle Amplitudes for the 1T Mode.

shown, however, that triggering of LT mode instability can be described when the  $O(\epsilon^3)$  terms are retained in the analysis.<sup>8,14</sup> The third order theory given in Refs. 8 and 14 is limited to a single mode in the approximating series expansions. A more general multi-mode third-order theory is now under development and the results will be presented in a future publication. It is also suspected that nonlinear unsteady combustion effects (not included in the present analysis) may play an important role in the triggering phenomenon.

For nozzles with complex admittances a study was conducted to determine the effect of the nozzle phase shift,  $\varphi$ , upon the limit-cycle amplitudes and waveforms for both standing and spinning LT mode instability. The effect of nozzle phase shift on the nonlinear pressure and velocity waveforms at the nozzle entrance plane is shown in Fig. 5 for spinning waves. This figure shows that, while  $\varphi$  has little or no effect on the pressure waveforms, the phase and shape of the velocity waveforms is strongly dependent on  $\varphi$ . The effect of  $\varphi$  on the limit-cycle amplitude for standing LT mode instability is shown in Fig. 6. For a given value of  $n$  and  $\bar{\tau}$  (in the linearly unstable region for the LT mode), Fig 6 shows a sinusoidal variation of limit-cycle amplitude with  $\varphi$  having a maximum amplitude at about  $\varphi = 200^\circ$  and a minimum amplitude at about  $\varphi = 20^\circ$ . In this connection, it should be pointed out that according to linear results nozzle damping is a maximum at  $\varphi = 0^\circ$  and a minimum at  $\varphi = 180^\circ$ ; thus the observed shifts must be due to nonlinearities.

In order to determine how well the solutions approximate the nozzle boundary condition, the amplitude ratio and phase shift between pressure and velocity at the nozzle entrance have been calculated from the nonlinear solutions and have been compared with the specified nozzle admittance condition. Since the waveforms are non-sinusoidal, an approximate amplitude ratio,  $A_c$ , was calculated by taking the ratio of peak-to-peak velocity amplitude to peak-to-peak pressure amplitude. The approximate phase shift,  $\varphi_c$  was calculated from the following formula:

$$\varphi_c = \left[ \frac{t_p - t_u}{T} \right] \times 360 \quad (15)$$

where  $t_p$  is the average of an ascending zero-crossing and the following descending zero-crossing for the pressure perturbation,  $t_u$  is a similar average

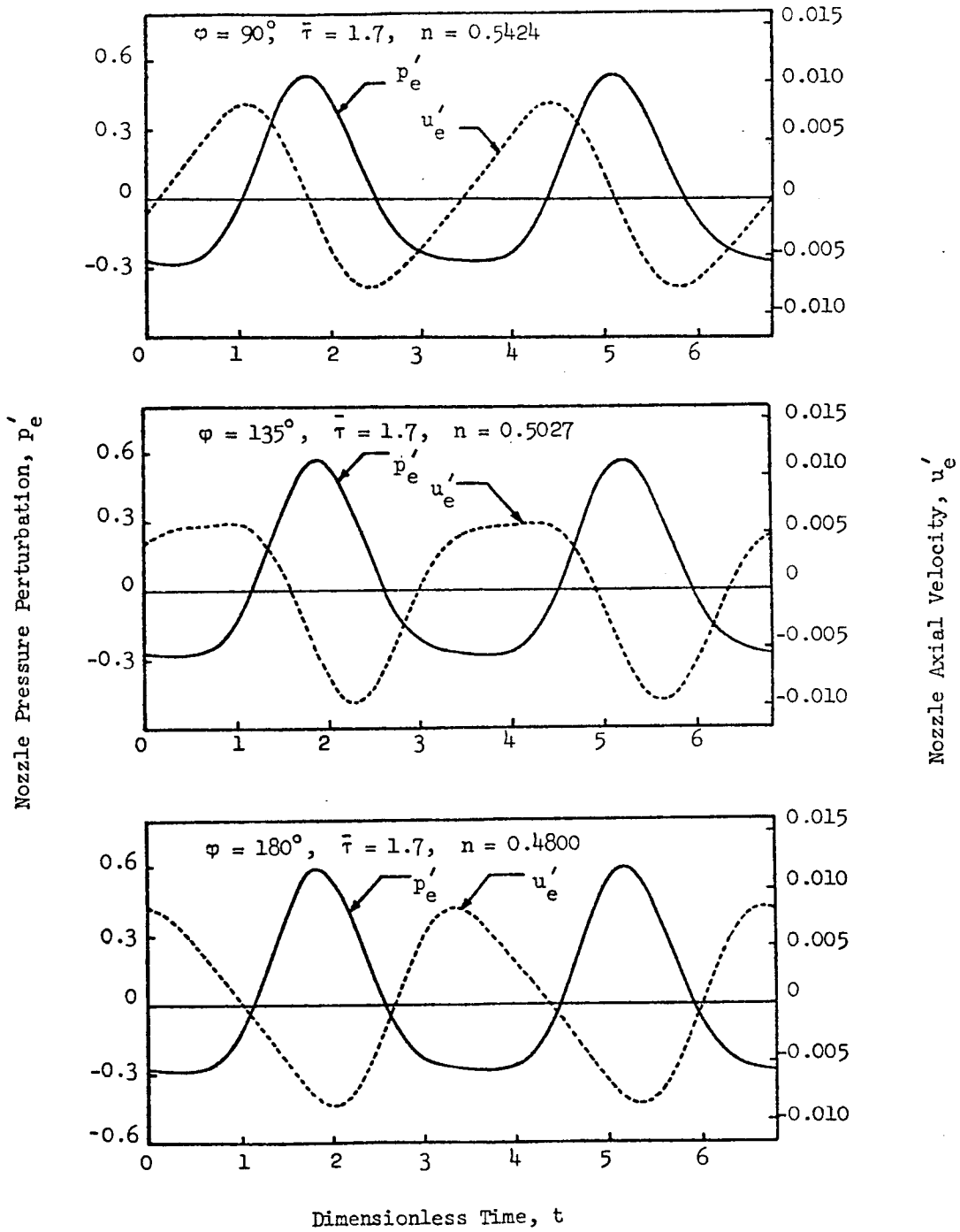


Figure 5. Effect of Nozzle Phase Shift,  $\varphi$ , on Nozzle Waveforms for Spinning 1T Modes.



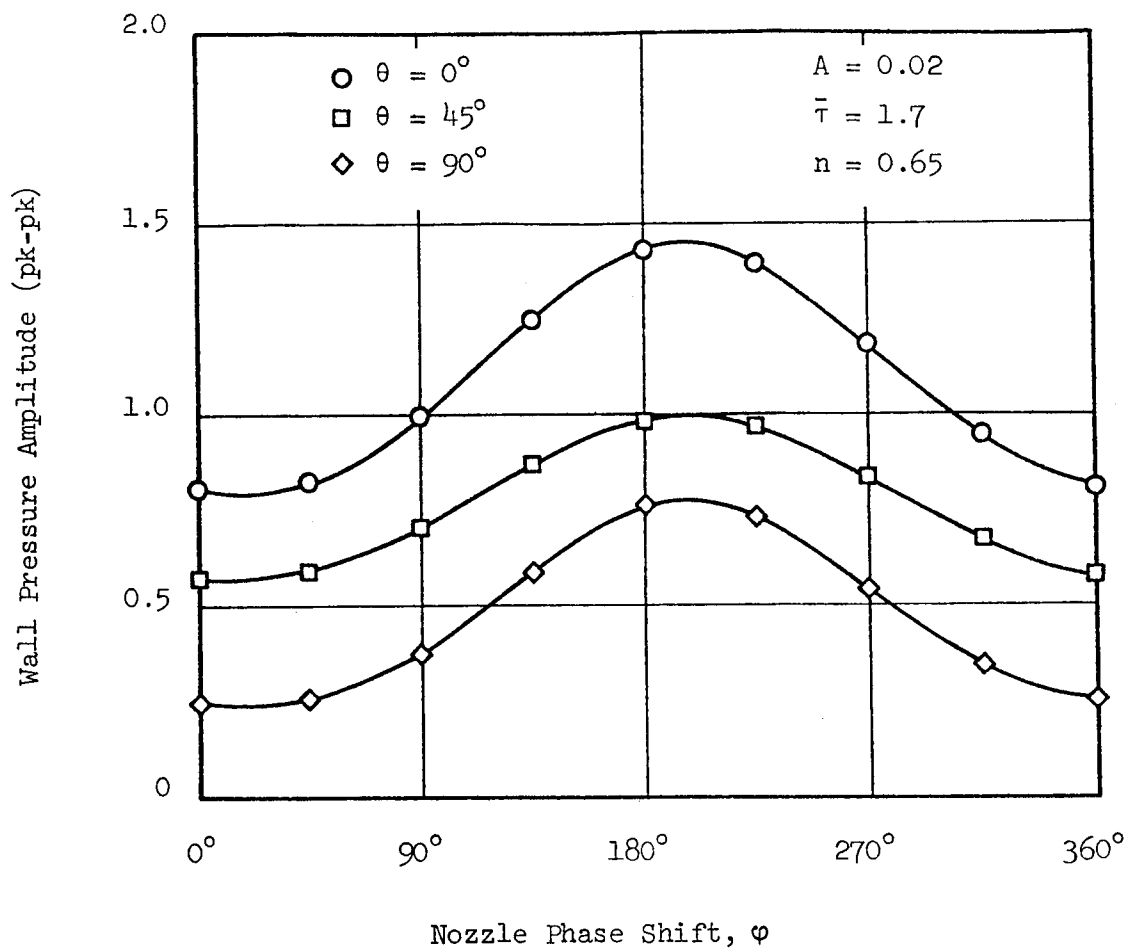


Figure 6. Effect of Nozzle Phase Shift on Limit-Cycle Amplitudes for the Standing 1T Mode.

for the velocity perturbation, and  $T$  is the period of oscillation. The results of this study are shown in Fig. 7 for both standing and spinning waves. For standing waves the calculated amplitude ratios are seen to be consistently higher than required by the nozzle admittance condition (dashed line), while for spinning waves the calculated amplitude ratios are lower than required. For both standing and spinning waves the calculated phase shifts are in excellent agreement with the imposed phase shifts. This study shows that the three-dimensional theory provides a good approximation to the nozzle boundary condition for the  $lT$  mode, considering that the nonlinear solutions are being forced to satisfy a linear boundary condition.

Longitudinal Mode Solutions. Letting  $m$  and  $n$  equal zero in Eq. (6) and using a series consisting of the first five longitudinal modes (i.e.,  $l = 1, 2, \dots, 5$ ), limit-cycle solutions were calculated for quasi-steady nozzles as well as for nozzles with complex admittances. The longitudinal mode solutions required somewhat longer computation times than the transverse mode solutions; the time required to reach a limit cycle was from three to four minutes on the Univac 1108 computer.

Longitudinal mode solutions for chambers with quasi-steady nozzles were compared with the solutions previously obtained by Lores and Zinn<sup>3,4</sup> using a one-dimensional theory. Pressure waveforms at the injector face are compared for both resonant and off-resonant conditions in Fig. 8 which shows excellent agreement between the two theories. Pressure and velocity waveforms at the nozzle entrance as well as injector face pressure waveforms are shown in Fig. 9 for quasi-steady nozzles, while Fig. 10 shows waveforms at the nozzle entrance for nozzles with complex admittance ( $\varphi = 45^\circ$  and  $\varphi = 90^\circ$ ). In each case the results indicate the presence of a steep-fronted pressure wave moving back and forth in the chamber. This behavior is in agreement with experimental observations of axial instabilities.<sup>2</sup> The relation between pressure and velocity waveforms at the nozzle entrance is a fairly good approximation to the nozzle admittance condition (see Figs. 9 and 10) in spite of the highly nonlinear waveforms. The results of this investigation indicate that the three-dimensional nonlinear theory is applicable to longitudinal instabilities as well as transverse instabilities. The theory can also be used to investigate the nonlinear behavior of combined

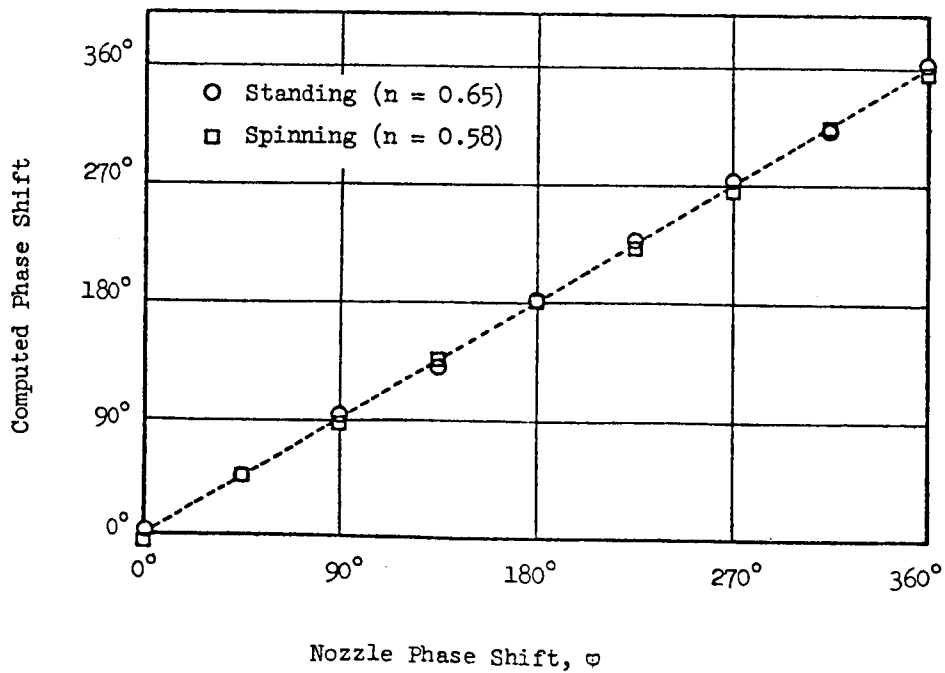
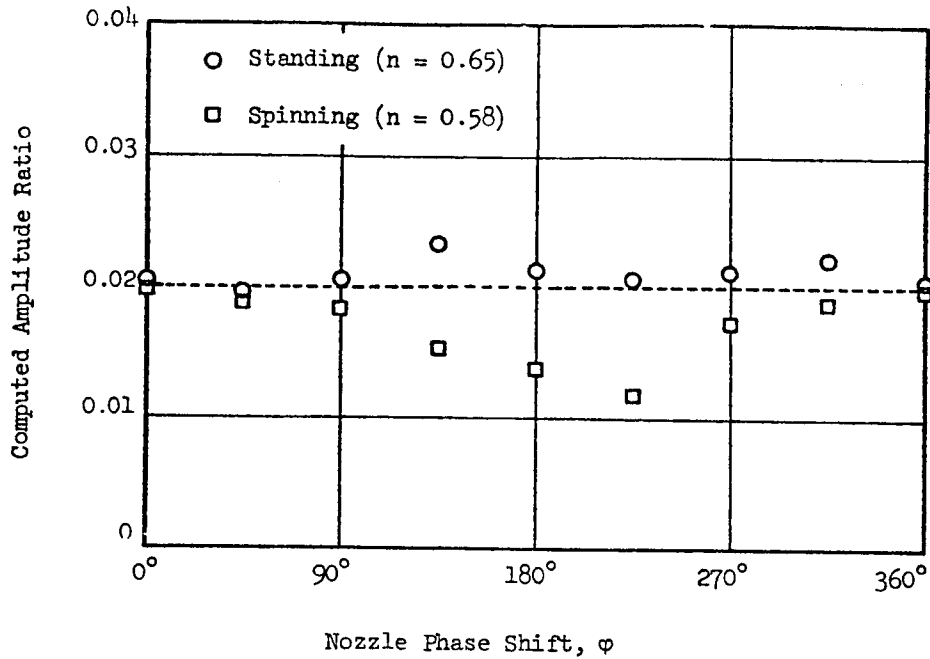


Figure 7. Nozzle Boundary Condition for Nonlinear 1T Mode Solutions.

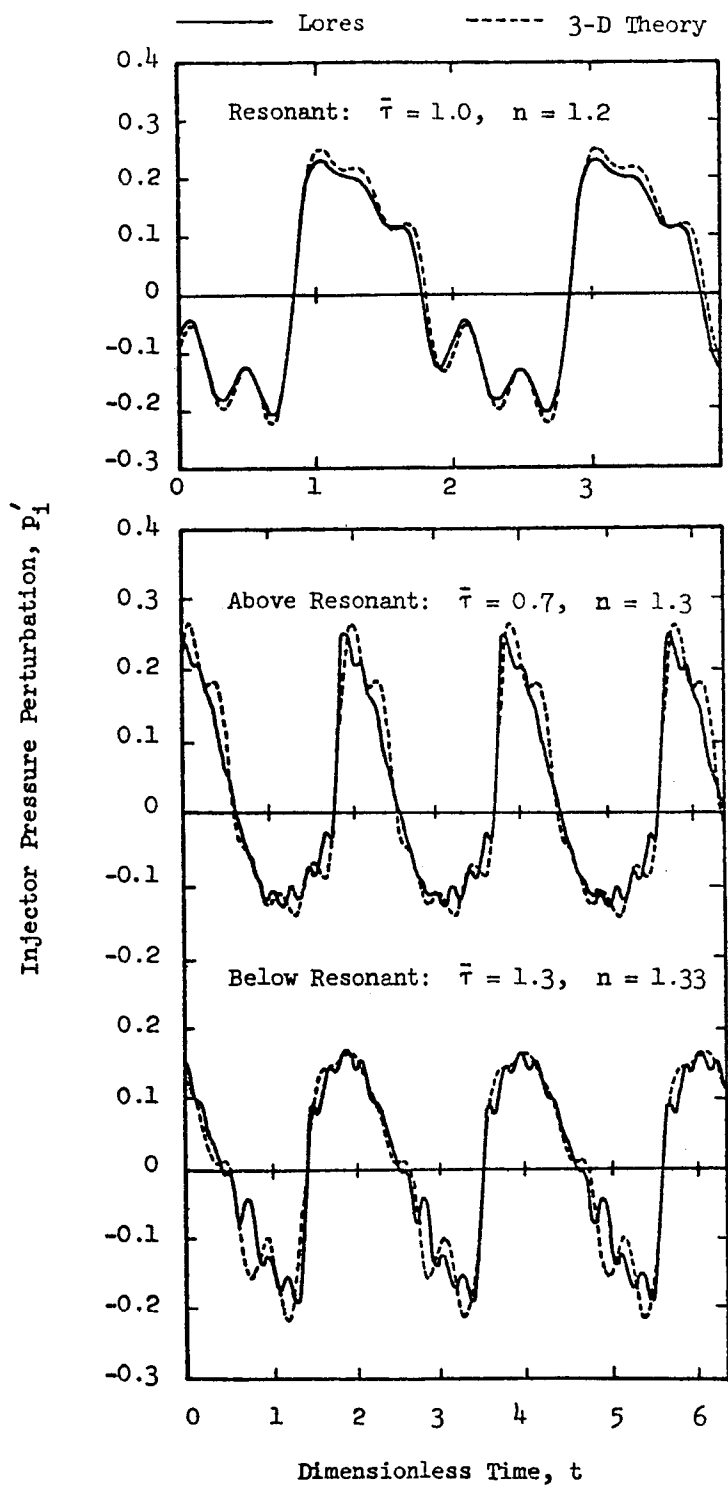


Figure 8. Comparison of Nonlinear 1L Mode Solutions for Quasi-Steady Nozzles.

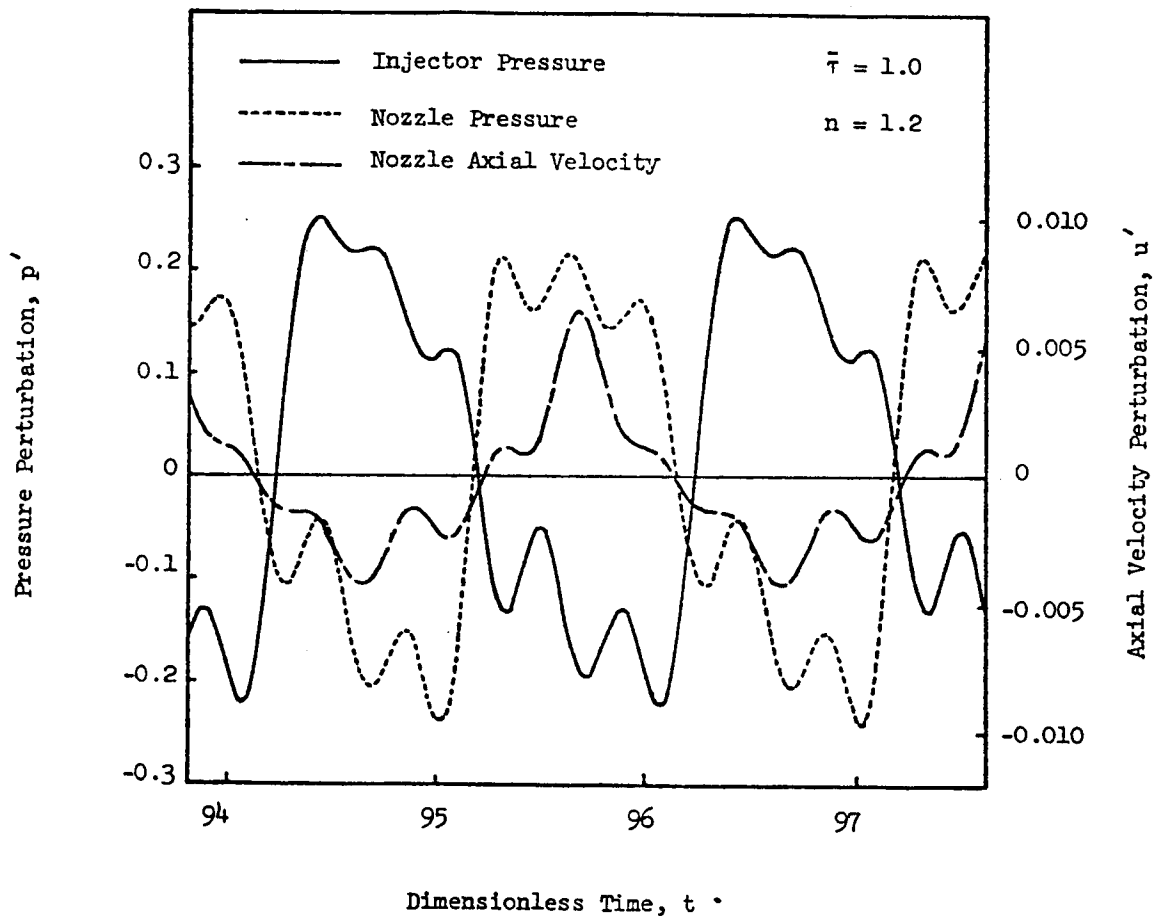


Figure 9. Longitudinal Mode Waveforms for Quasi-Steady Nozzles.

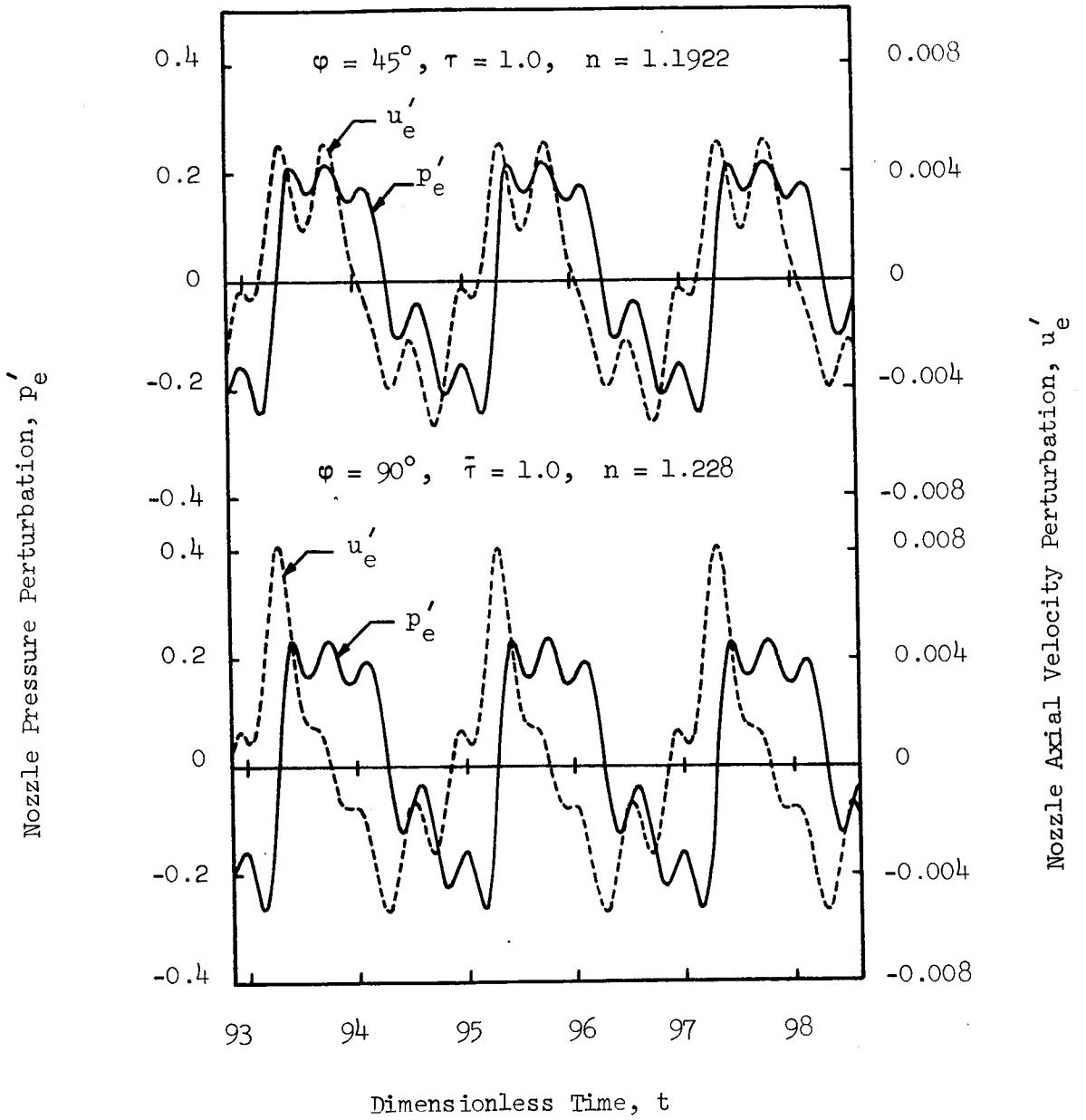


Figure 10. Longitudinal Mode Waveforms for Nozzles with Complex Admittances.

longitudinal-transverse instabilities, although no results for instabilities of this type are presented in this report.

#### CONCLUDING REMARKS

A general three-dimensional second-order nonlinear theory has been developed for predicting the linear and nonlinear behavior of combustion instability in liquid-propellant rocket combustors. This theory contains previous analyses of transverse and longitudinal instabilities as special cases. Furthermore it extends the previous analyses which were applicable only to combustors with quasi-steady nozzles, to the more practical cases of combustors with conventional DeLaval nozzles. The present theory can be used to predict the stability characteristics of longitudinal, transverse and combined longitudinal-transverse modes for various liquid-propellant rocket motor designs.

Results obtained for combustors with quasi-steady nozzles are in excellent agreement with the predictions of previous theories for both transverse and longitudinal instabilities. For combustors with conventional nozzles the limit-cycle amplitude varies sinusoidally with nozzle phase shift,  $\varphi$ , having a maximum value at  $\varphi = 200^\circ$  and a minimum value at  $\varphi = 20^\circ$ . The nozzle phase shift has a strong effect on the axial velocity waveforms at the nozzle entrance while having only a minor influence on the nonlinear pressure waveforms. In both cases, the nonlinear theory developed in this paper provides a good approximation to the unsteady flow conditions at the nozzle entrance plane. This is in contrast to the previous theories which provided a relatively poor approximation to the nozzle boundary condition.

The results presented in this report establish the relationship that exists between the resulting instability (i.e., waveform, final amplitude, and final frequency), the combustion parameters (i.e., interaction index,  $n$ , and time-lag  $\bar{\tau}$ ), and the chamber Mach number and length-to-diameter ratio. These results indicate that the limit-cycle amplitude increases with increasing sensitivity of the combustion process to pressure oscillations. For transverse instabilities, calculated pressure waveforms exhibit sharp peaks and shallow minima, and the frequency of oscillation is always within a few percent of the frequency of one of the chamber's acoustic modes. For axial instabilities, the theory predicts the presence of a steep-fronted wave moving back and forth along the combustor. In both cases the calculated pressure waveforms are in

good qualitative agreement with available experimental data.



## APPENDIX A

### MOMENTUM INTERCHANGE BETWEEN LIQUID AND GAS PHASES

The results presented in this report were obtained under the assumption that the momentum interchange between the liquid droplets and the burned gases is negligible. This assumption will now be relaxed for the special case of uniformly distributed combustion, and it will be shown that this momentum interchange is an important stabilizing effect.

#### Analysis

The momentum equation for two-phase flow was derived in Ref. 8 and is given by:

$$\rho \left[ \frac{\partial \vec{V}}{\partial t} + \vec{V} \cdot \nabla \vec{V} \right] + \frac{1}{\gamma} \nabla P = -(\vec{V} - \vec{V}_L)(C + W_m) \quad (\text{A-1})$$

where  $\vec{V}$  and  $\vec{V}_L$  are the gas and liquid velocity, respectively. The term on the right-hand-side of Eq. (A-1) represents a momentum source to the gas produced by the burning liquid drops. This momentum source consists of two parts: (1) the force necessary to accelerate the evolved gases from the droplet velocity to the gas velocity (i.e., the term  $-W_m(\vec{V} - \vec{V}_L)$ ) and (2) the aerodynamic drag of the droplets (i.e., the term  $-C(\vec{V} - \vec{V}_L)$ ).

In order to derive a wave equation for the velocity potential  $\phi$  it is necessary to make the following assumptions: (1) the drag term is negligible compared with the acceleration term, (2) liquid velocity fluctuations are negligible, and (3) the combustion is uniformly distributed throughout the chamber. Neglecting the drag term, perturbing, and neglecting third order quantities gives the following expression for the momentum source perturbation,  $\vec{M}'$ :

$$\vec{M}' = -(\vec{V}' - \vec{V}'_L) \bar{W}_m \quad (\text{A-2})$$

This is simplified further by neglecting the liquid velocity perturbation,

introducing the velocity potential, and using the steady-state relation,  $\bar{W}_m = d\bar{u}/dz$ , to obtain:

$$\vec{M}' = - \frac{d\bar{u}}{dz} \nabla\phi \quad (A-3)$$

Finally, the assumption of uniformly distributed combustion gives  $d\bar{u}/dz =$  constant which yields:

$$\vec{M}' = - \nabla \left[ \frac{d\bar{u}}{dz} \phi \right] \quad (A-4)$$

Perturbing the left-hand-side of Eq. (A-1), introducing the velocity potential, and combining with Eq. (A-4) gives:

$$\nabla \left[ \frac{\partial\phi}{\partial t} + \frac{1}{\gamma} p' + \bar{u}\phi_z + \frac{d\bar{u}}{dz}\phi + \frac{1}{2} \nabla\phi \cdot \nabla\phi - \frac{1}{2}\phi_t^2 \right] = 0 \quad (A-5)$$

which can be integrated to obtain:

$$p' = -\gamma \left[ \phi_t + \bar{u}\phi_z + \frac{d\bar{u}}{dz}\phi + \frac{1}{2} \nabla\phi \cdot \nabla\phi - \frac{1}{2}\phi_t^2 \right] \quad (A-6)$$

Equation (A-6) is similar to Eq. (13), where the additional term  $(d\bar{u}/dz)\phi$  arises from the droplet momentum source. Following the procedure outlined in Ref. 8, the momentum equation given by Eq. (A-6) is combined with the continuity and energy equations to obtain the desired wave equation:

$$\nabla^2\phi - \phi_{tt} = 2\bar{u}\phi_{zt} + (\gamma + 1)\frac{d\bar{u}}{dz}\phi_t + 2\nabla\phi \cdot \nabla\phi_t + (\gamma - 1)\phi_t \nabla^2\phi + W_m' \quad (A-7)$$

Comparing Eq. (A-7) with Eq. (1) shows that the droplet momentum source

appears only in the second term on the right-hand-side of this equation, where the factor  $\gamma$  in Eq. (1) becomes  $(\gamma + 1)$  in Eq. (A-7).

Applying the Method of Weighted Residuals to obtain approximate solutions to Eq. (A-7) yields a set of ordinary differential equations identical to Eqs. (12) where the coefficient  $C_2(j,p)$  is now given by:

$$C_2(j,p) = \left\{ 2 \int_0^{z_e} \bar{u}(z) Z_p' Z_j^* dz + (\gamma + 1) \int_0^{z_e} \frac{d\bar{u}}{dz} Z_p Z_j^* dz + \gamma Y Z_p(z_e) Z_j^*(z_e) \right\} \times \\ \times \int_0^{2\pi} \Theta_p \Theta_j d\theta \int_0^1 R_p R_j r dr \quad (A-8)$$

Equation (A-8) is readily obtained from Eq. (C-3) by replacing  $\gamma$  in the second term by  $\gamma + 1$ .

### Linear Stability Limits

Linear stability limits for the LL mode were calculated by the method described in Appendix E for the following two cases: (1) the droplet momentum source was included in the analysis and (2) the droplet momentum source was neglected. The results were compared with the linear stability limit calculated by Mitchell<sup>15</sup> on a plot of interaction index,  $n$ , versus stretched time-lag,  $\mu$ , where  $\mu = \omega \bar{r} / \pi$  (see Fig. A-1). This figure shows excellent agreement between the results of Mitchell (solid curve) and the present theory (circle symbols) when the droplet momentum source is included. Neglecting the droplet momentum source shifts the stability curve to much lower values of  $n$  (dashed curve), which indicates that the droplet momentum source is an important stabilizing effect.

### Nonlinear Solutions

In the second-order analysis presented in this report, the droplet momentum source affects the nonlinear solutions primarily by increasing the linear stability of the system. This is readily shown in Fig. (A-2) where the limit-cycle amplitude is plotted as a function of the displacement,  $\delta n$ , above the neutral stability limit. By plotting the limit-cycle amplitudes in this manner,

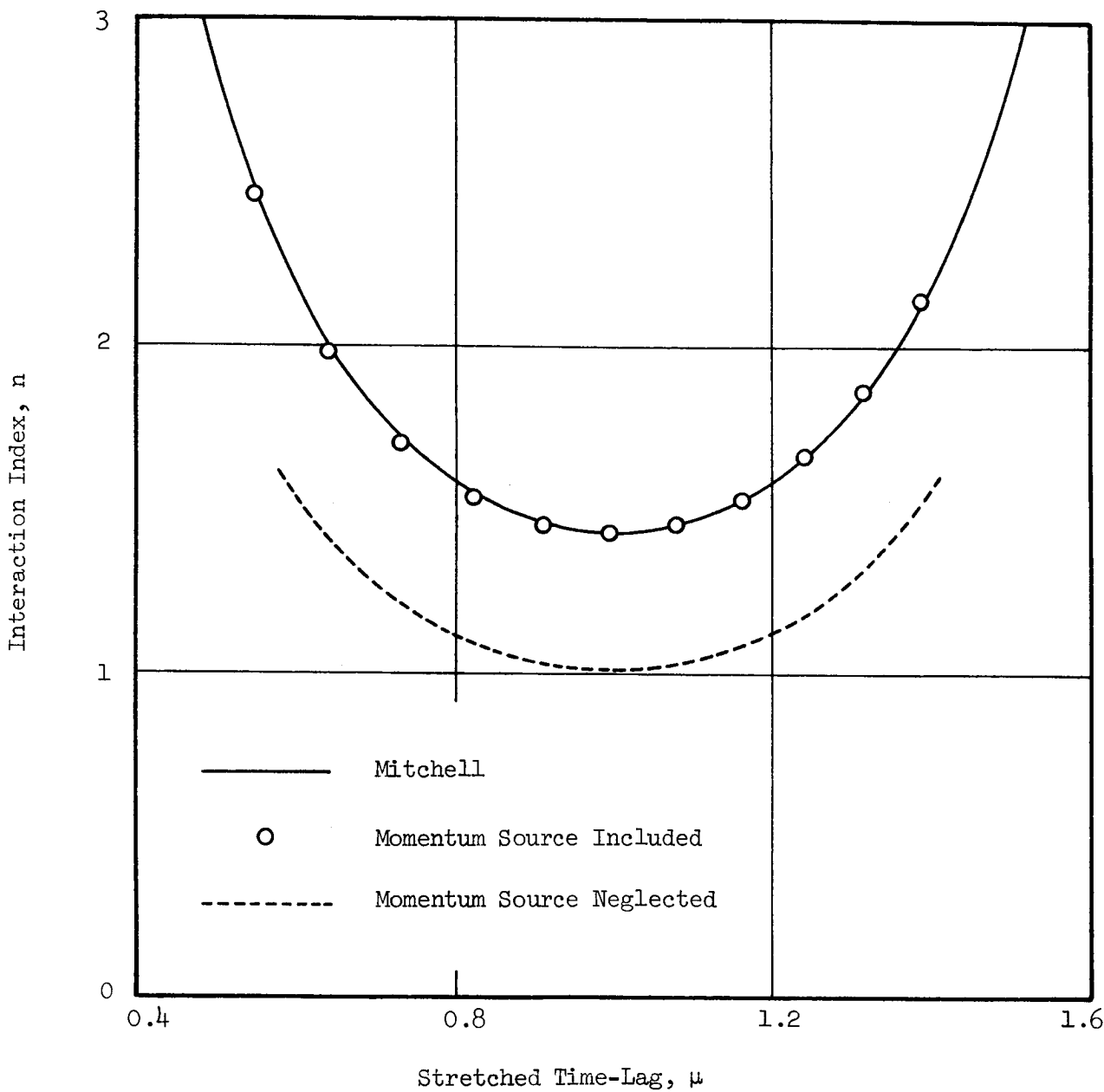


Figure A-1. Effect of Droplet Momentum Source on Linear Stability Limits for the 1L Mode.

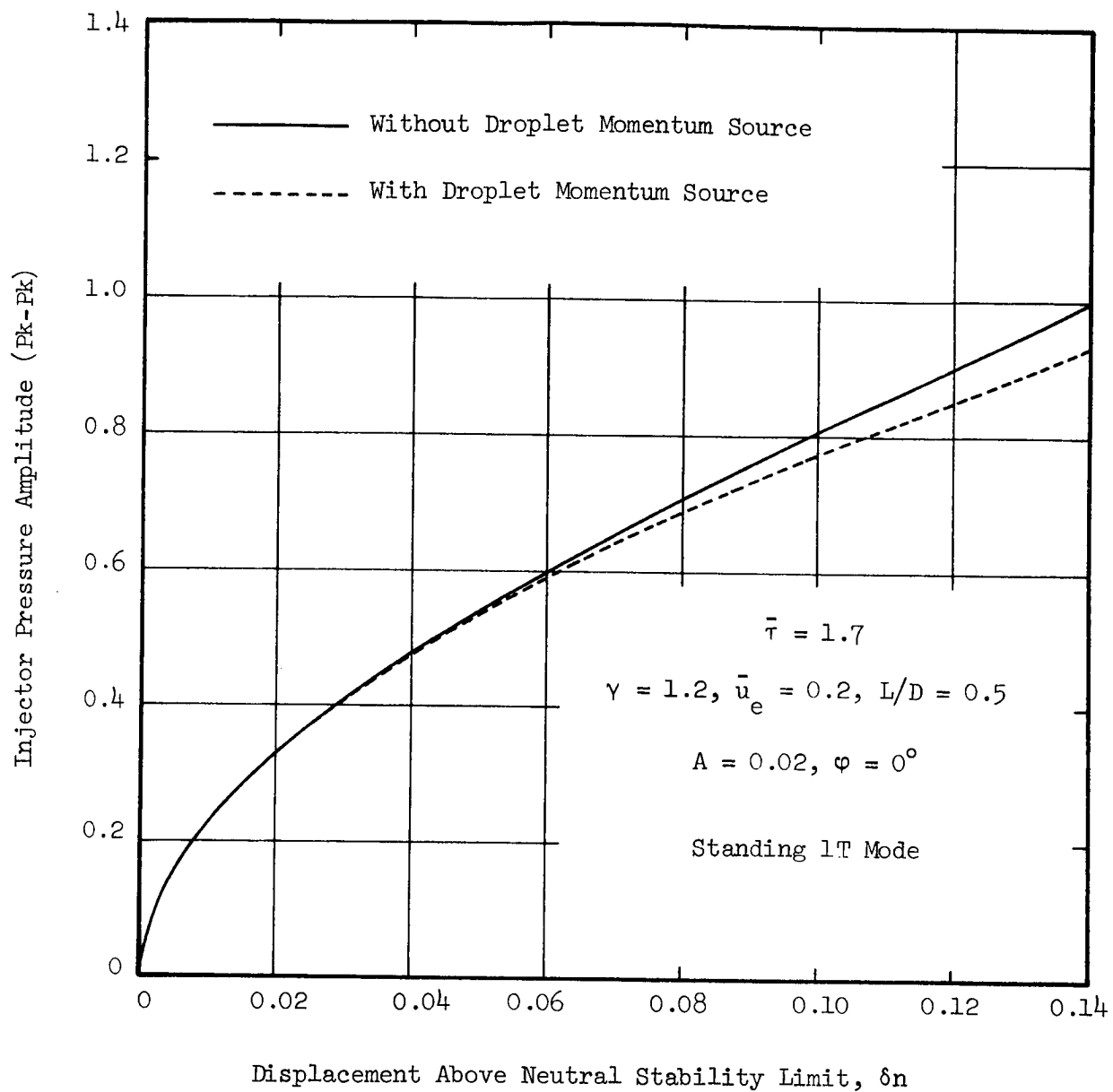


Figure A-2. Effect of Droplet Momentum Source on Limit-Cycle Amplitude.

the effect of the shift in the neutral stability curves is removed so that only the nonlinear effect of the momentum source is seen. Figure A-2 shows that, for equal displacements above the neutral stability limits, including the droplet momentum source results in a slightly smaller limit-cycle amplitude. This difference in limit-cycle amplitude is negligible for most practical purposes.

For combustors with uniformly distributed combustion it has been shown that the droplet momentum source is an important effect which is easily incorporated into the present analysis. Consequently the computer programs based on this theory include the droplet momentum source as an optional feature (see Appendices C, D, and E).

For chambers with non-uniform combustion distributions, Eqs. (A-6) and (A-7) are no longer applicable; however, the droplet momentum source can be taken into account in the following manner. Using the present theory with the droplet momentum source omitted, the neutral stability limit,  $n_1(\bar{\tau})$ , is calculated and the limit-cycle amplitudes are determined as a function of  $\delta n$  as in Fig. A-2. In addition, the linear stability limit,  $n_2(\bar{\tau})$ , is calculated using a linear theory which includes the droplet momentum source and is not restricted to uniformly distributed combustion (such as in Ref. (15)). Assuming that the nonlinear effect of the droplet momentum source is also small for non-uniformly distributed combustion and using the values of  $\delta n$  and  $n_2(\bar{\tau})$  calculated above, the desired plot of limit-cycle amplitude as a function of  $n$  is readily obtained.

## APPENDIX B

### USE OF COMPLEX VARIABLES IN THE SOLUTION OF NONLINEAR DIFFERENTIAL EQUATIONS

It is often convenient to use complex variables in the solution of the linear equations which arise in acoustics, combustion instability and related fields. In this case the solution is expressed in complex form, and the real part represents the physically meaningful solution. However, care must be used when applying this technique in the solution of nonlinear equations. The difficulties that are encountered in applying the complex variable technique to nonlinear problems will be illustrated by analyzing the following simplified example. Consider the nonlinear wave equation given by:

$$\nabla^2 \Phi - \Phi_{tt} = \Phi \Phi_t \quad (\text{B-1})$$

A complex solution of Eq. (B-1) of the form  $\Phi = \varphi + i\psi$  would be useful only if its real part,  $\varphi$ , satisfies Eq. (B-1), which would be the case if the equation were linear. However, straightforward substitution of  $\Phi = \varphi + i\psi$  into Eq. (B-1) and separating its real and imaginary parts yields the following equation for  $\varphi$  :

$$\nabla^2 \varphi - \varphi_{tt} = \varphi \varphi_t - \psi \psi_t \quad (\text{B-2})$$

indicating that the real part,  $\varphi$ , does not satisfy Eq. (B-1) because of the extra term,  $-\psi \psi_t$ , appearing on the right hand side. In order to eliminate this extra term, the form of the original differential equation (i.e., Eq. (B-1)) must be modified.

Since Eq. (B-1) supposedly describes some physical phenomenon, and since only the real part of the complex solution is physically meaningful, then the nonlinear term  $\Phi \Phi_t$  should really be expressed as the product  $\text{Re}(\Phi) \times \text{Re}(\Phi_t)$  which is equivalent to  $(\Phi \Phi_t + \Phi \Phi_t^* + \Phi^* \Phi_t + \Phi^* \Phi_t^*)/4$ . Substituting this expression into Eq. (B-1) yields:

$$\nabla^2 \bar{\Phi} - \bar{\Phi}_{tt} = \frac{1}{4} [\bar{\Phi}\bar{\Phi}_t + \bar{\Phi}\bar{\Phi}_t^* + \bar{\Phi}^*\bar{\Phi}_t + \bar{\Phi}^*\bar{\Phi}_t^*] \quad (\text{B-3})$$

Substituting  $\bar{\Phi} = \varphi + i\psi$  into Eq. (B-3) and separating its real and imaginary parts yield:

$$\nabla^2 \varphi - \varphi_{tt} = \varphi\varphi_t \quad (\text{B-4})$$

$$\nabla^2 \psi - \psi_{tt} = 0$$

which shows that the real part of the solution of Eq. (B-3) satisfies the desired equation (i.e., Eq. (B-1)) and the imaginary part satisfies a homogeneous linear wave equation. This technique was applied to the solution of nonlinear combustion instability problems (i.e., to Eq. (1)), and the resulting modified wave equation was solved using the Method of Weighted Residuals. Due to the approximate nature of the Method of Weighted Residuals, however, the resulting solution contained an error term which grew without limit. Consequently, the above procedure had to be modified in order to obtain satisfactory solutions of Eq. (1) using the Method of Weighted Residuals.

An alternate technique is to modify Eq. (B-1) such that both the real and imaginary parts satisfy the original equation. This can be done by replacing terms of the form  $\bar{\Phi}\bar{\Phi}_t$  with  $\text{Re}(\bar{\Phi})\text{Re}(\bar{\Phi}_t) + i\text{Im}(\bar{\Phi})\text{Im}(\bar{\Phi}_t)$ ; using the relations:

$$\begin{aligned} \text{Re}(\bar{\Phi})\text{Re}(\bar{\Phi}_t) &= \left( \frac{\bar{\Phi} + \bar{\Phi}^*}{2} \right) \left( \frac{\bar{\Phi}_t + \bar{\Phi}_t^*}{2} \right) = \frac{1}{4} [\bar{\Phi}\bar{\Phi}_t + \bar{\Phi}\bar{\Phi}_t^* + \bar{\Phi}^*\bar{\Phi}_t + \bar{\Phi}^*\bar{\Phi}_t^*] \\ i\text{Im}(\bar{\Phi})\text{Im}(\bar{\Phi}_t) &= -i \left( \frac{\bar{\Phi} - \bar{\Phi}^*}{2} \right) \left( \frac{\bar{\Phi}_t - \bar{\Phi}_t^*}{2} \right) = \frac{1}{4} [\bar{\Phi}\bar{\Phi}_t - \bar{\Phi}\bar{\Phi}_t^* - \bar{\Phi}^*\bar{\Phi}_t + \bar{\Phi}^*\bar{\Phi}_t^*] \end{aligned} \quad (\text{B-5})$$

in Eq. (B-1) gives:

$$\nabla^2 \bar{\Phi} - \bar{\Phi}_{tt} = \frac{1}{4} \left[ (1 - i)(\bar{\Phi}\bar{\Phi}_t + \bar{\Phi}^*\bar{\Phi}_t^*) + (1 + i)(\bar{\Phi}\bar{\Phi}_t^* + \bar{\Phi}^*\bar{\Phi}_t) \right] \quad (\text{B-6})$$

Substituting  $\bar{\Phi} = \varphi + i\psi$  into Eq. (B-6) and separating into its real and imagi-



nary parts gives:

$$\nabla^2 \varphi - \varphi_{tt} = \varphi \varphi_t \tag{B-7}$$

$$\nabla^2 \psi - \psi_{tt} = \psi \psi_t$$

which shows that both  $\varphi$  and  $\psi$  satisfy Eq. (B-1). Applying this method to the solution of Eq. (1) yields the modified wave equation (i.e., Eq. (10)) used in the present investigation.

APPENDIX C

PROGRAM COEFFS3D: A USER'S MANUAL

Statement of the Problem

Program COEFFS3D calculates the coefficients of both the linear and non-linear terms which appear in Eqs. (12). These coefficients are required as input for Program LCYC3D (see Appendix D) which numerically integrates this system of equations. The coefficients that are required depend on the choice of terms to be included in the series solution for  $\tilde{\Phi}$  (see Eq. (9)), therefore this information must be provided as input to Program COEFFS3D. The output of Program COEFFS3D is either punched onto cards or stored on drum (FASTRAND) for input to Program LCYC3D.

The coefficients to be calculated are functions of various integrals of hyperbolic, trigonometric, and Bessel functions and are given by the following expressions:

$$C_0(j,p) = \int_0^{z_e} Z_p Z_j^* dz \int_0^{2\pi} \Theta_p \Theta_j d\theta \int_0^1 R_p R_j r dr \quad (C-1)$$

$$C_1(j,p) = \left\{ S_{mn}^2(p) \int_0^{z_e} Z_p Z_j^* dz - \int_0^{z_e} Z_p'' Z_j^* dz + Z_p'(z_e) Z_j^*(z_e) \right\} \int_0^{2\pi} \Theta_p \Theta_j d\theta \int_0^1 R_p R_j r dr \quad (C-2)$$

$$C_2(j,p) = \left\{ 2 \int_0^{z_e} \bar{u}(z) Z_p' Z_j^* dz + \gamma \int_0^{z_e} \frac{d\bar{u}}{dz} Z_p Z_j^* dz + \gamma Y Z_p(z_e) Z_j^*(z_e) \right\} \int_0^{2\pi} \Theta_p \Theta_j d\theta \int_0^1 R_p R_j r dr \quad (C-3)$$

$$C_3(j,p) = \left\{ \gamma \int_0^{z_e} \frac{d\bar{u}}{dz} Z_p Z_j^* dz \int_0^{2\pi} \Theta_p \Theta_j d\theta \int_0^1 R_p R_j r dr \right\} \quad (C-4)$$

$$D_1(j,p,q) = \frac{1}{2}(1-i) \left\{ T_1 \int_0^{z_e} Z_p Z_q Z_j^* dz + T_2 \left[ \int_0^{z_e} Z_p' Z_q' Z_j^* dz + \frac{\gamma-1}{2} \int_0^{z_e} Z_p'' Z_q Z_j^* dz \right] \right\} \quad (C-5)$$

$$D_2(j,p,q) = \frac{1}{2}(1+i) \left\{ T_1 \int_0^{z_e} Z_p Z_q^* Z_j^* dz + T_2 \left[ \int_0^{z_e} Z_p'(Z_q^*)' Z_j^* dz + \frac{\gamma-1}{2} \int_0^{z_e} Z_p'' Z_q^* Z_j^* dz \right] \right\} \quad (C-6)$$

$$D_3(j,p,q) = \frac{1}{2}(1+i) \left\{ T_1 \int_0^{z_e} Z_p^* Z_q Z_j^* dz + T_2 \left[ \int_0^{z_e} (Z_p^*)' Z_q' Z_j^* dz + \frac{\gamma-1}{2} \int_0^{z_e} (Z_p^*)'' Z_q Z_j^* dz \right] \right\} \quad (C-7)$$

$$D_4(j,p,q) = \frac{1}{2}(1-i) \left\{ T_1 \int_0^{z_e} Z_p^* Z_q^* Z_j^* dz + T_2 \left[ \int_0^{z_e} (Z_p^*)' (Z_q^*)' Z_j^* dz + \frac{\gamma-1}{2} \int_0^{z_e} (Z_p^*)'' Z_q^* Z_j^* dz \right] \right\} \quad (C-8)$$

where

$$T_1 = \int_0^{2\pi} \Theta_p \Theta_q \Theta_j d\theta \int_0^1 R_p' R_q' R_j r dr + \int_0^{2\pi} \Theta_p' \Theta_q' \Theta_j d\theta \int_0^1 R_p R_q R_j \frac{dr}{r} - \frac{\gamma-1}{2} S_{mn}^2(p) \times$$

$$T_2 = \int_0^{2\pi} \Theta_p \Theta_q \Theta_j d\theta \int_0^1 R_p R_q R_j r dr$$

$$\times \int_0^{2\pi} \Theta_p \Theta_q \Theta_j d\theta \int_0^1 R_p R_q R_j r dr$$

In the equations on the prior page the notation of Eq. (9) is used; that is, a single index (i.e.,  $j$ ,  $p$ , or  $q$ ) is used to identify a particular series term rather than the mode numbers used in Eq. (6). The index  $j$  identifies the equations in which a given coefficient appears which corresponds to the weighting function used in deriving that equation. For the coefficients of the linear terms (i.e., the  $C$ 's) the index  $p$  identifies the amplitude function which the coefficient multiplies. For coefficients of the nonlinear terms, (i.e., the  $D$ 's)  $p$  identifies the factor which is not differentiated with respect to time, (i.e.,  $A_p$  or  $A_p^*$ ), while  $q$  identifies the differentiated factor (i.e.  $dA_p/dt$  or  $dA_p^*/dt$ ). Due to the complex nature of the axial eigenfunctions, the above coefficients are complex numbers.

### Structure of the Numerical Calculations

A flow chart for Program COEFFS3D is shown in Figure (C-1). The program can be divided into five major sections: (1) input, (2) calculation of the complex linear coefficients, (3) calculation of the complex nonlinear coefficients, (4) obtaining coefficients of the equivalent uncoupled real system, and (5) output.

The inputs to the program include the various parameters describing the chamber geometry, the nozzle boundary condition, the modes included in the approximating series expansion, and various control numbers, as well as the roots of the Bessel functions.

In the second section the axial acoustic eigenvalues are calculated by means of Subroutines EIGVAL and FCNS, and the integrals of the products of two axial eigenfunctions are computed by means of Subroutines AXIAL1 and UBAR. The integrals involving radial and tangential eigenfunctions are evaluated by using the orthogonality properties of these functions. The complex linear coefficients are then calculated according to Eqs. (C-1) through (C-4) and are normalized by dividing by  $C_0(j, j)$ .

In the third section the integrals of products of three Bessel functions are calculated using Subroutines RADIAL and JBES, while similar integrals involving azimuthal eigenfunctions and axial eigenfunctions are computed using Subroutines AZIMTL and AXIAL2 respectively. The normalized complex nonlinear coefficients are obtained from Eqs. (C-5) through (C-8) by dividing by  $C_0(j, j)$ .

In the fourth section the normalized complex coefficients are used to

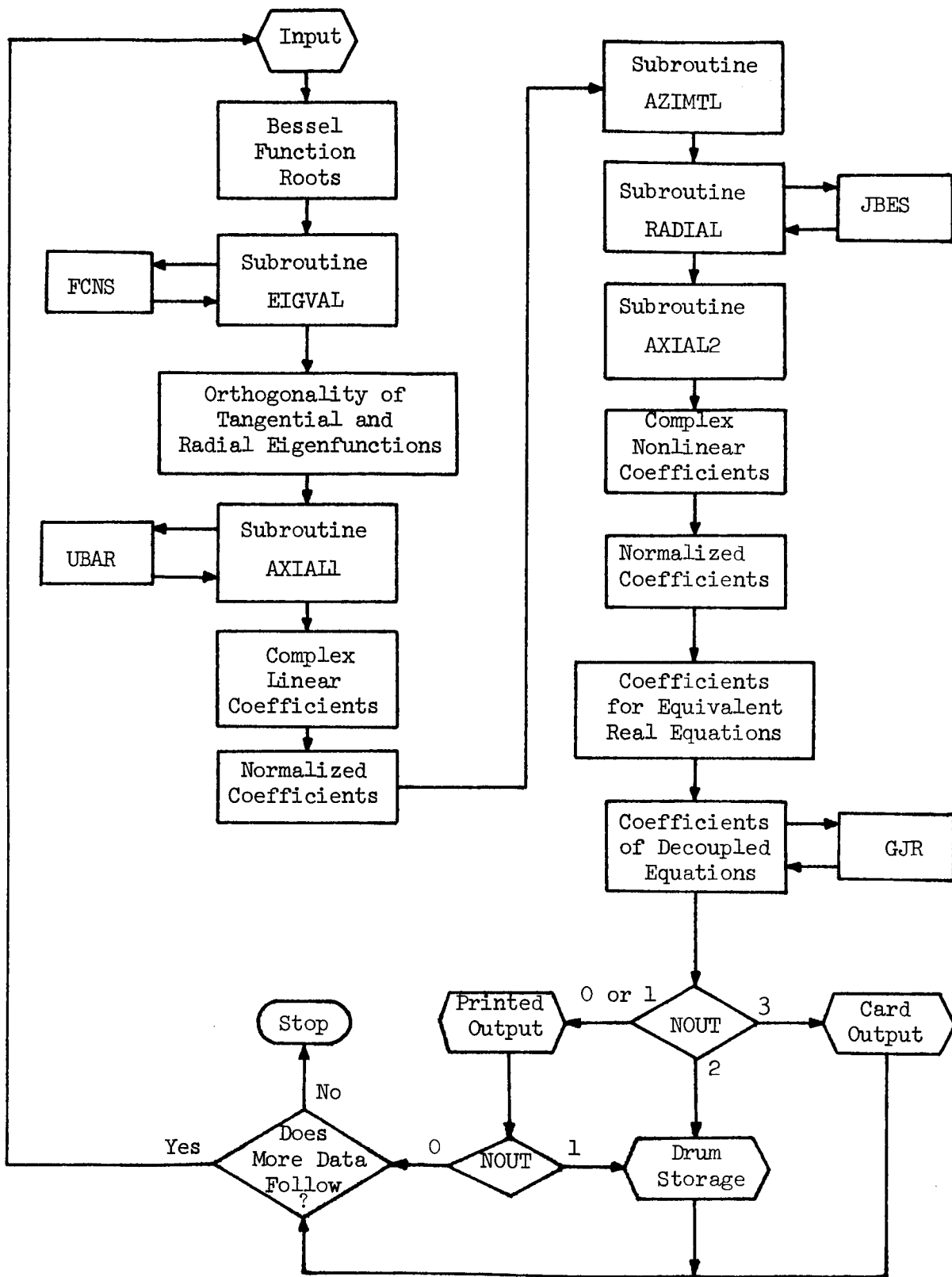


Figure C-1. Flow Chart for Program COEFFS3D

obtain the coefficients for the equivalent system of real differential equations obtained by separating the real and imaginary parts of the complex equations. Since the axial eigenfunctions are non-orthogonal, the resulting system of equations may be coupled in the second derivative terms. Therefore, a matrix inversion procedure is used to obtain the coefficients of an equivalent system which is not coupled in the second derivatives.

In the last section the computed values of the coefficients are either printed out, punched onto cards, or stored on drum (FASTRAND file) as desired.

### Input Data

The input data consists of the chamber parameters (i.e., ratio of specific heats, steady state Mach number, and length-to-diameter ratio), the nozzle admittance ratio, various control numbers, and information indicating which modes are included in the approximate series expansion. Regarding the latter information, each term in the series is identified by the integer variable  $J$ . The nature of each term is specified by the four integers  $L(J)$ ,  $M(J)$ ,  $N(J)$ , and  $NS(J)$ , and each term is given a four character name  $NAME(J)$ . In this manner the coefficients are identified by the integers  $J$  associated with the modes involved rather than the corresponding axial, azimuthal, and radial mode numbers.

The following comments pertain to the detailed description of the input. The location number refers to columns of the card. Three formats are used for input: "A" indicates alphanumeric characters, "I" indicates integers, and "F" indicates real numbers with a decimal point. For the "I" and "F" formats the values are placed in fields of five and ten locations, respectively, and the numbers must be placed in the rightmost locations of the allocated field.

<u>No. of Cards</u>	<u>Location</u>	<u>Type</u>	<u>Input Item</u>	<u>Comments</u>
1	1-72	A	TITLE	Title of Case
1	1-10	F	GAMMA	Ratio of specific heats, $\gamma$ .
	11-20	F	UE	Steady state Mach number at nozzle entrance, $\bar{u}_e$ .
	21-30	F	RLD	Length-to-diameter ratio, $L/D = z_e/2$
	31-40	F	ZCOMB	Length of combustion zone, $z_c/z_e$ .

<u>No. of Cards</u>	<u>Location</u>	<u>Type</u>	<u>Input Item</u>	<u>Comments</u>
	41-45	I	NDROPS	If 0: droplet momentum source neglected. If 1: droplet momentum source included.
	46-50	I	NOZZLE	If 0: quasi-steady nozzle. If 1: conventional nozzle.
1	1-5	I	NJMAX	Number of series terms (complex). (NJMAX $\leq$ 10)
	6-10	I	NONLIN	If 0: linear terms only. If 1: linear and nonlinear terms.
	11-15	I	NEGL	If 0: Nonzero coefficients calculated. If 1: Small coefficients neglected.
	16-20	I	NOUJ	If 0: printed output only. If 1: printed and written into FASTRAND file. If 2: FASTRAND only. If 3: card output only.
If NEGL = 1:				
1	1-10	F	SML	Linear coefficients with absolute value less than SML neglected.
	11-20	F	SM2	Nonlinear coefficients with absolute value less than SM2 neglected.
End of input for NEGL = 1.				
If NOZZLE = 1:				
NJMAX	1-5	I	J	Integer which identifies series term.
	6-15	F	AMPL(J)	Amplitude factor of nozzle admittance, A.
	16-25	F	PHASE(J)	Phase of nozzle admittance, $\varphi$ .
End of Input for NOZZLE = 1.				
NJMAX	1-5	I	J	Integer which identifies series term.
	6-10	I	L(J)	Axial mode number, $l$ . ( $0 \leq L(J) \leq 10$ )

<u>No. of Cards</u>	<u>Location</u>	<u>Type</u>	<u>Input Item</u>	<u>Comments</u>
	11-15	I	M(J)	Tangential mode number, m. ( $0 \leq L(J) \leq 8$ )
	16-20	I	N(J)	Radial mode number, n. ( $0 \leq N(J) \leq 5$ )
	21-25	I	NS(J)	NS(J) = 1: $\Theta_j = \sin(m\theta)$ NS(J) = 2: $\Theta_j = \cos(m\theta)$
	26-30	A	NAME(J)	Four character name.

The first card gives a title (maximum 72 characters) used to identify the run. The second card gives the chamber parameters (i.e.,  $\gamma$ ,  $\bar{u}_e$ ,  $L/D$ ,  $z_c$ ), determines whether the droplet momentum source is included in the analysis (see Appendix A), and specifies the type of nozzle (quasi-steady or conventional). If a quasi-steady nozzle is specified the nozzle admittance is calculated using Eqs. (14), and no further information concerning the nozzle is required. The control numbers are given on the third card. Due to computer storage limitations the series expansion is limited to ten terms, thus NJMAX  $\leq$  10. The control number NEGL gives the option to neglect all coefficients with absolute value smaller than a given number, thus allowing a considerable saving in computation time when the equations are numerically integrated by Program LCYC3D. It has been found that neglecting coefficients with absolute value smaller than 0.1 (i.e., SML = SM2 = 0.1) reduces the computation time by half and has a negligible effect on the resulting solutions. For conventional nozzles a series of NJMAX cards is read which gives the nozzle admittance (amplitude and phase) for each term in the series. This is followed by another series of NJMAX cards giving the mode numbers for each series term.

The proper input for program COEFFS3D will be illustrated with the following example. Suppose the velocity potential  $\Phi$  is expressed in terms of the first tangential (1T), the second tangential (2T), and the first radial (1R) modes. It is also desired to investigate instability of the spinning type, therefore both  $\sin(m\theta)$  and  $\cos(m\theta)$  terms are included in the series. However, for the 1R mode ( $m=0$ ) there is no corresponding  $\sin(m\theta)$  term, therefore the resulting series will contain five terms. A nozzle admittance of  $A = 0.02$  and  $\varphi = 45^\circ$  will be assumed for each term in the series, and coefficients smaller than 0.1 as well as the droplet momentum source will be neglected.





### Complex Linear Coefficients

For NDROPS = 0 the complex linear coefficients are computed from Eqs. (C-1) through (C-4) and are stored in the complex array CC(KC,NJ,NP). For NDROPS = 1 the coefficients  $C_2(j,p)$  are computed from Eq. (A-8).

In order to calculate these coefficients the following information is needed: (1) the axial acoustic eigenvalues,  $b_{l,mn}$ , (2) the steady state Mach number distribution,  $\bar{u}(z)$ , (3) the orthogonality properties of the transverse eigenfunctions, and (4) the integrals of products of two axial eigenfunctions. The calculation of these quantities is described below.

Axial Acoustic Eigenvalues. The axial acoustic eigenvalues are determined by numerically solving the transcendental equation given by Eq. (8). This is done by first substituting  $b_{l,mn} = \epsilon_{l,mn} + i\eta_{l,mn}$  and  $Y = Y_r + iY_i$  into Eq. (8) and separating real and imaginary parts. This yields a pair of simultaneous equations of the form:

$$f(\epsilon, \eta) = 0 \tag{C-9}$$

$$g(\epsilon, \eta) = 0$$

where

$$\begin{aligned} f(\epsilon, \eta) = & (\epsilon^2 - \eta^2)F(\epsilon, \eta) - 4\epsilon\eta H(\epsilon, \eta) \\ & + \gamma^2 \left\{ \left[ (Y_r^2 - Y_i^2)(S_{mn}^2 + \epsilon^2 - \eta^2) - 4Y_r Y_i \epsilon \eta \right] G(\epsilon, \eta) \right. \\ & \left. + 4 \left[ Y_r Y_i (S_{mn}^2 + \epsilon^2 - \eta^2) + (Y_r^2 - Y_i^2) \epsilon \eta \right] H(\epsilon, \eta) \right\} \end{aligned} \tag{C-10}$$

$$\begin{aligned}
g(\epsilon, \eta) &= (\epsilon^2 - \eta^2)H(\epsilon, \eta) + \epsilon\eta F(\epsilon, \eta) \\
&+ \gamma^2 \left\{ \left[ Y_r Y_i (S_{mn}^2 + \epsilon^2 - \eta^2) + (Y_r^2 - Y_i^2) \epsilon \eta \right] G(\epsilon, \eta) \right. \\
&\left. - \left[ (Y_r^2 - Y_i^2) (S_{mn}^2 + \epsilon^2 - \eta^2) + 4Y_r Y_i \epsilon \eta \right] H(\epsilon, \eta) \right\} \quad (C-11)
\end{aligned}$$

and

$$\begin{aligned}
F(\epsilon, \eta) &= \sin^2(\epsilon z_e) \cosh^2(\eta z_e) - \cos^2(\epsilon z_e) \sinh^2(\eta z_e) \\
G(\epsilon, \eta) &= \cos^2(\epsilon z_e) \cosh^2(\eta z_e) - \sin^2(\epsilon z_e) \sinh^2(\eta z_e) \quad (C-12) \\
H(\epsilon, \eta) &= \sin(\epsilon z_e) \cos(\epsilon z_e) \sinh(\eta z_e) \cosh(\eta z_e)
\end{aligned}$$

In the above equations the subscripts on  $\epsilon$  and  $\eta$  have been omitted.

Equations (C-9) are solved by Subroutine EIGVAL using Newton's Method for two unknowns.<sup>17</sup> In this method successive approximations to the roots are generated by the recursion formulas:

$$\begin{aligned}
\epsilon_{i+1} &= \epsilon_i - \left[ \frac{fg_\eta - gf_\eta}{J(f, g)} \right]_i \\
\eta_{i+1} &= \eta_i - \left[ \frac{gf_\epsilon - fg_\epsilon}{J(f, g)} \right]_i \quad (C-13)
\end{aligned}$$

where the Jacobian  $J(f, g)$  is given by:

$$J(f, g) = f_\epsilon g_\eta - g_\epsilon f_\eta \quad (C-14)$$

and the subscripts indicate partial differentiation with respect to  $\epsilon$  and  $\eta$ . The quantities  $f$ ,  $g$ ,  $f_{\epsilon}$ ,  $f_{\eta}$ ,  $g_{\epsilon}$ ,  $g_{\eta}$  are calculated by the Subroutine FCNS. The iteration is started by assuming the following values for  $\epsilon$  and  $\eta$ :

$$\epsilon_0 = \epsilon_m + a \cos(\beta) \tag{C-15}$$

$$\eta_0 = a \sin(\beta)$$

where for  $\ell = 0$ :

$$\epsilon_m = 0$$

$$a = 10A/z_e$$

$$\beta = \varphi/2 + 45 \text{ (degrees)}$$

(C-16)

and for  $\ell \neq 0$ :

$$\epsilon_m = \ell\pi/z_e$$

$$a = A/z_e$$

$$\beta = \varphi + 90 \text{ (degrees)}$$

The iteration is terminated when the errors  $\Delta\epsilon$  and  $\Delta\eta$  are smaller than  $10^{-7}$ . If the iteration fails to converge after 40 iterations or the Jacobian vanishes a warning message is printed. FORTRAN listings of Subroutines EIGVAL and FCNS are given at the end of this appendix.

Steady State Mach Number Distribution. The steady state Mach number distribution is calculated by means of Subroutine UBAR which must be supplied by the user. This distribution must be of the form shown in Fig. (C-2) where the Mach number varies from zero at the injector face ( $z = 0$ ) to its maximum value at the end of the combustion zone ( $z = z_c$ ) and remains constant until the nozzle entrance ( $z = z_e$ ) is reached. Thus the Mach number is given by

$$\bar{u}(z) = U(z)\bar{u}_e \quad (0 \leq z \leq z_c)$$

(C-17)

$$\bar{u}(z) = \bar{u}_e \quad (z_c \leq z \leq z_e)$$

where  $U(0) = 0$  and  $U(z_c) = 1$ . Although the function  $U(z)$  may be arbitrary, the results presented in this report were obtained using a linear Mach number distribution in the combustion zone (i.e., uniformly distributed combustion). Thus the function  $U(z)$  in the listing of UBAR provided herein is given by:

$$U(z) = z/z_c \quad (C-18)$$

In addition to the Mach number distribution (NOPT = 1), the first (NOPT = 2) and second (NOPT = 3) derivatives are also calculated.

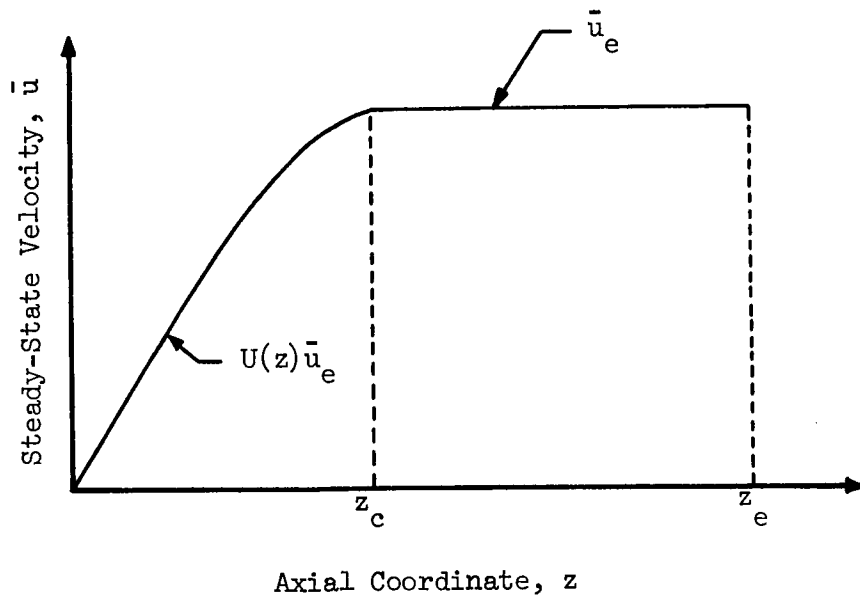


Figure C-2. Steady-State Mach Number Distribution.

Orthogonality of Transverse Eigenfunctions. The tangential eigenfunctions have the following orthogonality properties:

$$\begin{aligned}
 \int_0^{2\pi} \sin(m_p \theta) \sin(m_j \theta) d\theta &= \int_0^{2\pi} \cos(m_p \theta) \cos(m_j \theta) d\theta = 0 & m_p \neq m_j \\
 &= \pi & m_p = m_j \neq 0 \\
 \int_0^{2\pi} \cos(m_p \theta) \cos(m_j \theta) d\theta &= 2\pi & m_p = m_j = 0 \\
 \int_0^{2\pi} \sin(m_p \theta) \cos(m_j \theta) d\theta &= 0 & \text{for all } m_p \text{ and } m_j
 \end{aligned} \tag{C-19}$$

For the special case of  $m_p = m_j = 0$  the integral involving sines vanishes. The orthogonality property of the radial eigenfunctions is given by:

$$\begin{aligned}
 \int_0^1 R_p R_j r dr &= 0 & n_p \neq n_j \quad (m_p = m_j) \\
 \int_0^1 R_p R_j r dr &= \frac{s_{mn}^2 - m^2}{2s_{mn}^2} [J_m(s_{mn})]^2 & n_p = n_j \quad (m_p = m_j)
 \end{aligned} \tag{C-20}$$

Since the tangential integrals vanish when  $m_p \neq m_j$  it is not necessary to calculate the radial integrals for  $m_p \neq m_j$ . These orthogonality properties are used to calculate the integrals,  $\int_0^{2\pi} \Theta_p \Theta_j d\theta$  and  $\int_0^1 R_p R_j r dr$ , which appear in Eqs. (C-1) through (C-4). For a series containing pure transverse modes only ( $l = 0$ ), it is easily seen that all of the linear coefficients vanish except those corresponding to  $p = j$ , yielding a system of equations which are not coupled in the linear terms.

Axial Integrals. The integrals of products of two axial eigenfunctions are calculated by Subroutine AXIAL1. According to the value of the input parameter NOPT these integrals are calculated as follows:

$$\text{NOPT} = 1: \int_0^{z_e} Z_p Z_j^* dz = \frac{1}{2} \left\{ \frac{\sinh[i(b_p + b_j^*)z_e]}{i(b_p + b_j^*)} + \frac{\sinh[i(b_p - b_j^*)z_e]}{i(b_p - b_j^*)} \right\} \quad (\text{C-21})$$

$$\text{NOPT} = 2: \int_0^{z_e} Z_p'' Z_j^* dz = -b_p^2 \int_0^{z_e} Z_p Z_j^* dz \quad (\text{C-22})$$

$$\text{NOPT} = 3: \int_0^{z_e} \frac{d\bar{u}}{dz} Z_p Z_j^* dz \quad (\text{evaluated numerically})$$

$$\text{NOPT} = 4: \int_0^{z_e} \bar{u}(z) Z_p' Z_j^* dz \quad (\text{evaluated numerically})$$

The last two integrals, which involve the mean flow Mach number, are evaluated by means of Simpson's Rule. A FORTRAN listing of AXIAL1 is provided at the end of this appendix.

#### Complex Nonlinear Coefficients.

The complex nonlinear coefficients are calculated from Eqs. (C-5) through (C-8) and are stored in the complex arrays, CD1(NJ, NP, NQ), CD2(NJ, NP, NQ), CD3(NJ, NP, NQ), and CD4(NJ, NP, NQ).

In order to calculate these coefficients, the various integrals of axial, azimuthal, and radial eigenfunctions must be evaluated. Since many of the azimuthal integrals are zero they are evaluated first, and the remaining integrals are computed only if the corresponding azimuthal integral is nonzero. The subroutines used to calculate these integrals are described in the following paragraphs.

Azimuthal Integrals. The azimuthal integrals are calculated by Subroutine AZIMPL according to the value of NOPT as follows:

$$\text{NOPT} = 1: \int_0^{2\pi} \Theta_p \Theta_q \Theta_j^* d\theta$$

$$\text{NOPT} = 2 : \int_0^{2\pi} \Theta_p \Theta_q \Theta_j d\theta$$

These integrals are easily evaluated analytically; for most values of  $p$ ,  $q$ , and  $j$  they are zero. The nonzero integrals are readily expressed in terms of the following integrals:

$$\int_0^{2\pi} \cos(m_p \theta) \cos(m_q \theta) \cos(m_j \theta) d\theta = \pi/2 \quad \text{for } m_j = m_p + m_q,$$

$$m_p = m_j + m_q, \text{ or}$$

$$m_q = m_j + m_p \quad (\text{C-23})$$

$$\int_0^{2\pi} \cos(m_p \theta) \sin(m_q \theta) \sin(m_j \theta) d\theta = \pi/2 \quad \text{for } m_q = m_p + m_j \text{ or}$$

$$m_j = m_p + m_q \quad (\text{C-24})$$

$$\int_0^{2\pi} \cos(m_p \theta) \sin(m_q \theta) \sin(m_j \theta) d\theta = -\pi/2 \quad \text{for } m_p = m_q + m_j \quad (\text{C-25})$$

where  $m_p$ ,  $m_q$ , and  $m_j$  are nonzero. If any one of the tangential mode numbers is zero (corresponding to a radial mode) the following values are obtained:

$$\int_0^{2\pi} \cos(m_p \theta) \cos(m_q \theta) \cos(m_j \theta) d\theta = 2\pi \quad m_p = m_q = m_j = 0$$

$$= \pi \quad m_p = 0, m_q = m_j;$$

$$m_q = 0, m_p = m_j;$$

$$m_j = 0, m_p = m_q \quad (\text{C-26})$$



$$\int_0^{2\pi} \cos(m_p \theta) \sin(m_q \theta) \sin(m_j \theta) d\theta = \pi \quad m_p = 0, m_q = m_j \quad (C-27)$$

Subroutine AZIMTL consists of two sections. In the first section the azimuthal integral is expressed as the product of a constant factor and one of the basic forms given in Eqs. (C-23) and (C-24). The second section is essentially a series of logical tests to determine if the mode numbers,  $m_p$ ,  $m_q$ , and  $m_j$  satisfy any of the conditions for Eqs. (C-23) through (C-27). If any of these conditions is satisfied the appropriate value is multiplied by the corresponding factor determined in the first section and the product is assigned to the output variable (i.e., RESULT), otherwise the value zero is assigned.

Radial Integrals. Subroutine RADIAL calculates the radial integrals which appear in Eqs. (C-5) through (C-8) according to NOPT as follows:

$$\begin{aligned} \text{NOPT} = 1 : & \int_0^1 R_p R_q R_j r dr \\ \text{NOPT} = 2 : & \int_0^1 R_p R_q R_j \frac{1}{r} dr \\ \text{NOPT} = 3 : & \int_0^1 R_p' R_q' R_j' r dr \end{aligned}$$

where the R's are the Bessel functions,  $J_m(S_{mn} r)$ . These integrals are computed numerically using Simpson's Rule with 100 subdivisions. In calculating the integrands the derivatives of the Bessel functions are given by:

$$\begin{aligned} J_m'(S_{mn} r) &= \frac{1}{2} [J_{m-1}(S_{mn} r) - J_{m+1}(S_{mn} r)] \quad \text{for } m = 1, 2, 3, \dots \\ J_0'(S_{mn} r) &= -J_1(S_{mn} r) \end{aligned} \quad (C-28)$$

The integrand of the second integral (NOPT = 2) is indeterminate at the lower limit of integration. However a limit exists, denoted by L, which vanishes with the following exceptions:

$$\begin{aligned}
 L &= S_{mn}(p)/2 \quad \text{for} \quad m_p = 1, m_q = m_j = 0 \\
 L &= S_{mn}(q)/2 \quad \text{for} \quad m_q = 1, m_p = m_j = 0 \\
 L &= S_{mn}(j)/2 \quad \text{for} \quad m_j = 1, m_p = m_q = 0
 \end{aligned}
 \tag{C-29}$$

All of the calculations in Subroutine RADIAL are carried out in double precision arithmetic. The results are given as a single precision number.

Subroutine JBES computes the double precision Bessel functions which are needed for the above calculations. A description of this subroutine and a program listing are given in Chapter 23 of Ref. (18).

Axial Integrals. The integrals of the products of three axial eigenfunctions (see Eqs. (C-5) through (C-8)) are computed by Subroutine AXIAL2 according to the input parameters NOPT and NCONJ. The three basic forms are specified by NOPT as follows:

$$\begin{aligned}
 \text{NOPT} = 1 : & \int_0^z e^{z} Z_p Z_q Z_j^* dz \\
 \text{NOPT} = 2 : & \int_0^z e^{z} Z_p' Z_q' Z_j^* dz \\
 \text{NOPT} = 3 : & \int_0^z e^{z} Z_p'' Z_q'' Z_j^* dz
 \end{aligned}$$

When NCONJ = 1 these basic forms are calculated; these are the forms appearing in the expression for  $D_1(j, p, q)$  (see Eq. (C-5)). For NCONJ = 2 the second function in the integrand is replaced by its complex conjugate to obtain the

integrals appearing in the expression for  $D_2(j,p,q)$ . The integrals appearing in the expressions for  $D_3(j,p,q)$  and  $D_4(j,p,q)$  are obtained by setting  $NCONJ = 3$  and  $NCONJ = 4$  respectively.

The basic forms are calculated from the following analytical formulas:

$$\int_0^z e^{Z_p Z_q Z_j^*} dz = \frac{1}{4} \left\{ \frac{\sinh[i(b_p + b_q + b_j^*)z_e]}{i(b_p + b_q + b_j^*)} + \frac{\sinh[i(b_p + b_q - b_j^*)z_e]}{i(b_p + b_q - b_j^*)} + \frac{\sinh[i(b_p - b_q + b_j^*)z_e]}{i(b_p - b_q + b_j^*)} + \frac{\sinh[i(b_p - b_q - b_j^*)z_e]}{i(b_p - b_q - b_j^*)} \right\} \quad (C-30)$$

$$\int_0^z e^{Z_p' Z_q' Z_j^*} dz = -\frac{1}{4} b_p b_q \left\{ \frac{\sinh[i(b_p + b_q + b_j^*)z_e]}{i(b_p + b_q + b_j^*)} + \frac{\sinh[i(b_p + b_q - b_j^*)z_e]}{i(b_p + b_q - b_j^*)} - \frac{\sinh[i(b_p - b_q + b_j^*)z_e]}{i(b_p - b_q + b_j^*)} - \frac{\sinh[i(b_p - b_q - b_j^*)z_e]}{i(b_p - b_q - b_j^*)} \right\} \quad (C-31)$$

$$\int_0^z e^{Z_p'' Z_q Z_j^*} dz = -b_p^2 \int_0^z e^{Z_p Z_q Z_j^*} dz \quad (C-32)$$

The remaining forms are obtained from Eqs. (C-30) through (C-32) by replacing the appropriate eigenvalues with their complex conjugates; thus, for NOPT = 2  $b_q$  is replaced by  $b_q^*$ , for NOPT = 3  $b_p$  is replaced with  $b_p^*$ , and both  $b_p$  and  $b_q$  are replaced by their conjugates for NOPT = 4.

FORTTRAN listings for Subroutines AZIMTL, RADIAL, and AXIAL2 are given at the end of this appendix.

#### Coefficients for Equivalent Real System.

Equations (12) are a system of complex differential equations to be solved for the unknown complex amplitude functions,  $A_p(t)$ . In order to solve these equations numerically they must first be separated into their real and imaginary parts. This is done by assuming that  $A_p(t) = F_p(t) + iG_p(t)$ , substituting into Eqs. (12), and separating real and imaginary parts to obtain an equivalent system of real differential equations that describe the behavior of the  $F_p$ 's and  $G_p$ 's. Since these equations contain twice as many unknown functions (i.e.,  $F_p(t)$  and  $G_p(t)$ ) as Eqs. (12), it is convenient to re-index the unknown functions and their coefficients as follows:

$$\begin{aligned} F_p(t) &= B_{2p-1}(t) \\ G_p(t) &= B_{2p}(t) \end{aligned} \tag{C-33}$$

Thus the B's with odd indices correspond to the real parts,  $F_p(t)$ , and the B's with even indices correspond to the imaginary parts,  $G_p(t)$ . The corresponding set of differential equations is given by:

$$\sum_{p=1}^{2N} \left\{ c_0'(j,p) \frac{d^2 B_p}{dt^2} + c_1'(j,p) B_p(t) + [c_2'(j,p) - nc_3'(j,p)] \frac{dB_p}{dt} + \right.$$

$$+ nC'_3(j,p) \frac{d[B_p(t-\bar{\tau})]}{dt} \} + \sum_{p=1}^{2N} \sum_{q=1}^{2N} \left\{ D'(j,p,q) B_p \frac{dB_q}{dt} \right\} = 0$$

$$j = 1, 2, 3, \dots, 2N \quad (C-34)$$

The real coefficients in Eqs. (C-34) (i.e.,  $C'_0, C'_1, C'_2, C'_3$ , and  $D'$ ) are related to the complex coefficients in Eqs. (12) (i.e.,  $C_0, \dots, C_3, D_1, \dots, D_4$ ) as follows:

$$\begin{aligned} C'_k(2j-1, 2p-1) &= \text{Re} [C_k(j,p)] \\ C'_k(2j-1, 2p) &= -\text{Im} [C_k(j,p)] \\ C'_k(2j, 2p-1) &= \text{Im} [C_k(j,p)] \\ C'_k(2j, 2p) &= \text{Re} [C_k(j,p)] \end{aligned} \quad (C-35)$$

for  $k = 0, 1, 2, 3$ ,  $j = 1, 2, \dots, N$ ,  $p = 1, 2, \dots, N$  and:

$$\begin{aligned} D'(2j-1, 2p-1, 2q-1) &= \text{Re} [D_1(j,p,q) + D_2(j,p,q) + D_3(j,p,q) + D_4(j,p,q)] \\ D'(2j-1, 2p-1, 2q) &= \text{Im} [-D_1(j,p,q) + D_2(j,p,q) - D_3(j,p,q) + D_4(j,p,q)] \\ D'(2j-1, 2p, 2q-1) &= \text{Im} [-D_1(j,p,q) - D_2(j,p,q) + D_3(j,p,q) + D_4(j,p,q)] \\ D'(2j-1, 2p, 2q) &= \text{Re} [-D_1(j,p,q) + D_2(j,p,q) + D_3(j,p,q) - D_4(j,p,q)] \end{aligned} \quad (C-36)$$

$$D'(2j, 2p-1, 2q-1) = \text{Im} \left[ D_1(j, p, q) + D_2(j, p, q) + D_3(j, p, q) + D_4(j, p, q) \right]$$

$$D'(2j, 2p-1, 2q) = \text{Re} \left[ D_1(j, p, q) - D_2(j, p, q) + D_3(j, p, q) - D_4(j, p, q) \right]$$

$$D'(2j, 2p, 2q-1) = \text{Re} \left[ D_1(j, p, q) + D_2(j, p, q) - D_3(j, p, q) - D_4(j, p, q) \right]$$

$$D'(2j, 2p, 2q) = \text{Im} \left[ -D_1(j, p, q) + D_2(j, p, q) + D_3(j, p, q) - D_4(j, p, q) \right]$$

for  $j = 1, 2, \dots, N$ ,  $p = 1, 2, \dots, N$ ,  $q = 1, 2, \dots, N$ . The linear coefficients are stored in the arrays  $Cl(NJ, NP)$  for  $k = 0$  and  $C(KC, NJ, NP)$  for  $k = 1, 2, 3$ . The nonlinear coefficients are stored in the array  $D(NJ, NP, NQ)$ .

In general Eqs. (C-34) are coupled in the second derivatives; that is, they are of the form:

$$\sum_{p=1}^{2N} \left\{ C'_0(j, p) \frac{d^2 B_p}{dt^2} \right\} = g_j(B_1, B_2, \dots, B_{2N}) \quad (C-37)$$

where there are two or more  $C'_0$  terms in each equation. This coupling results from the non-orthogonality of the axial eigenfunctions. In order to numerically integrate Eqs. (C-34), they must be decoupled by transforming to the form:

$$\frac{d^2 B_j}{dt^2} = f_j(B_1, B_2, \dots, B_{2N}) \quad (C-38)$$

in which only one second derivative appears in each equation. Using Eq. (C-38), it is seen that Eq. (C-37) can be expressed as

$$C'_0 f = g \quad (C-39)$$

where  $C'_0$  is the  $2N \times 2N$  matrix of coefficients of the coupled system,  $f$  is

the column matrix corresponding to the right-hand-side of the decoupled system, and  $g$  is the column matrix corresponding to the right-hand-side of the coupled system. To decouple Eqs. (C-37), therefore, Eq. (C-39) is solved for  $f$ , thus:

$$f = C_0^{-1}g \quad (C-40)$$

where  $C_0^{-1}$  is the inverse of the matrix  $C_0'$ . Performing these operations and equating the coefficients of like terms in  $f$  and  $C_0^{-1}g$  gives the following relations:

$$\begin{aligned} \tilde{C}_i(j,p) &= \sum_{k=1}^{2N} C_0^{-1}(j,k)C_i'(k,p) \quad i = 1,2,3 \\ \tilde{D}(j,p,q) &= \sum_{k=1}^{2N} C_0^{-1}(j,k)D'(k,p,q) \end{aligned} \quad (C-41)$$

where  $\tilde{C}_i$  and  $\tilde{D}$  are the corresponding coefficients of the decoupled system. The matrix inverse,  $C_0^{-1}$ , is computed by the subroutine GJR, which is a standard Univac 1108 library program, and is stored in the array C1(NJ, NP). A listing of GJR and instructions for its use are given in Ref. (19).

The calculation of  $\tilde{C}_i(j,p)$  and  $\tilde{D}(j,p,q)$ , which are the coefficients for the equivalent set of real, decoupled equations, is the final step in the computations performed by COEFFS3D. The coefficients are stored in the arrays C(KC, NJ, NP) and D(NJ, NP, NQ), replacing those computed from Eqs. (C-35) and (C-36). The output of these coefficients is described below.

#### Output

According to the value of the control number NOUT, the coefficients calculated by Program COEFFS3D are printed, punched onto cards, or stored on drum (FASTRAND). These three output modes will now be discussed individually.

Printed Output. Since the printed output cannot be used as input to

Program LCYC3D, the option "printed output only" (NOUT = 0) is only used for checkout purposes. Printed output can also be obtained in conjunction with the drum storage mode (NOUT = 1). Since the printed output format can only accommodate five series terms (complex), it should only be used for NJMAX  $\leq$  5.

The first page of printed output gives a restatement of the input parameters. This page is headed by the title of the case (TITLE) which is followed by the ratio of specific heats (GAMMA), the steady state Mach number at the nozzle entrance (UE), the length-to-diameter ratio (L/D), and the length of the combustion zone as a fraction of the chamber length (ZCOMB). After statements concerning the presence or absence of the liquid droplet momentum source and the type of nozzle considered, a restatement of the input parameters J, L(J), M(J), N(J), NS(J), and NAME(J) which describe the terms in the series expansion of  $\Phi$  is given. This tabulation also includes additional parameters needed by Program LCYC3D:  $S_{mn}$ , the dimensionless frequency of the mode (SMN);  $J_m(S_{mn})$ , the associated value of the Bessel function (JM(SMN)); the real part (EPS) and the imaginary part (ETA) of the axial acoustic eigenvalue; and the real part (YR) and imaginary part (YI) of the nozzle admittance.

The next three pages give the decoupled linear coefficients,  $\tilde{C}_1(j,p)$ ,  $\tilde{C}_2(j,p)$ , and  $\tilde{C}_3(j,p)$ . These coefficients are presented in the matrix format with the rows corresponding to the index j and the columns corresponding to the index p. The remaining pages give the decoupled nonlinear coefficients  $\tilde{D}(j,p,q)$  for each value of j. Here the rows correspond to the index p and the columns correspond to the index q.

A sample printed output for the five term series used in the sample input is given in Tables (C-2) through (C-4).

Drum Storage. When available drum storage, such as the FASTRAND system used with the Univac 1108, is the most convenient means of storing the output of Program COEFFS3D. In the absence of such a system, the program can be easily modified to store the coefficients on magnetic tape. In either case magnetic tape can be used as a back-up file or for permanent storage of the data. The control statements needed to execute these procedures depend upon the computer facilities being used and cannot be described in



Table C-2. Sample Printed Output, Page 1.

## IT,2T,1R SPINNING.

GAMMA = 1.20    UE = .20    L/D = .50000    ZCOMB = 1.00

## DROPLET MOMENTUM SOURCE NEGLECTED

NAME	J	L	M	N	NS	SMN	JM(SMN)	EPS	ETA	YR	YI
A011	1	0	1	1	1	1.84118	.58187	.08122	.19451	.01414	.01414
B011	2	0	1	1	2	1.84118	.58187	.08122	.19451	.01414	.01414
A021	3	0	2	1	1	3.05424	.48650	.10617	.25115	.01414	.01414
B021	4	0	2	1	2	3.05424	.48650	.10617	.25115	.01414	.01414
B001	5	0	0	1	2	3.83171	-.40276	.11993	.28170	.01414	.01414

Table C-3. Sample Printed Output, Page 2.

DECOUPLED COEFFICIENT OF B(P):		C(1,J,P)									
J	P	1	2	3	4	5	6	7	8	9	10
1	3.390599	.000000	.000000	.000000	.000000	.000000	.000000	.000000	.000000	.000000	.000000
2	-.000000	3.390599	.000000	.000000	.000000	.000000	.000000	.000000	.000000	.000000	.000000
3	.000000	.000000	3.390599	.000000	.000000	.000000	.000000	.000000	.000000	.000000	.000000
4	.000000	.000000	-.000000	3.390599	.000000	.000000	.000000	.000000	.000000	.000000	.000000
5	.000000	.000000	.000000	.000000	9.330212	.000000	.000000	.000000	.000000	.000000	.000000
6	.000000	.000000	.000000	.000000	.000000	9.330212	.000000	.000000	.000000	.000000	.000000
7	.000000	.000000	.000000	.000000	.000000	.000000	9.330212	.000000	.000000	.000000	.000000
8	.000000	.000000	.000000	.000000	.000000	.000000	.000000	9.330212	.000000	.000000	.000000
9	.000000	.000000	.000000	.000000	.000000	.000000	.000000	.000000	14.684905	.000000	.000000
10	.000000	.000000	.000000	.000000	.000000	.000000	.000000	.000000	.000000	14.684905	.000000

Table C-4. Sample Printed Output, Page 5.

DECOUPLED COEFFICIENT OF B(P) \* DB(Q)/DT IN EQUATION FOR B( 1)

P	Q	1	2	3	4	5	6	7	8	9	10
1	.000000	.000000	.000000	.000000	.000000	.000000	.000000	-1.735038	-.015812	-2.338657	-.026798
2	.000000	.000000	.000000	.000000	.000000	.000000	.000000	-.010650	.008834	-.013979	.011946
3	.000000	.000000	.000000	.000000	.000000	1.735038	.015812	.000000	.000000	.000000	.000000
4	.000000	.000000	.000000	.000000	.000000	.010650	-.008834	.000000	.000000	.000000	.000000
5	.000000	.000000	1.497831	.008314	.000000	.000000	.000000	.000000	.000000	.000000	.000000
6	.000000	.000000	.015813	-.007594	.000000	.000000	.000000	.000000	.000000	.000000	.000000
7	-1.497831	-.008314	.000000	.000000	.000000	.000000	.000000	.000000	.000000	.000000	.000000
8	-.015813	.007594	.000000	.000000	.000000	.000000	.000000	.000000	.000000	.000000	.000000
9	-1.962811	-.010896	.000000	.000000	.000000	.000000	.000000	.000000	.000000	.000000	.000000
10	-.024780	.009986	.000000	.000000	.000000	.000000	.000000	.000000	.000000	.000000	.000000

this manual.

Card Output. When a drum or magnetic tape storage is not available, punched card output can be used (NOUT = 3). This method becomes unwieldy, however, when a large number of coefficients is involved since only one coefficient can be punched on a card. The format for both drum and card output is the same and is given below:

<u>Number of Cards</u>	<u>Location</u>	<u>Type</u>	<u>Output Item</u>	<u>Comments</u>
1	1-10	F	GAMMA	Same as for input.
	11-20	F	UE	Same as for input.
	21-30	F	ZE	Dimensionless chamber length, (2L/D).
	31-40	F	ZCOMB	Same as for input.
	41-45	I	NDROPS	Same as for input.
	46-50	I	NJMAX	Number of unknown functions, $B_p(t)$ (see Eq. (C-34)).
NJMAX/2	1-5	I	J	Same as input.
	6-10	I	L(J)	"
	11-15	I	M(J)	"
	16-20	I	N(J)	"
	21-25	I	NS(J)	"
	26-35	F	S(J)	Root of Bessel function, $S_{mn}$ .
	36-45	F	SJ(J)	Associated value of Bessel function, $J_m(S_{mn})$ .
	46-50	A	NAME(J)	Same as input.
NJMAX/2	1-5	I	J	Same as input.
	6-15	F	YR	Real part of nozzle admittance, $Y_r$ .
	16-25	F	YI	Imaginary part of nozzle admittance, $Y_i$ .
	26-35	F	EPS	Real part of axial eigenvalue, $\epsilon$ .
	36-45	F	ETA	Imaginary part of axial eigenvalue, $\eta$ .

<u>Number of Cards</u>	<u>Location</u>	<u>Type</u>	<u>Output Item</u>	<u>Comments</u>
1	1-5	I	KMAX(1)	Number of nonzero linear coefficients of type $\tilde{C}_1(j,p)$ .
KMAX(1)	1-5	I	NJ	Index, j.
	6-10	I	NP	Index, p.
	11-25	F	C(1,NJ,NP)	Linear coefficient, $\tilde{C}_1(j,p)$ .
1	1-5	I	KMAX(2)	Number of nonzero linear coefficients of type $\tilde{C}_2(j,p)$ .
KMAX(2)	1-5	I	NJ	Index, j.
	6-10	I	NP	Index, p.
	11-25	F	C(2,NJ,NP)	Linear coefficient, $\tilde{C}_2(j,p)$ .
1	1-5	I	KMAX(3)	Number of nonzero linear coefficients of type $\tilde{C}_3(j,p)$ .
KMAX(3)	1-5	I	NJ	Index, j.
	6-10	I	NP	Index, p.
	11-25	F	C(3,NJ,NP)	Linear coefficient, $\tilde{C}_3(j,p)$ .
1	1-5	I	KMAX(4)	Number of nonzero nonlinear coefficients.
KMAX(4)	1-5	I	NJ	Index, j.
	6-10	I	NP	Index, p.
	11-15	I	NQ	Index, q.
	16-30	F	D(NJ,NP,NQ)	Nonlinear coefficient, D(j,p,q).

The first card of output gives the chamber parameters  $\gamma$ ,  $\bar{u}_e$ ,  $L/D$ , and  $z_c/z_e$ ; the droplet momentum source control number, NDROPS; and the number of unknown real functions (i.e.,  $B_p(t)$ ), NJMAX. This is followed by NJMAX/2 cards (the number of unknown complex functions,  $A_p(t)$ ) describing the terms included in the series expansion of  $\phi$ . The next NJMAX/2 cards gives the complex nozzle admittance ( $Y_r$  and  $Y_i$ ) and the corresponding complex axial eigenvalue ( $\epsilon$  and  $\eta$ ) for each complex series term. The linear coefficients are given in three sets of cards. The first card in the set gives the number of coefficients of the given type, while the remaining





FORTRAN Listing.

```
C
C
C *****PROGRAM COEFS3D *****
C
C     THIS PROGRAM COMPUTES THE COEFFICIENTS WHICH APPEAR
C     IN THE DIFFERENTIAL EQUATIONS WHICH GOVERN THE MODE-AMPLITUDE
C     FUNCTIONS.  THESE COEFFICIENTS ARE STORED ON DRUM OR
C     PUNCHED ONTO CARDS FOR INPUT INTO PROGRAM LCYC3D.
C
C     THE FOLLOWING INPUTS ARE REQUIRED:
C     THE TITLE OF THE CASE.
C     GAMMA IS THE SPECIFIC HEAT RATIO.
C     UE IS THE STEADY STATE MACH NUMBER AT THE NOZZLE ENTRANCE.
C     RLD IS THE LENGTH-TO-DIAMETER RATIO.
C     ZCOMB IS THE LENGTH OF THE REGION OF UNIFORMLY DISTRIBUTED
C     COMBUSTION, EXPRESSED AS A FRACTION OF THE CHAMBER LENGTH.
C     NDROPS DETERMINES THE PRESENCE OF DROPLET MOMENTUM SOURCES:
C     NDROPS = 0  DROPLET MOMENTUM SOURCE NEGLECTED.
C     NDROPS = 1  DROPLET MOMENTUM SOURCE INCLUDED.
C     NOZZLE SPECIFIES THE TYPE OF NOZZLE USED:
C     NOZZLE = 0  QUASI-STEADY.
C     NOZZLE = 1  CONVENTIONAL NOZZLE.
C     FOR CONVENTIONAL NOZZLE:
C     AMPL IS THE NOZZLE AMPLITUDE RATIO.
C     PHASE IS THE NOZZLE PHASE SHIFT.
C     NJMAX IS THE NUMBER OF MODE-AMPLITUDE FUNCTIONS IN THE ASSUMED
C     SERIES SOLUTION.  NJMAX MUST NOT EXCEED 10.
C     THE COEFFICIENTS COMPUTED ARE DETERMINED BY NONLIN AS FOLLOWS:
C     NONLIN = 0  LINEAR COEFFICIENTS ONLY.
C     NONLIN = 1  BOTH LINEAR AND NONLINEAR COEFFICIENTS.
C     COEFFICIENTS TO BE NEGLECTED ARE DETERMINED BY NEGL
C     AS FOLLOWS:
C     NEGL = 0  TERMS SMALLER THAN 0.00001 ARE NEGLECTED.
C     NEGL = 1  LINEAR TERMS SMALLER THAN SM1 AND NONLINEAR
C              TERMS SMALLER THAN SM2 ARE NEGLECTED.
C     THE OUTPUT IS DETERMINED BY NOUT AS FOLLOWS:
C     NOUT = 0  PRINTED OUTPUT ONLY.
C     NOUT = 1  PRINTED AND STORED ON DRUM (FASTRAND FILE).
C     NOUT = 2  FASTRAND FILE ONLY.
C     NOUT = 3  CARD OUTPUT ONLY.
C     EACH MODE-AMPLITUDE IS ASSIGNED AN INTEGER J.
C     THE MODE IS SPECIFIED BY THE INDICES L(J), M(J), AND N(J).
C     L(J) IS THE AXIAL MODE NUMBER AND MUST NOT EXCEED 10.
C     M(J) IS THE AZIMUTHAL MODE NUMBER AND MUST NOT EXCEED 8.
C     N(J) IS THE RADIAL MODE NUMBER AND MUST NOT EXCEED 5.
C     THE INTEGER NS(J) IS ASSIGNED AS FOLLOWS:
C     NS = 1  A-FUNCTION  SIN(M*THETA) * COSH(I*B*Z)
C     NS = 2  B-FUNCTION  COS(M*THETA) * COSH(I*B*Z)
C     NAME(J) IS A FOUR-CHARACTER NAME.
C
```



C \*\*\*\*\*  
C

DIMENSION L(10), N(10), NAME(10), S(10), SJ(10), TITLE(80),  
1 RJROOT(10,5), RJVAL(10,5), C1(20,20), C(3,20,20),  
2 D(20,20,20), AMPL(10), PHASE(10), AZI(2),  
3 BES1(9,9,9), BES2(9,9,9), BES3(9,9,9),  
4 V(2), JC(20), TS(3,20), TSQ(20), KMAX(4)  
COMPLEX  
1 CRSLT, C1, ZEJ, ZEP1, ZEP2, CZE, CAZ, CRAD,  
2 G1, DCOEF, CGAM, CAX, B(10), BC(10), YNOZ(10),  
3 CNORM(10), CSSQ(10), TANINT(2), RADINT(3),  
4 AXINT(4,3), CC(4,10,10), CD1(10,10,10),  
5 CD2(10,10,10), AX(4), T1, T2, D1, D2, D3, D4,  
6 CD3(10,10,10), CD4(10,10,10)  
COMMON B /ELK2/ M(10), NS(10)

C  
C  
C

DATA INPUT.

PI = 3.1415927  
SM1 = 0.00001  
SM2 = 0.00001  
CI = (0.0,1.0)

C  
C

INPUT ROOTS AND VALUES OF BESSEL FUNCTIONS.

DATA ((RJROOT(I,J), J = 1,5), I = 1,9)/  
1 3.83171, 7.01559, 10.17347, 13.32369, 16.47063,  
2 1.84118, 5.33144, 8.53632, 11.70600, 14.86359,  
3 3.05424, 6.70613, 9.96947, 13.17037, 16.34752,  
4 4.20119, 8.01524, 11.34592, 14.58585, 17.78875,  
5 5.31755, 9.28240, 12.68191, 15.96411, 19.19603,  
6 6.41562, 10.51986, 13.98719, 17.31284, 20.57551,  
7 7.50127, 11.73494, 15.26818, 18.63744, 21.93172,  
8 8.57784, 12.93239, 16.52937, 19.94185, 23.26805,  
9 9.64742, 14.11552, 17.77401, 21.22906, 24.58720/  
DATA ((RJVAL(I,J), J = 1,5), I = 1,9)/  
1 -0.40276, 0.30012, -0.24970, 0.21836, -0.19647,  
2 0.58187, -0.34613, 0.27330, -0.23330, 0.20701,  
3 0.48650, -0.31353, 0.25474, -0.22088, 0.19794,  
4 0.43439, -0.29116, 0.24074, -0.21097, 0.19042,  
5 0.39965, -0.27438, 0.22959, -0.20276, 0.18403,  
6 0.37409, -0.26109, 0.22039, -0.19580, 0.17849,  
7 0.35414, -0.25017, 0.21261, -0.18978, 0.17363,  
8 0.33793, -0.24096, 0.20588, -0.18449, 0.16929,  
9 0.32438, -0.23303, 0.19998, -0.17979, 0.16539/

C  
C

INPUT PARAMETERS.

4 READ (5,5000, END = 600) (TITLE(I), I = 1, 72)  
READ (5,5001) GAMMA, UE, RLD, ZCOMB, NDROPS, NOZZLE  
IF (GAMMA) 600, 600, 8  
8 READ (5,5004) NJMAX, NONLIN, NEGL, NOUT  
IF (NEGL .EQ. 1) READ (5,5005) SM1, SM2

```

C      IF (NOZZLE .EQ. 1) GO TO 5
      COMPUTE ADMITTANCE FOR QUASI-STEADY NOZZLE.
      Y = (GAMMA - 1.0) * UE/(2.0 * GAMMA)
      DO 3 J = 1, NJMAX
        AMPL(J) = Y
        PHASE(J) = 0.0
3     CONTINUE
      GO TO 7
5     DO 6 I = 1, NJMAX
      READ (5,5003) J, AMPL(J), PHASE(J)
6     CONTINUE
7     DO 10 I = 1, NJMAX
      READ (5,5002) J, L(J), M(J), N(J), NS(J), NAME(J)
10    CONTINUE
C
      DO 12 J = 1, NJMAX
        THETA = PHASE(J) * PI/180.0
        YR = AMPL(J) * COS(THETA)
        YI = AMPL(J) * SIN(THETA)
        YNOZ(J) = CMLPX(YR,YI)
12    CONTINUE
C
      ZE = 2.0 * RLD
      CZE = CMLPX(ZE,0.0)
      CGAM = CMLPX(GAMMA,0.0)
      CAX = CGAM
      IF (NDROPS .EQ. 1) CAX = CGAM + (1.0,0.0)
C
C
C
C      *****
      ASSIGN ARRAYS FOR ROOTS OF BESSEL FUNCTIONS.
      DO 20 J = 1, NJMAX
        IF ((M(J) .EQ. 0) .AND. (N(J) .EQ. 0)) GO TO 15
        MM = M(J) + 1
        NN = N(J)
        S(J) = RJROOT(MM,NN)
        SJ(J) = RJVAL(MM,NN)
        GO TO 25
15    S(J) = 0.0
        SJ(J) = 1.0
25    SSQ = S(J) * S(J)
        CSSQ(J) = CMLPX(SSQ,0.0)
20    CONTINUE
C
C
C
C      *****
      CALCULATE AXIAL ACOUSTIC EIGENVALUES.
C
      FIND MAXIMUM VALUES OF L(J), M(J), AND N(J).
      KN = 0

```

```

    LMAX = 0
    MMAX = 0
    NMAX = 0
    DO 30 J = 1, NJMAX
    IF (L(J) .GT. LMAX) LMAX = L(J)
    IF (M(J) .GT. MMAX) MMAX = M(J)
    IF (N(J) .GT. NMAX) NMAX = N(J)
    IF (N(J) .NE. N(1)) KN = 1
30 CONTINUE
    LMAX = LMAX + 1
    MMAX = MMAX + 1
C
C   COMPUTE EIGENVALUES.
    DO 40 J = 1, NJMAX
    LL = L(J)
    SMN = S(J)
    YAMPL = AMPL(J)
    YPHASE = PHASE(J)
    CALL EIGVAL(LL, SMN, GAMMA, ZE, YAMPL, YPHASE, CRSLT)
    B(J) = CRSLT
    BC(J) = CONJG(CRSLT)
40 CONTINUE
C
C   *****
C
C   CALCULATE LINEAR COEFFICIENTS.
    DO 100 NJ = 1, NJMAX
    DO 100 NP = 1, NJMAX
C
C   ZERO COEFFICIENT ARRAYS.
    DO 105 KC = 1, 4
    CC(KC, NJ, NP) = (0.0, 0.0)
105 CONTINUE
C
C   ORTHOGONALITY PROPERTY OF TANGENTIAL EIGENFUNCTIONS.
    IF ( NS(NP) .NE. NS(NJ) ) GO TO 100
    IF ( M(NP) .NE. M(NJ) ) GO TO 100
    IF ( M(NJ) .EQ. 0 ) GO TO 112
    AZ = PI
    GO TO 120
112 IF ( NS(NJ) .EQ. 1 ) GO TO 100
    AZ = 2.0 * PI
C
C   ORTHOGONALITY PROPERTY OF RADIAL EIGENFUNCTIONS.
120 IF ( N(NP) .NE. N(NJ) ) GO TO 100
    IF ( S(NP) ) 125, 122, 125
125 SGM = M(NJ) * M(NJ)
    SSQ = S(NP) * S(NP)
    SJSQ = SJ(NJ) * SJ(NJ)

```

```

RAD = (SSQ - SQM) * SJSQ/(2.0 * SSQ)
GO TO 127
122 RAD = 0.5
C
C   CALCULATE AXIAL INTEGRALS.
127 DO 130 NOPT = 1, 4
    CALL AXIAL1(NOPT, NP, NJ, UE, ZE, ZCOMB, CRSLT)
    AX(NOPT) = CRSLT
130 CONTINUE
C
C   EVALUATE FUNCTIONS AT NOZZLE END.
ZEJ = CCOSH(CI*BC(NJ)*CZE)
ZEP1 = CCOSH(CI*B(NP)*CZE)
ZEP2 = CI * B(NP) * CSINH(CI*B(NP)*CZE)
C
CAZ = CMPLX(AZ, 0.0)
CRAD = CMPLX(RAD, 0.0)
C
C   COEFFICIENT OF THE SECOND DERIVATIVE OF A(P).
CC(1, NJ, NP) = AX(1) * CAZ * CRAD
C
C   COEFFICIENT OF A(P).
CC(2, NJ, NP) = (CSSQ(NP)*AX(1) - AX(2) + ZEP2*ZEJ) * CAZ * CRAD
C
C   COEFFICIENT OF THE FIRST DERIVATIVE OF A(P).
CC(3, NJ, NP) = (CAX*AX(3) + (2.0, 0.0)*AX(4)
1          + CGAM*YNOZ(NP)*ZEP1*ZEJ) * CAZ * CRAD
C
C   COEFFICIENT OF THE RETARDED DERIVATIVE OF A(P).
CC(4, NJ, NP) = CGAM * AX(3) * CAZ * CRAD
C
100 CONTINUE
C
C   NORMALIZE LINEAR COEFFICIENTS.
DO 140 NJ = 1, NJMAX
    CNORM(NJ) = CC(1, NJ, NJ)
    DO 140 NP = 1, NJMAX
        DO 140 KC = 1, 4
            CC(KC, NJ, NP) = CC(KC, NJ, NP)/CNORM(NJ)
140 CONTINUE
C
C   *****
C
C   COMPUTE NONLINEAR COEFFICIENTS.
C
IF (NONLIN .EQ. 0) GO TO 402
G1 = (CGAM - (1.0, 0.0)) * (0.5, 0.0)
C
C   COMPUTATIONS OF BESSEL INTEGRALS WHEN ALL SERIES TERMS HAVE THE
C   SAME RADIAL MODE NUMBER N(J).

```

```

IF (KN .EQ. 1) GO TO 170
DO 150 MP = 1, MMAX
DO 150 MQ = 1, MMAX
DO 150 MJ = 1, MMAX
BES1(MP,MQ,MJ) = 0.0
BES2(MP,MQ,MJ) = 0.0
BES3(MP,MQ,MJ) = 0.0
L1 = MP - 1
L2 = MQ - 1
L3 = MJ - 1
LM = L1 + L2
LN = L1 + L3
MN = L2 + L3
IF ((L3.EQ.LM) .OR. (L2.EQ.LN) .OR. (L1.EQ.MN)) GO TO 160
GO TO 150
160 IF (NMAX .EQ. 0) GO TO 165
A1 = RJROOT(MP,NMAX)
A2 = RJROOT(MQ,NMAX)
A3 = RJROOT(MJ,NMAX)
GO TO 167
165 A1 = 0.0
A2 = 0.0
A3 = 0.0
167 CALL RADIAL(1,L1,L2,L3,A1,A2,A3,RESULT)
BES1(MP,MQ,MJ) = RESULT
CALL RADIAL(2,L1,L2,L3,A1,A2,A3,RESULT)
BES2(MP,MQ,MJ) = RESULT
CALL RADIAL(3,L1,L2,L3,A1,A2,A3,RESULT)
BES3(MP,MQ,MJ) = RESULT
150 CONTINUE
C
170 DO 200 NJ = 1, NJMAX
DO 200 NP = 1, NJMAX
DO 200 NQ = 1, NJMAX
C
CD1(NJ,NP,NQ) = (0.0,0.0)
CD2(NJ,NP,NQ) = (0.0,0.0)
C
DO 210 J = 1, 2
CALL AZIMTL(J,NP,NQ,NJ,RESULT)
AZI(J) = RESULT
TANINT(J) = CMPLX(RESULT,0.0)
210 CONTINUE
C
IF (AZI(1)) 220, 225, 220
225 IF (AZI(2)) 220, 200, 220
C
220 IF (KN .EQ. 0) GO TO 222
L1 = M(NP)
L2 = M(NQ)

```

```

L3 = M(NJ)
A1 = S(NP)
A2 = S(NQ)
A3 = S(NJ)
GO TO 244
C
222 MP = M(NP) + 1
MQ = M(NQ) + 1
MJ = M(NJ) + 1
RADINT(1) = CMPLX(BES1(MP,MQ,MJ),0.0)
RADINT(2) = CMPLX(BES2(MP,MQ,MJ),0.0)
RADINT(3) = CMPLX(BES3(MP,MQ,MJ),0.0)
C
244 DO 240 J = 1, 3
IF (KN .EQ. 0) GO TO 242
CALL RADIAL (J,L1,L2,L3,A1,A2,A3,RESULT)
RADINT(J) = CMPLX(RESULT,0.0)
242 DO 240 NC = 1,4
CALL AXIAL2(J,NC,NP,NQ,NJ,ZE,CRSLT)
AXINT(NC,J) = CRSLT
240 CONTINUE
C
C
DO 250 J = 1,4
T1 = G1 * CSSQ(NP) * AXINT(J,1)
T2 = G1 * AXINT(J,3)
D1 = AXINT(J,1) * TANINT(1) * RADINT(3)
D2 = AXINT(J,1) * TANINT(2) * RADINT(2)
D3 = AXINT(J,2) * TANINT(1) * RADINT(1)
D4 = (T2 - T1) * TANINT(1) * RADINT(1)
DCOEF = (0.5,0.0) * (D1 + D2 + D3 + D4)/CNORM(NJ)
IF (J .EQ. 1) CD1(NJ,NP,NQ) = (1.0,-1.0) * DCOEF
IF (J .EQ. 2) CD2(NJ,NP,NQ) = (1.0,1.0) * DCOEF
IF (J .EQ. 3) CD3(NJ,NP,NQ) = (1.0,1.0) * DCOEF
IF (J .EQ. 4) CD4(NJ,NP,NQ) = (1.0,-1.0) * DCOEF
250 CONTINUE
200 CONTINUE
C
C
*****
C
CALCULATE COEFFICIENTS FOR EQUIVALENT REAL SYSTEM.
C
402 DO 350 NJ = 1, NJMAX
NEWJ = (2 * NJ) - 1
NEWJ1 = NEWJ + 1
DO 350 NP = 1, NJMAX
NEWP = (2 * NP) - 1
NEWP1 = NEWP + 1
C
C
COEFFICIENTS OF LINEAR TERMS.

```

```

CCR = REAL(CC(1,NJ,NP))
CCI = AIMAG(CC(1,NJ,NP))
C1(NEWJ,NEWP) = CCR
C1(NEWJ,NEWP1) = -CCI
C1(NEWJ1,NEWP) = CCI
C1(NEWJ1,NEWP1) = CCR
DO 360 KC = 1,3
CCR = REAL(CC(KC+1,NJ,NP))
CCI = AIMAG(CC(KC+1,NJ,NP))
C(KC,NEWJ,NEWP) = CCR
C(KC,NEWJ,NEWP1) = -CCI
C(KC,NEWJ1,NEWP) = CCI
C(KC,NEWJ1,NEWP1) = CCR

```

360 CONTINUE

C  
C

COEFFICIENTS OF NONLINEAR TERMS.

IF (NONLIN .EQ. 0) GO TO 350

DO 370 NQ = 1, NJMAX

NEWQ = (2 \* NQ) - 1

NEWQ1 = NEWQ + 1

CD1R = REAL(CD1(NJ,NP,NQ))

CD1I = AIMAG(CD1(NJ,NP,NQ))

CD2R = REAL(CD2(NJ,NP,NQ))

CD2I = AIMAG(CD2(NJ,NP,NQ))

CD3R = REAL(CD3(NJ,NP,NQ))

CD3I = AIMAG(CD3(NJ,NP,NQ))

CD4R = REAL(CD4(NJ,NP,NQ))

CD4I = AIMAG(CD4(NJ,NP,NQ))

D(NEWJ,NEWP,NEWQ) = CD1R + CD2R + CD3R + CD4R

D(NEWJ,NEWP,NEWQ1) = -CD1I + CD2I - CD3I + CD4I

D(NEWJ,NEWP1,NEWQ) = -CD1I - CD2I + CD3I + CD4I

D(NEWJ,NEWP1,NEWQ1) = -CD1R + CD2R + CD3R - CD4R

D(NEWJ1,NEWP,NEWQ) = CD1I + CD2I + CD3I + CD4I

D(NEWJ1,NEWP,NEWQ1) = CD1R - CD2R + CD3R - CD4R

D(NEWJ1,NEWP1,NEWQ) = CD1R + CD2R - CD3R - CD4R

D(NEWJ1,NEWP1,NEWQ1) = -CD1I + CD2I + CD3I - CD4I

370 CONTINUE

350 CONTINUE

C  
C  
C  
C  
C  
C

\*\*\*\*\*

COMPUTE COEFFICIENTS FOR THE EQUATIONS WHICH ARE DECOUPLED  
IN THE SECOND DERIVATIVES.

DO 405 KC = 1, 4

KMAX(KC) = 0

405 CONTINUE

C  
C

CALCULATE INVERSE OF THE MATRIX C1(I,J).  
JMAX = NJMAX

```

      NJMAX = 2 * NJMAX
C
C
      V(1) = 1
      CALL GJR(C1,20,20,NJMAX,0,$500,JC,V)
C
C      USE INVERSE TO CALCULATE DECOUPLED COEFFICIENTS.
C
      DO 410 NP = 1, NJMAX
C
C      LINEAR COEFFICIENTS.
      DO 420 NJ = 1, NJMAX
      DO 420 KC = 1, 3
      TS(KC,NJ) = 0.0
      DO 420 K = 1, NJMAX
      TS(KC,NJ) = TS(KC,NJ) + C1(NJ,K) * C(KC,K,NP)
420 CONTINUE
      DO 430 NJ = 1, NJMAX
      DO 430 KC = 1, 3
      C(KC,NJ,NP) = TS(KC,NJ)
      ABSVAL = ABS(C(KC,NJ,NP))
      IF (ABSVAL .GE. SM1) KMAX(KC) = KMAX(KC) + 1
430 CONTINUE
C
C      NONLINEAR COEFFICIENTS.
      IF (NONLIN .EQ. 0) GO TO 410
      DO 415 NQ = 1, NJMAX
      DO 440 NJ = 1, NJMAX
      TSQ(NJ) = 0.0
      DO 440 K = 1, NJMAX
      TSQ(NJ) = TSQ(NJ) + C1(NJ,K) * D(K,NP,NQ)
440 CONTINUE
      DO 445 NJ = 1, NJMAX
      D(NJ,NP,NQ) = TSQ(NJ)
      ABSVAL = ABS(D(NJ,NP,NQ))
      IF (ABSVAL .GE. SM2) KMAX(4) = KMAX(4) + 1
445 CONTINUE
415 CONTINUE
C
410 CONTINUE
C
C      *****
C      OUTPUT.
C
      IF (NOUT .GE. 2) GO TO 455
C
C      PRINTED OUTPUT.
      WRITE (6,6001) (TITLE(I), I = 1, 72)
      WRITE (6,6002) GAMMA, UE, RLD, ZCOMB
      IF (NDROPS .EQ. 0) WRITE (6,6020)

```



```

        IF (NDROPS .EQ. 1) WRITE (6,6021)
        IF (NOZZLE .EQ. 0) WRITE (6,6012)
        WRITE (6,6004)
        DO 310 J = 1, JMAX
        WRITE (6,6003) NAME(J), J, L(J), M(J), N(J), NS(J),
1          S(J), SJ(J), B(J), YNOZ(J)
310 CONTINUE
        IF (NONLIN .EQ. 0) WRITE (6,6013)

C
C   OUTPUT OF LINEAR COEFFICIENTS.
        DO 320 KC = 1, 3
        IF (KC .EQ. 1) WRITE (6,6005)
        IF (KC .EQ. 2) WRITE (6,6006)
        IF (KC .EQ. 3) WRITE (6,6007)
        WRITE (6,6008) (J, J = 1, NJMAX)
        WRITE (6,6014)
        DO 320 NJ = 1, NJMAX
        WRITE (6,6009) NJ, (C(KC,NJ,NP), NP = 1, NJMAX)
320 CONTINUE

C
C   OUTPUT OF NONLINEAR COEFFICIENTS.
        IF (NONLIN .EQ. 0) GO TO 452
        DO 400 NJ = 1, NJMAX
        WRITE (6,6010) NJ
        WRITE (6,6011) (J, J = 1, NJMAX)
        WRITE (6,6015)
        DO 400 NP = 1, NJMAX
        WRITE (6,6009) NP, (D(NJ,NP,NQ), NQ = 1, NJMAX)
400 CONTINUE
452 IF (NOUT .EQ. 0) GO TO 4

C
455 IF (NOUT .EQ. 3) GO TO 480

C
C   WRITE COEFFICIENTS ON FASTRAND FILE.
C
        WRITE (9,7001) GAMMA, UE, ZE, ZCOMB, NDROPS, NJMAX

C
        DO 450 J = 1, JMAX
        WRITE (9,7002) J, L(J), M(J), N(J), NS(J), S(J), SJ(J),
1          NAME(J)
450 CONTINUE

C
        DO 457 J = 1, JMAX
        WRITE (9,7006) J, YNOZ(J), B(J)
457 CONTINUE

C
        DO 460 KC = 1, 3
        WRITE (9,7003) KMAX(KC)
        DO 460 NJ = 1, NJMAX
        DO 460 NP = 1, NJMAX

```

```

      ABSVAL = ABS(C(KC,NJ,NP))
      IF (ABSVAL .GE. SM1) WRITE (9,7004) NJ, NP, C(KC,NJ,NP)
460 CONTINUE
C
      WRITE (9,7003) KMAX(4)
      IF (NONLIN .EQ. 0) GO TO 4
      DO 470 NJ = 1, NJMAX
      DO 470 NP = 1, NJMAX
      DO 470 NQ = 1, NJMAX
      ABSVAL = ABS(D(NJ,NP,NQ))
      IF (ABSVAL .GE. SM2) WRITE (9,7005) NJ, NP, NQ, D(NJ,NP,NQ)
470 CONTINUE
      GO TO 4
C
C      PUNCHED CARD OUTPUT.
C
480 PUNCH 7001 GAMMA, UE, ZE, ZCOMB, NDROPS, NJMAX
C
      DO 482 J = 1, JMAX
      PUNCH 7002 J, L(J), M(J), N(J), NS(J), S(J), SJ(J),
1      NAME(J)
482 CONTINUE
C
      DO 484 J = 1, JMAX
      PUNCH 7006 J, YNOZ(J), B(J)
484 CONTINUE
C
      DO 486 KC = 1, 3
      PUNCH 7003 KMAX(KC)
      DO 486 NJ = 1, NJMAX
      DO 486 NP = 1, NJMAX
      ABSVAL = ABS(C(KC,NJ,NP))
      IF (ABSVAL .GE. SM1) PUNCH 7004 NJ, NP, C(KC,NJ,NP)
486 CONTINUE
C
      PUNCH 7003 KMAX(4)
      IF (NONLIN .EQ. 0) GO TO 4
      DO 488 NJ = 1, NJMAX
      DO 488 NP = 1, NJMAX
      DO 488 NQ = 1, NJMAX
      ABSVAL = ABS(D(NJ,NP,NQ))
      IF (ABSVAL .GE. SM2) PUNCH 7005 NJ, NP, NQ, D(NJ,NP,NQ)
488 CONTINUE
      GO TO 4
C
C      ERROR EXIT
C
500 IF (JC(1)) 510, 510, 520
510 JC(1) = ABS(JC(1))
      WRITE (6,6017) JC(1)
      GO TO 4

```

520 WRITE (6,6018) JC(1)  
GO TO 4  
600 CONTINUE

C

C

\*\*\*\*\*

C

C

FORMAT SPECIFICATIONS.

5000 FORMAT (72A1)  
5001 FORMAT (4F10.0,2I5)  
5002 FORMAT (5I5,1X,A4)  
5003 FORMAT (I5,2F10.0)  
5004 FORMAT (4I5)  
5005 FORMAT (2F10.0)  
6001 FORMAT (1H1,1X,72A1//)  
6002 FORMAT (2X,8HGAMMA = ,F5.2,5X,5HUE = ,F5.2,5X,6HL/D = ,F8.5,  
1 5X,8HZCOMB = ,F5.2//)  
6003 FORMAT (2X,A4,5I5,6F10.5//)  
6004 FORMAT (2X///2X,29HNAME J L M N NS,7X,3HSMN,3X,  
1 7HJM(SMN),7X,3HEPS,7X,3HETA,8X,2HYR,8X,2HYI//)  
6005 FORMAT (1H1,45H DECOUPLED COEFFICIENT OF B(P): C(1,J,P)///)  
6006 FORMAT (1H1,44H DECOUPLED COEFFICIENT OF THE DERIVATIVE OF,  
1 6H B(P):,5X,8HC(2,J,P)///)  
6007 FORMAT (1H1,39H DECOUPLED COEFFICIENT OF THE RETARDED,  
1 20H DERIVATIVE OF B(P):,5X,8HC(3,J,P)///)  
6008 FORMAT (7X,1HF,18,9I12)  
6009 FORMAT (2X//2X,I3,3X,10F12.6)  
6010 FORMAT (1H1,42H DECOUPLED COEFFICIENT OF B(P) \* DB(Q)/DT,  
1 19H IN EQUATION FOR B(,12,1H)///)  
6011 FORMAT (7X,1HQ,18,9I12)  
6012 FORMAT (2X,19HQUASI-STEADY NOZZLE//)  
6013 FORMAT (2X//2X,24HLINEAR COEFFICIENTS ONLY)  
6014 FORMAT (4X,1HJ)  
6015 FORMAT (4X,1HF)  
6017 FORMAT (1H1,31H OVERFLOW DETECTED, LAST ROW = ,I5)  
6018 FORMAT (1H1,34H SINGULARITY DETECTED, LAST ROW = ,I5)  
6020 FORMAT (2X,'DROPLET MOMENTUM SOURCE NEGLECTED')  
6021 FORMAT (2X,'DROPLET MOMENTUM SOURCE INCLUDED')  
7001 FORMAT (4F10.5,2I5)  
7002 FORMAT (5I5,2F10.5,1X,A4)  
7003 FORMAT (I5)  
7004 FORMAT (2I5,F15.6)  
7005 FORMAT (3I5,F15.6)  
7006 FORMAT (I5,4F10.5)  
END

```

C      SUBROUTINE EIGVAL(L, SMN, GAMMA, ZE, YAMPL, YPHASE, RESULT)
C
C      COMPLEX    RESULT
C      COMMON  /BLK1/ GSQ, ABSQ, ALBET, SMNSQ
C
C      *****
C      THIS SUBROUTINE COMPUTES THE COMPLEX AXIAL ACOUSTIC EIGENVALUES
C      FOR A CYLINDRICAL CHAMBER WITH A NOZZLE AND STORES THEM IN
C      RESULT.
C      THE EIGENVALUES ARE COMPUTED BY MEANS OF NEWTONS METHOD.
C
C      THE INPUT PARAMETERS ARE AS FOLLOWS:
C      L IS THE AXIAL MODE NUMBER.
C      SMN IS THE DIMENSIONLESS ACOUSTIC FREQUENCY.
C      GAMMA IS THE SPECIFIC HEAT RATIO.
C      ZE IS THE LENGTH-TO-RADIUS RATIO.
C      YAMPL IS THE NOZZLE AMPLITUDE FACTOR.
C      YPHASE IS THE NOZZLE PHASE SHIFT IN DEGREES.
C
C      *****
C
C      PI = 3.1415927
C      ERR = 0.0000001
C
C      IF (YAMPL) 5, 60, 5
C      CALCULATE CONSTANTS.
C      5 PHASE = YPHASE * PI/180.0
C      ALPHA = YAMPL * COS(PHASE)
C      BETA  = YAMPL * SIN(PHASE)
C      GSQ  = GAMMA * GAMMA
C      ABSQ = (ALPHA * ALPHA) - (BETA * BETA)
C      ALBET = ALPHA * BETA
C      SMNSQ = SMN * SMN
C
C      ASSIGN INITIAL GUESS FOR EIGENVALUE.
C      IF (L .EQ. 0) GO TO 45
C      RL = L
C      PHI = PI/2.0 + PHASE
C      XM = RL * PI/ZE
C      A = YAMPL/ZE
C      XO = XM + A*COS(PHI)
C      YO = A*SIN(PHI)
C      GO TO 47
C      45 PHI = PI/4.0 + 0.5*PHASE
C      A = YAMPL * 10.0/ZE
C      XO = A * COS(PHI)
C      YO = A * SIN(PHI)
C
C      ITERATION USING NEWTONS METHOD FOR A SYSTEM OF TWO EQUATIONS

```

```

C      IN TWO UNKNOWN.
47 L1 = 0
   X = X0
   Y = Y0
40 CALL FCNS(X,Y,Z,E,F,G,FX,FY,GX,GY)
   IF (L1 .EQ. 40) GO TO 50
   RJFG = (FX * GY) - (GX * FY)
   IF (RJFG) 20, 30, 20
20 DELTAX = (-F * GY + G * FY)/RJFG
   DELTAY = (-G * FX + F * GX)/RJFG
   L1 = L1 + 1
   X = X + DELTAX
   Y = Y + DELTAY

C
C      TEST FOR CONVERGENCE.
   IF (ABS(DELTAX) .GE. ERR .OR. ABS(DELTAY) .GE. ERR) GO TO 40
   GO TO 10

C
C      WARNING MESSAGES
30 WRITE (6,6005)
   GO TO 10
50 WRITE (6,6006)
   GO TO 10

C
C      CASE OF HARD WALL (YAMPL = 0).
60 RL = L
   X = RL * PI/ZE
   Y = 0.0

C
10 RESULT = CPLX(X,Y)

C
C      FORMAT SPECIFICATIONS.
6005 FORMAT (2X//2X,16HJACOBIAN IS ZERO//)
6006 FORMAT (2X//2X,35HFAILED TO CONVERGE IN 40 ITERATIONS//)
RETURN
END

```

```

SUBROUTINE FCNS(X,Y,ZE,F,G,FX,FY,GX,GY)
C
C THIS SUBROUTINE COMPUTES THE FUNCTIONS F(X,Y) AND G(X,Y)
C AND THEIR PARTIAL DERIVATIVES WITH RESPECT TO X AND Y.
C
COMMON /ELK1/ GSQ, ABSQ, ALBET, SMNSQ
C
C COMPUTE THE TRIGONOMETRIC FUNCTIONS, THE HYPERBOLIC FUNCTIONS
C AND THEIR SQUARES.
C
I = 1
ARGX = ZE * X
ARGY = ZE * Y
10 SX = SIN(ARGX)
CX = COS(ARGX)
SHY = SINH(ARGY)
CHY = COSH(ARGY)
IF (I .EQ. 2) GO TO 20
SXSQ = SX * SX
CXSQ = CX * CX
SHYSQ = SHY * SHY
CHYSQ = CHY * CHY
ARGX = 2.0 * ARGX
ARGY = 2.0 * ARGY
I = 2
GO TO 10
C
C COMPUTE TRANSCENDENTAL FUNCTIONS AND THEIR DERIVATIVES
C
20 FF = (SXSQ * CHYSQ) - (CXSQ * SHYSQ)
GG = (CXSQ * CHYSQ) - (SXSQ * SHYSQ)
HH = 0.25 * SX * SHY
FFX = ZE * SX * CHY
GGY = ZE * CX * SHY
FFY = -GGY
GGX = -FFX
HHX = 0.5 * GGY
HHY = 0.5 * FFX
C
C COMPUTE FACTORS
C
XYSQ = (X * X) - (Y * Y)
XY = X * Y
SMNXY = SMNSQ + YYSQ
F1 = (ABSQ * SMNXY) - (4.0 * ALBET * XY)
F2 = (ALBET * SMNXY) + (ABSQ * XY)
G1 = (ABSQ * SMNXY) + (4.0 * ALBET * XY)
FX1 = (2.0 * X * ABSQ) - (4.0 * ALBET * Y)
FX2 = (2.0 * X * ALBET) + (ABSQ * Y)
FY1 = (-2.0 * Y * ABSQ) - (4.0 * ALBET * X)
FY2 = (-2.0 * Y * ALBET) + (ABSQ * X)

```

```

      GX1 = (2.0 * X * ABSQ) + (4.0 * ALBET * Y)
      GY1 = (-2.0 * Y * ABSQ) + (4.0 * ALBET * X)
C
C
      COMPUTE F(X,Y) AND G(X,Y)
      F = (XYSQ * FF) - (4.0 * XY * HH)
1      + GSQ * ((F1 * GG) + (4.0 * F2 * HH))
      G = (XYSQ * HH) + (XY * FF)
1      + GSQ * ((F2 * GG) - (G1 * HH))
C
C
      COMPUTE THE PARTIAL DERIVATIVES OF F AND G
      FX = (2.0 * X * FF) + (XYSQ * FFX)
1      -4.0 * ((Y * HH) + (XY * HHX))
2      + GSQ * ((FX1 * GG) + (F1 * GGX)
3      + (4.0 * FX2 * HH) + (4.0 * F2 * HHX))
      FY = (-2.0 * Y * FF) + (XYSQ * FFY)
1      -4.0 * ((X * HH) + (XY * HHY))
2      + GSQ * ((FY1 * GG) + (F1 * GGY)
3      + (4.0 * FY2 * HH) + (4.0 * F2 * HHY))
      GX = (2.0 * X * HH) + (XYSQ * HHX)
1      + (Y * FF) + (XY * FFX)
2      + GSQ * ((FX2 * GG) + (F2 * GGX)
3      -(GX1 * HH) - (G1 * HHX))
      GY = (-2.0 * Y * HH) + (XYSQ * HHY)
1      + (X * FF) + (XY * FFY)
2      + GSQ * ((FY2 * GG) + (F2 * GGY)
3      -(GY1 * HH) - (G1 * HHY))
      RETURN
      END

```

```

SUBROUTINE AXIAL1(NOPT, NP, NJ, UE, ZE, ZCOMB, RESULT)
C
C
C THIS SUBROUTINE CALCULATES THE INTEGRAL OVER THE INTERVAL
C (0,ZE) OF THE FOLLOWING FUNCTIONS ACCORDING TO THE VALUE
C OF NOPT:
C
C NOPT = 1      Z(NP) * ZC(NJ)
C NOPT = 2      ZPP(NP) * ZC(NJ)
C NOPT = 3      UP * Z(NP) * ZC(NJ)
C NOPT = 4      U * ZP(NP) * ZC(NJ)
C
C IN THE ABOVE EQUATIONS:
C Z(NP) IS THE AXIAL ACOUSTIC EIGENFUNCTION OF INDEX NP.
C Z(NJ) IS THE AXIAL ACOUSTIC EIGENFUNCTION OF INDEX NJ.
C ZC IS THE COMPLEX CONJUGATE OF THE AXIAL EIGENFUNCTION.
C ZP AND ZPP ARE THE FIRST AND SECOND DERIVATIVES OF THE
C AXIAL EIGENFUNCTIONS RESPECTIVELY.
C U IS THE STEADY STATE VELOCITY DISTRIBUTION AND UP IS ITS
C AXIAL DERIVATIVE.
C THE VELOCITY DISTRIBUTION IS COMPUTED BY THE SUBROUTINE UBAR.
C
C
C REAL      MAG
C COMPLEX  CI, CZE, BP, BJ, T1, T2, CH, F1, F2, F3, CZ, ARG,
1          S1, S2, S3, RESULT, FUNCT(500), B(10)
C COMMON   B
C
C
C CI = (0.0,1.0)
C CZE = CMPLX(ZE,0.0)
C BP = B(NP)
C BJ = CONJG(B(NJ))
C
C IF (NOPT .GT. 2) GO TO 50
C CALCULATE INTEGRALS BY MEANS OF ANALYTICAL EXPRESSIONS FOR
C NOPT = 1 AND NOPT = 2.
C ARG = (BP + BJ) * CI
C MAG = CABS(ARG)
C IF (MAG) 20, 25, 20
20 T1 = CSINH(ARG*CZE)/ARG
C GO TO 30
25 T1 = CZE
30 ARG = (BP - BJ) * CI
C MAG = CABS(ARG)
C IF (MAG) 35, 40, 35
35 T2 = CSINH(ARG*CZE)/ARG
C GO TO 45
40 T2 = CZE
45 RESULT = (T1 + T2) * (0.5,0.0)
C IF (NOPT .EQ. 2) RESULT = -B(NP) * B(NP) * RESULT
C GO TO 100
C

```



```

C   NUMERICAL EVALUATION OF INTEGRALS FOR NOPT = 3 AND NOPT = 4.
C
C   COMPUTE STEP SIZE FOR SIMPSON INTEGRATION.
50  N = 50
    RN = N
    RESULT = (0.0,0.0)
    IC = ZCOMB
    IC = 2 - IC
C
    DO 90 J = 1, IC
    IF (J .EQ. 1) H = ZCOMB * ZE/RN
    IF (J .EQ. 2) H = (1.0 - ZCOMB) * ZE/RN
    IF (J .EQ. 1) Z0 = 0.0
    IF (J .EQ. 2) Z0 = ZCOMB * ZE
    NP1 = N + 1
    CH = CMPLX(H,0.0)
C
C   COMPUTE INTEGRANDS.
DO 60 I = 1, NP1
    STEP = I - 1
    Z = (STEP * H) + Z0
    IF ((I.EQ.1) .AND. (J.EQ.2)) Z = Z + H/100.0
    IF (NOPT .EQ. 3) CALL UBAR(2,UE,ZE,ZCOMB,Z,F)
    IF (NOPT .EQ. 4) CALL UBAR(1,UE,ZE,ZCOMB,Z,F)
    F1 = CMPLX(F,0.0)
    CZ = CMPLX(Z,0.0)
    ARG = CI * BP
    IF (NOPT .EQ. 3) F2 = CCOSH(ARG*CZ)
    IF (NOPT .EQ. 4) F2 = ARG * CSINH(ARG*CZ)
    ARG = CI * BJ
    F3 = CCOSH(ARG*CZ)
    FUNCT(I) = F1 * F2 * F3
60  CONTINUE
C
C   PERFORM SIMPSON INTEGRATION.
NM1 = N - 1
S1 = FUNCT(1) + FUNCT(NP1)
S2 = (0.0,0.0)
S3 = (0.0,0.0)
DO 70 I = 2, N, 2
    S2 = S2 + FUNCT(I)
70  CONTINUE
DO 80 I = 3, NM1, 2
    S3 = S3 + FUNCT(I)
80  CONTINUE
    RESULT = RESULT +
1    CH * (S1 + (4.0,0.0)*S2 + (2.0,0.0)*S3)/(3.0,0.0)
90  CONTINUE
C
100 CONTINUE
    RETURN
    END

```

```

SUBROUTINE UBAR(NOPT, UE, ZE, ZCOMB, Z, RESULT)
C
C THIS SUBROUTINE CALCULATES THE STEADY STATE VELOCITY
C DISTRIBUTION FOR UNIFORMLY DISTRIBUTED COMBUSTION COMPLETED AT
C  $Z = ZCOMB * ZE$  WHERE:
C UE IS THE EXIT MACH NUMBER.
C ZE IS THE DIMENSIONLESS LENGTH.
C Z IS THE AXIAL COORDINATE.
C
C IF NOPT = 1 THE DISTRIBUTION IS CALCULATED.
C IF NOPT = 2 THE DERIVATIVE IS CALCULATED.
C IF NOPT = 3 THE SECOND DERIVATIVE IS CALCULATED.
C
C
      ECZ = ZCOMB * ZE
      GO TO (10,20,30), NOPT
10 IF (Z .LE. ECZ) RESULT = UE * Z/ECZ
      IF (Z .GT. ECZ) RESULT = UE
      GO TO 40
20 IF (Z .LE. ECZ) RESULT = UE/ECZ
      IF (Z .GT. ECZ) RESULT = 0.0
      GO TO 40
30 RESULT = 0.0
40 CONTINUE
      RETURN
      END

```

```

SUBROUTINE AZIMTL(NOPT, NP, NQ, NJ, RESULT)
C
C   DIMENSION   NFCN(3), SG(2)
COMMON /BLK2/   M(10), NS(10)
C
C *****
C
C THIS SUBROUTINE CALCULATES THE INTEGRAL OVER THE INTERVAL
C (0, 2*PI) OF THE FOLLOWING FUNCTIONS ACCORDING TO THE VALUE
C OF NOPT:
C
C NOPT = 1      TH(NP) * TH(NQ) * TH(NJ)
C
C NOPT = 2      THP(NP) * THP(NQ) * TH(NJ)
C
C IN THE ABOVE EQUATIONS:
C TH(NP), TH(NQ), AND TH(NJ) ARE THE TANGENTIAL EIGENFUNCTIONS
C AND NP, NQ, AND NJ ARE THEIR INDICES.
C THP IS THE DERIVATIVE OF THE TANGENTIAL EIGENFUNCTIONS.
C
C IF NS = 1    TH = SIN(M*THETA)
C IF NS = 2    TH = COS(M*THETA)
C
C *****
C
C RESULT = 0.0
C FACTOR = 1.0
C PI = 3.1415927
C
C DISTINGUISH BETWEEN SINES AND COSINES.
C DO 10 K1 = 1, 3
C   NFCN(K1) = 1
10 CONTINUE
C   IF (NS(NJ).EQ.2) NFCN(3) = 2
C   IF (NOPT .EQ. 2) GO TO 20
C   IF (NS(NP).EQ.2) NFCN(1) = 2
C   IF (NS(NQ).EQ.2) NFCN(2) = 2
C   GO TO 30
20 IF (NS(NP).EQ.1) NFCN(1) = 2
C   IF (NS(NQ).EQ.1) NFCN(2) = 2
C   DO 40 K1 = 1, 2
C     SG(K1) = 1.0
C   IF (NFCN(K1) .EQ. 1) SG(K1) = -1.0
40 CONTINUE
C   FACTOR = SG(1) * SG(2) * M(NP) * M(NQ)
C
C 30 NSUM = 0
C   DO 50 K1 = 1, 3
C     NSUM = NSUM + NFCN(K1)
50 CONTINUE
C

```

```

IF ((NSUM .EQ. 3) .OR. (NSUM .EQ. 5)) GO TO 60
IF (NSUM .EQ. 4) GO TO 70
IF (NSUM .EQ. 6) GO TO 80
C
70 KOPT = 2
IF (NFCN(1) .EQ. 2) GO TO 72
GO TO 74
72 LL = M(NP)
MM = M(NQ)
NN = M(NJ)
GO TO 90
74 IF (NFCN(2) .EQ. 2) GO TO 76
GO TO 78
76 LL = M(NQ)
MM = M(NP)
NN = M(NJ)
GO TO 90
78 LL = M(NJ)
MM = M(NP)
NN = M(NQ)
GO TO 90
C
80 KOPT = 1
LL = M(NP)
MM = M(NQ)
NN = M(NJ)
C
C COMPUTE VALUES OF THE INTEGRALS.
C
90 IF ((LL.NE.0) .AND. (MM.NE.0) .AND. (NN.NE.0)) GO TO 101
GO TO 103
101 LM = LL + MM
LN = LL + NN
MN = MM + NN
IF ((NN.EQ.LM) .OR. (MM.EQ.LN)) RESULT = PI/2.0
IF (LL .EQ. MN) GO TO 102
GO TO 104
102 IF (KOPT .EQ. 1) RESULT = PI/2.0
IF (KOPT .EQ. 2) RESULT = -PI/2.0
GO TO 104
103 IF ((LL.EQ.0) .AND. (MM.EQ.0) .AND. (NN.EQ.0)) GO TO 105
IF ((KOPT.EQ.1) .AND. (NN.EQ.0) .AND. (LL.EQ.MM)) RESULT = PI
IF ((KOPT.EQ.1) .AND. (MM.EQ.0) .AND. (LL.EQ.NN)) RESULT = PI
IF ((LL .EQ. 0) .AND. (MM .EQ. NN)) RESULT = PI
GO TO 104
105 IF (KOPT .EQ. 1) RESULT = 2.0 * PI
104 CONTINUE
RESULT = FACTOR * RESULT
60 CONTINUE
RETURN
END

```

```

SUBROUTINE RADIAL(NOPT,L,M,N,A,B,C,RESULT)
C
C THIS SUBROUTINE CALCULATES THE INTEGRAL OVER THE INTERVAL
C (0,1) OF THE FOLLOWING PRODUCTS OF THREE BESSEL FUNCTIONS:
C
C NOPT = 1 JL(A*R) * JM(B*R) * JN(C*R) * R
C
C NOPT = 2 JL(A*R) * JM(B*R) * JN(C*R)/R
C
C NOPT = 3 JPL(A*R) * JPM(B*R) * JN(C*R) * R
C
C JL IS THE BESSEL FUNCTION OF FIRST KIND OF ORDER L
C JPL IS THE DERIVATIVE OF JL WITH RESPECT TO R
C L, M, N ARE NON-NEGATIVE INTEGERS
C A, B, C ARE REAL NUMBERS
C
DIMENSION FUNCT(200)
DOUBLE PRECISION DN, DH, DSTEP, DR, ARG1, ARG2, ARG3,
1 BES1, BES2, BES3, BESH, BESL, PROD,
2 FUNCT, BESLIM, S1, S2, S3
C
NN = 100
DN = NN
DH = 1.0/DN
NP1 = NN + 1
C
DO 10 I = 1, NP1
DSTEP = I - 1
DR = DH * DSTEP
ARG1 = A * DR
ARG2 = B * DR
ARG3 = C * DR
C
CALL JBES(N,ARG3,BES3,$500)
IF (NOPT .EQ. 3) GO TO 101
CALL JBES(L,ARG1,BES1,$500)
CALL JBES(M,ARG2,BES2,$500)
GO TO 102
101 IF (L .EQ. 0) GO TO 103
CALL JBES(L+1,ARG1,BESH,$500)
CALL JBES(L-1,ARG1,BESL,$500)
BES1 = A * (BESL - BESH)/2.0
GO TO 104
103 CALL JBES(1,ARG1,BES1,$500)
BES1 = -BES1 * A
104 IF (M .EQ. 0) GO TO 105
CALL JBES(M+1,ARG2,BESH,$500)
CALL JBES(M-1,ARG2,BESL,$500)
BES2 = B * (BESL - BESH)/2.0
GO TO 102

```

```

105 CALL JBES(1,ARG2,BES2,$500)
    BES2 = -BES2 * B
102 PROD = BES1 * BES2 * BES3
C
    IF (NOPT .EQ. 2) GO TO 110
    FUNCT(I) = PROD * DR
    GO TO 10
110 IF (I .EQ. 1) GO TO 111
    FUNCT(I) = PROD/DR
    GO TO 10
111 BESLIM = 0.0
    IF ((L.EQ.1) .AND. (M.EQ.0) .AND. (N.EQ.0)) BESLIM = A/2.0
    IF ((L.EQ.0) .AND. (M.EQ.1) .AND. (N.EQ.0)) BESLIM = B/2.0
    IF ((L.EQ.0) .AND. (M.EQ.0) .AND. (N.EQ.1)) BESLIM = C/2.0
    FUNCT(I) = BESLIM
10 CONTINUE
C
    NM1 = NN - 1
    S1 = FUNCT(1) + FUNCT(NP1)
    S2 = 0.0
    S3 = 0.0
    DO 20 I = 2, NN, 2
        S2 = S2 + FUNCT(I)
    20 CONTINUE
    DO 30 I = 3, NM1, 2
        S3 = S3 + FUNCT(I)
    30 CONTINUE
    RESULT = DH * (S1 + 4.0*S2 + 2.0*S3)/3.0
    GO TO 501
500 WRITE (6, 6000)
6000 FORMAT (1H1,10HERROR JBES)
501 CONTINUE
    RETURN
    END

```



```

ARG(2) = (BP + BQ - BJ) * CI
ARG(3) = (BP - BQ + BJ) * CI
ARG(4) = (BP - BQ - BJ) * CI
DO 10 J = 1,4
MAG = CABS(ARG(J))
IF (MAG) 12, 15, 12
12 FUNCT(J) = CSINH(ARG(J)*CZE)/ARG(J)
GO TO 10
15 FUNCT(J) = CZE
10 CONTINUE
IF (NOPT .EQ. 2) GO TO 30
SUM = FUNCT(1) + FUNCT(2) + FUNCT(3) + FUNCT(4)
RESULT = CF * SUM
IF (NOPT .EQ. 3) RESULT = -BP * BP * RESULT
GO TO 50
30 SUM = FUNCT(1) + FUNCT(2) - FUNCT(3) - FUNCT(4)
RESULT = -CF * BP * BQ * SUM
50 CONTINUE
RETURN
END

```



## APPENDIX D

### PROGRAM LCYC3D: A USER'S MANUAL

#### General Description

Using the three-dimensional second-order theory described in this report Program LCYC3D calculates the nonlinear stability characteristics of a cylindrical combustion chamber with distributed combustion and a conventional nozzle. The response of the burning rate to pressure oscillations is described by Crocco's time-lag model. For given values of the operating parameters (i.e.,  $n$ ,  $\bar{\tau}$ ,  $\gamma$ ,  $\bar{u}_e$ , and  $L/D$ ), a given series expansion, and a given initial disturbance Program LCYC3D integrates Eqs. (C-38) to obtain the time behavior of the unknown mode-amplitude functions (i.e.,  $B_j(t)$ ). From this information a time history of the pressure oscillation is determined. The program determines the final amplitude of the pressure oscillation attained in a linearly unstable engine (i.e., limit-cycle amplitude). Since the second-order analysis does not predict "triggering", however, the threshold amplitude above which a finite amplitude disturbance can trigger instability in a linearly stable engine (i.e., triggering limit) is not calculated by Program LCYC3D. For either transient or limit-cycle conditions, the program prints out time histories of both pressure and axial velocity perturbations from which the amplitude, frequency, and wave shapes can be determined. The option to produce plotted output using a CALCOMP plotter is also provided.

#### Program Structure

A flow chart for Program LCYC3D is given in Fig. (D-1). This program performs the following operations: (1) reads the input data, (2) calculates the initial conditions, (3) numerically integrates the differential equations, (4) tests for limit cycles (optional), and (5) prints and plots the resulting solutions.

The inputs to the program include the data generated by Program COEFFS3D, the combustion parameters  $n$  and  $\bar{\tau}$ , various control numbers, and a description of the initial disturbance. The data from COEFFS3D is read first and then printed out. Next the space dependent coefficients appearing in the series

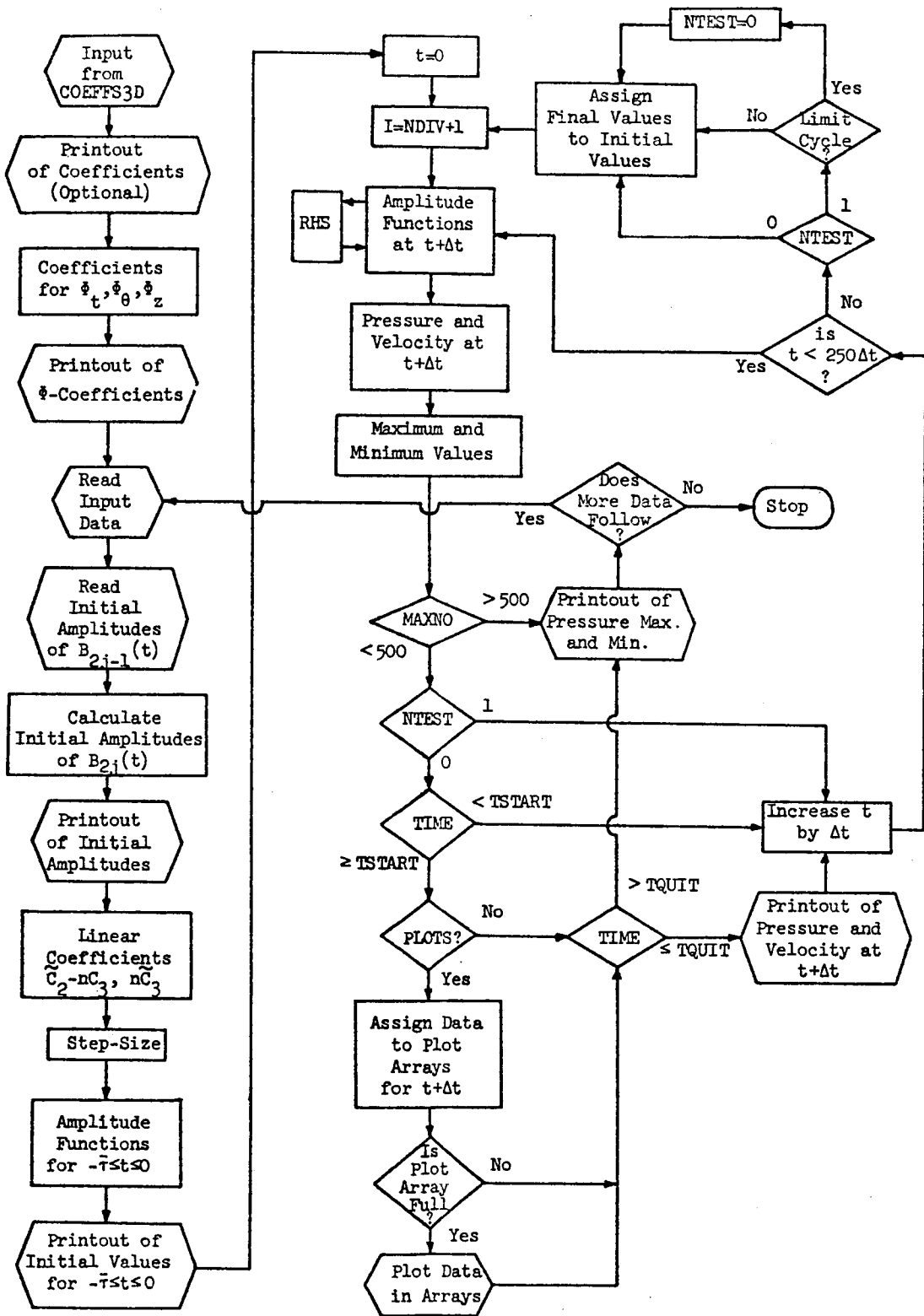


Figure D-1. Flow Chart for Program LCYC3D.

expansions for  $\bar{\Phi}_t$ ,  $\bar{\Phi}_\theta$ , and  $\bar{\Phi}_z$  are computed and printed out. These coefficients are calculated by Subroutine PHICFS for use in the computation of the pressure and axial velocity perturbations. The remaining input data is then read, and following program execution, control is returned to this point (see Fig. D-1) so that several cases (i.e., different values of  $n$  and  $\bar{\tau}$ ) may be run for a given set of coefficients generated by COEFFS3D.

After input of the initial amplitudes of the real parts (i.e.,  $B_{2j-1}(t)$ ) of the complex amplitude functions, the initial amplitudes of the imaginary parts (i.e.,  $B_{2j}(t)$ ) are calculated such that the nozzle admittance condition is satisfied for  $-\bar{\tau} \leq t \leq 0$ . These amplitudes are then printed out. Next the integration step-size,  $\Delta t$ , is calculated such that the interval  $-\bar{\tau} \leq t \leq 0$  is divided into NDIV equal increments. Assuming a sinusoidal initial disturbance, the initial amplitudes of  $B_{2j-1}(t)$  and  $B_{2j}(t)$  are used to calculate these functions and their derivatives at each of the NDIV + 1 discrete points in  $-\bar{\tau} \leq t \leq 0$ . These values are needed in order to start the numerical solution of the differential equations (i.e., Eqs. (C-38)). The initial values of the amplitude functions are stored in the array U(I,J) where the index I varies from 1 ( $t = -\bar{\tau}$ ) to NDIV + 1 ( $t = 0$ ) and the index J identifies the function. The corresponding initial values of the pressure and velocity perturbations are then printed out. This section also calculates the coefficients  $\tilde{C}_2(j,p) - n\tilde{C}_3(j,p)$  and  $n\tilde{C}_3(j,p)$  which are the coefficients of  $dB_p/dt$  and  $d[B_p(t - \bar{\tau})]/dt$  in Eqs. (C-38).

After the starting values are calculated, Eqs. (C-38) are solved using a modified form of the fourth order Runge Kutta method. Starting at  $t = 0$  ( $I = \text{NDIV} + 1$ ), the amplitude functions at  $t + \Delta t$  are calculated, using the Subroutine RHS to evaluate the functions  $f_j(B_1, B_2, \dots, B_{2N})$  on the right hand sides of Eqs. (C-38). The amplitude functions and the coefficients from PHICFS are then used to compute the pressure and axial velocity perturbations by Subroutine PRSVEL. The values of the amplitude functions at  $t + \Delta t$  are stored in U(I + 1, J), while the pressure and axial velocity perturbations are stored in the arrays PRESS(NPRES) and AXVEL(NPRES) where NPRES specifies the locations in the chamber where the data is calculated. Pressure data at one location (specified by NLOC) is also stored in the array PRS(I + 1). After checking for maximum and minimum values of U(I, J) and PRS(I), the data may

be printed out (if NTEST = 0 and TSTART  $\leq$  t  $\leq$  TQUIT) or stored in plot arrays as desired. The time is then increased by  $\Delta t$  (i.e., I is increased by 1) and the calculations are repeated. This process continues until 250 integration steps have been computed (t = 250 $\Delta t$ ), after which transfer is made to the limit-cycle section.

In the limit-cycle section a test for a limit-cycle is made if NTEST = 1. If the test is satisfied, NTEST is set to zero so that no further tests will be made and the results can be printed or plotted. In either case the final values (for 250-NDIV  $\leq$  I  $\leq$  250) replace the initial values (for 1  $\leq$  I  $\leq$  NDIV+1) in the arrays U(I,J) and PRS(I), I is again assigned the value NDIV+1, and another 250 integration steps are calculated. This process continues until one of the following conditions is satisfied: (1) NTEST = 0 and t  $>$  TQUIT, (2) a limit-cycle is reached and t  $>$  TQUIT, and (3) more than 250 cycles of the pressure oscillation have been computed (MAXNO  $>$  500). At this point the numerical calculations are terminated and the time history of the pressure amplitude (maxima and minima) are printed out and/or plotted as desired.

As can be seen from Fig. D-1 the output is not confined to a single section of the program but is produced in several different sections. Thus data is printed out or plotted shortly after it is calculated, which greatly reduces the amount of core storage required. All plots are generated by Subroutine GRAPHS which uses standard Univac 1108 plot routines.<sup>20</sup>

FORTTRAN listings of Program LCYC3D and Subroutines PHICFS, PRSVEL, RHS, and GRAPHS are provided at the end of this appendix.

### Input Data

A precise definition of the input data required to run the computer program is given below. This input data consists of three parts: (1) the control number NOUTCF, (2) the parameters and coefficients generated by Program COEFFS3D and (3) the data describing the cases to be run (see Fig. D-1). For each input case the following information must be provided: (1) the combustion parameters n and  $\bar{\tau}$ ; (2) a series of control numbers; and (3) information describing the initial disturbance.

The control number NOUTCF determines whether the coefficients from COEFFS3D will be printed, and it appears on the first card of input. This

card is followed by the coefficient deck generated by COEFFS3D and the data describing the cases to be run. Since the coefficient data has already been described in Appendix C, it will be omitted from the following detailed description of the input. As in Appendix C the location number refers to the columns of the card. Again three formats are used for input: "A" indicates alphanumeric characters, "I" indicates integers, and "F" indicates real numbers with a decimal point. For the "I" formats the values are placed in fields of five locations, while a field of ten locations is used with the "F" formats. In either case the numbers must be placed in the rightmost locations of the allocated field.

<u>No. of Cards</u>	<u>Location</u>	<u>Type</u>	<u>Input Item</u>	<u>Comments</u>
1	1-5	I	NOUTC	If 0: coefficients are not printed out. If 1: linear coefficients only are printed out. If 2: all coefficients are printed out.
1	1-72	A	TITLE	Title used to label plots.
1	1-10	F	EN	Interaction index, n.
	11-20	F	TAU	Time-lag, $\bar{\tau}$ .
	21-30	F	H	Time-increment for numerical integration, $\Delta t$ . *
	31-40	F	TSTART	Time at which output of solutions begins.
	41-50	F	TQUIT	Time at which output of solutions ends.
1	1-5	I	NTEST	If 0: compute transient behavior. If 1: compute limit-cycle behavior.
	6-10	I	JMODE	Identifies the amplitude function used to test for limit-cycles.

\* This value is adjusted slightly by the program to divide the interval  $-\bar{\tau} \leq t \leq 0$  into NDIV equal parts.

<u>No. of Cards</u>	<u>Location</u>	<u>Type</u>	<u>Input Item</u>	<u>Comments</u>
	11-15	I	NLOC	Determines location for wall pressure maxima and minima. If 1: $z = 0, \theta = 0^\circ$ If 2: $z = 0, \theta = 45^\circ$ If 3: $z = 0, \theta = 90^\circ$
	16-20	I	NTERMS	Number of amplitude functions given initial values.
	21-25	I	NPZ	Determines how secondary instability zones are handled. If 0: all instability zones retained. If 1: secondary zones eliminated.
	26-30	I	NOUT	Determines output. If 0: printed output only. If $1 \leq NOUT \leq 6$ : both printed and plotted output, NOUT gives number of last plot produced.

If  $1 \leq NOUT \leq 6$  the following two cards are read:

1	1-10	F	YHI(1)	Maximum ordinate for pressure plots.
	11-20	F	YHI(5)	Maximum ordinate for velocity plots.
	21-30	F	YLAB(1)	Interval for ordinate labeling of pressure plots.
	31-40	F	YLAB(5)	Interval for ordinate labeling of velocity plots.
1	1-5	I	ITICY(1)	Number of ordinate tic marks for pressure plots.
	6-10	I	ITICY(5)	Number of ordinate tic marks for velocity plots.
	11-15	I	NFIRST	Gives the number of the first plot produced.
	16-20	I	NOMIT	If 0: amplitude plot produced. If 1: amplitude plot omitted.

<u>No. of Cards</u>	<u>Location</u>	<u>Type</u>	<u>Input Item</u>	<u>Comments</u>
End of input for $1 \leq \text{NOUT} \leq 6$ .				
NTERMS	1-5	I	J	Identifies complex amplitude function.
	6-15	I	AST	Amplitude of $\sin(\omega t)$ term in initial conditions.
	16-25	I	ACT	Amplitude of $\cos(\omega t)$ term in initial conditions.

The input data describing the cases to be run is given on a series of three or more cards. These cards are preceded by a title card which gives a title (TITLE) to be used to identify any plots produced by the run. This title appears before the first plot generated and does not appear on the printed output. The title card is included only for the first case of the run; on all subsequent cases it is omitted.

The first card of the series gives the interaction index,  $n$ , and the time-lag,  $\bar{\tau}$ , for the motor under consideration (EN and TAU); the time-increment,  $\Delta t$ , used in the numerical integrations (H); and the times (TSTART and TQUIT) at which output begins and ends. For all cases considered in this report a time-increment (dimensionless) of  $H = 0.050$  was used, which gives about 70 steps per cycle for the 1T mode. For  $\bar{\tau} = 1.7$  this input value was adjusted by the program to obtain  $H = 0.04857$  which divides  $-\bar{\tau} \leq t \leq 0$  into 35 equal parts. For transient cases (NTEST = 0) printed output is given for  $TSTART \leq t \leq TQUIT$ . When the limit-cycle behavior is calculated (NTEST = 1), TSTART and TQUIT are measured from the time at which the limit-cycle is reached,  $t_{LC}$ . Thus the limit-cycle solutions are printed out for  $(t_{LC} + TSTART) \leq t \leq (t_{LC} + TQUIT)$ . Two or three cycles of limit-cycle data for the 1T mode are obtained with TSTART = 0 and TQUIT = 10. For plotted output, the time axis is always 10 units long, therefore  $(TQUIT - TSTART) > 10$  to obtain plots.

The second card of the series gives the control numbers, NTEST, JMODE, NLOC, NTERMS, NPZ, and NOUT. The task to be performed by Program LCYC3D is specified by NTEST. If NTEST = 0 the transient behavior (growth or decay) of the pressure oscillation is determined, while for NTEST = 1 the program

searches for a limit-cycle amplitude. JMODE identifies the "principal" series term, the amplitude function used in the limit-cycle test. This is usually the lowest frequency mode (i.e., 1T or 1L) in the approximating series expansion. NLOC gives the location at which the amplitude-time history (maxima and minima) of the wall pressure perturbation is calculated. The number of complex series terms  $A_j(t)$  receiving initial values is specified by NTERMS, while all other series terms are initially zero. The parameter NPZ determines how the secondary instability zones (phantom zones) are handled by Program LCYC3D. For NPZ = 1 the phantom zones are eliminated by dropping the combustion terms for a given mode when  $\bar{\tau} > \bar{\tau}_{cut}$  where:

$$\bar{\tau}_{cut} = \frac{2\pi}{\omega} = 2\pi \left[ S_{mn}^2 + \frac{t^2 \pi^2}{z_e^2} \right]^{-\frac{1}{2}} \quad (D-1)$$

A similar procedure was used in the axial instability studies by Loes and Zinn.<sup>3</sup> The transverse instability data presented herein was obtained with NPZ = 0, while NPZ = 1 was used in the axial instability studies to facilitate comparison with the results of Ref. (3). The last control number NOUT determines which plots, if any, are produced. For NOUT = 0 no plots are produced. For  $1 \leq NOUT \leq 6$ , NOUT gives the number of the last plot produced, where the plots are numbered as given in Table D-1 below:

Table D-1. Numbering of Plots.

<u>No. of Plot (N PLOT)</u>	<u>Quantity Plotted</u>	<u>Axial Location</u>	<u>Azimuthal Coordinate</u>
1	Pressure	Injector	0°
2	"	"	45°
3	"	"	90°
4	"	Nozzle	0°
5	Axial Velocity	"	0°
6	Nozzle Boundary Term	"	0°



The nozzle boundary term given on the last plot is discussed later in this appendix.

If plots are produced, two additional cards are needed to give the maximum and minimum values of the variables to be plotted, YHI(NPLOT) and YLO(NPLOT); the intervals for ordinate labeling (YLAB(NPLOT)); and the number of ordinate tic marks, ITICY(NPLOT). All of the plots are symmetric about the time-axis so that YLO(NPLOT) = -YHI(NPLOT), and ITICY(NPLOT) must be negative to obtain the centerline. Since the ordinate scales and labeling are the same for all pressure plots (NPLOT = 1,2,3,4) this data is read for NPLOT = 1 only; likewise the data for the last two plots is read for NPLOT = 5 only. In addition NFIRST gives the number of the first plot produced, giving additional control over the number of plots produced. NOMIT determines whether a plot of pressure amplitude versus time (location specified by NLOC) is produced.

The remaining cards give the initial amplitudes of the complex series terms,  $A_j(t)$ , needed to start the numerical integration. Only the amplitudes of the real parts,  $B_{2j-1}(t)$ , are given on these cards, while the amplitudes of the imaginary parts,  $B_{2j}(t)$ , are determined from the nozzle admittance condition. For each value of J the amplitudes AST and ACT are assigned to the arrays AS(NP) and AC(NP) where NP = 2J - 1. The computation of the amplitudes of the imaginary parts, AS(NP + 1) and AC(NP + 1), is discussed later. The initial values of the series terms are then calculated from the formula:

$$B_p(t) = AS(NP)\sin(\omega_p t) + AC(NP)\cos(\omega_p t) \quad (-\bar{\tau} \leq t \leq 0) \quad (D-2)$$

where  $\omega_p$  is the acoustic frequency. The derivatives,  $dB_p/dt$ , are also required for starting the numerical integration; they are obtained simply by differentiating Eq. (D-2).

The proper input for pure standing and pure spinning single-mode initial disturbances is given as follows. For a standing mode, only the  $\cos(m\theta)$  terms are retained in the series and NTERMS = 1. A single card is read giving the amplitude of the initial disturbance. For a spinning mode, both  $\sin(m\theta)$  and

$\cos(m\theta)$  terms are included in the series expansion. It is convenient to pair these terms such that the index  $J$  corresponds to a  $\sin(m\theta)$  term and  $J + 1$  corresponds to a  $\cos(m\theta)$  term. For an initial disturbance of amplitude  $A$  spinning in the counterclockwise direction ( $\theta$  increasing),  $NTERMS = 2$  and two cards are read giving the following data:

$$J : \quad AST = A \text{ and } ACT = 0 \tag{D-3}$$

$$J + 1 : \quad AST = 0 \text{ and } ACT = A$$

In both cases above initial amplitudes are required only for the mode initially present, and the initial amplitudes of all other modes included in the series expansion are zero.

The proper input for Program LCYC3D will be illustrated with the following example. Assuming that the velocity potential  $\phi$  is expressed in terms of the 1R, 1T, and 2T modes<sup>\*</sup>, it is desired to determine the limit-cycle behavior of a linearly unstable engine ( $n = 0.57486$ ,  $\bar{\tau} = 1.7$ ,  $\bar{u}_e = 0.2$ ,  $L/D = 0.5$ ) with a nozzle admittance of  $A = 0.02$  and  $\varphi = 45^\circ$ . Sample input is given for the case of a spinning 1T mode disturbance of amplitude 0.3. The principal series term is the  $\cos(m\theta)$  term for the 1T mode (i.e.,  $B_{011}(t)$ ), thus  $JMODE = 2$ . Plots are desired for the pressure, axial velocity, and nozzle boundary condition at the nozzle entrance, thus  $NOUT = 6$  and  $NFIRST = 4$ .

To run the case described above the data deck must be assembled as follows. The card specifying NOUTCF is followed by the coefficient deck produced by Program COEFFS3D; in this example it contains the information given in the sample output for COEFFS3D shown in Appendix C. The coefficient deck is followed by the data for the case to be run as shown in the sample input below:

---

\* This is the same case used to illustrate Program COEFFS3D.



$$\Phi_z = \sum_{p=1}^N A_p(t) Z_p'(z) \Theta_p(\theta) R_p(1) = \sum_{p=1}^N C_z(p, z, \theta) A_p(t) \quad (D-6)$$

where the complex coefficients  $C_t$ ,  $C_\theta$ , and  $C_z$  are functions of  $z$  and  $\theta$ . The quantity,  $\Phi_r$ , is not needed since  $\Phi_r = 0$  at the chamber wall. The complex coefficients  $C_t$ ,  $C_\theta$ , and  $C_z$  are calculated by Subroutine PHICFS and are assigned to the variables, C1, C2, and C3 respectively. The coefficients in the series expansions for the corresponding real parts (i.e.,  $\varphi_t$ ,  $\varphi_\theta$ ,  $\varphi_z$ ) are related to the complex coefficients by:

$$\begin{aligned} C_t'(2p-1, z, \theta) &= \text{Re}[C_t(p, z, \theta)] \\ C_t'(2p, z, \theta) &= -\text{Im}[C_t(p, z, \theta)] \end{aligned} \quad (D-7)$$

where similar relations hold for  $C_\theta'$  and  $C_z'$ . The real coefficients are stored in the arrays CFT(NPRES, NP), CFTH(NPRES, NP), and CFZ(NPRES, NP) where NPRES determines the location in the chamber as given in Table D-3 below:

Table D-3. Chamber Locations for Pressure Calculations.

<u>NPRES</u>	<u>Axial Location (z)</u>	<u>Azimuthal Location (<math>\theta</math>)</u>
1	0	0°
2	0	45°
3	0	90°
4	$z_e$	0°
5	$z_e$	45°
6	$z_e$	90°

#### Initial Amplitudes

The initial amplitudes of the real parts of the complex series terms (i.e.,  $B_{2j-1}(t)$ ) are specified in the input to the program. The initial

amplitudes of the imaginary parts (i.e.,  $B_{2j}(t)$ ), however, are calculated such that the nozzle admittance condition is satisfied for  $-\bar{\tau} \leq t \leq 0$ . This is done by introducing the linear expressions for  $u'$  and  $p'$  into the nozzle admittance relation and assuming periodic solutions. This yields a set of linear algebraic equations relating the amplitudes of the real and imaginary parts of the complex series terms. For given values of the amplitudes of the real parts,  $AS(NP)$  and  $AC(NP)$ , these equations are solved to obtain the amplitudes of the imaginary parts,  $AS(NP + 1)$  and  $AC(NP + 1)$ . The following formulas are used in this calculation.

$$\begin{aligned} AS(NJ + 1) &= -(r_2 a_1 - r_1 a_2) / (a_1^2 + a_2^2) \\ AC(NJ + 1) &= (r_1 a_1 + r_2 a_2) / (a_1^2 + a_2^2) \end{aligned} \tag{D-8}$$

where

$$\begin{aligned} r_1 &= a_3 [AC(NJ)] - a_4 [AS(NJ)] \\ r_2 &= -a_4 [AC(NJ)] - a_3 [AS(NJ)] \end{aligned} \tag{D-9}$$

and

$$\begin{aligned} a_1 &= (1 + \gamma_r^Y \bar{u}_e) CFZ(NPRES, NJ+1) - \gamma_i^Y \omega_j CFT(NPRES, NJ+1) \\ a_2 &= \gamma_r^Y \omega_j CFT(NPRES, NJ+1) + \gamma_i^Y \bar{u}_e CFZ(NPRES, NJ+1) \\ a_3 &= -(1 + \gamma_r^Y \bar{u}_e) CFZ(NPRES, NJ) + \gamma_i^Y \omega_j CFT(NPRES, NJ) \\ a_4 &= \gamma_r^Y \omega_j CFT(NPRES, NJ) + \gamma_i^Y \bar{u}_e CFZ(NPRES, NJ) \end{aligned} \tag{D-10}$$

In Eqs. (D-8) through (D-10)  $\omega_j$  is the acoustic frequency and CFT and CFZ are

the coefficients in the series for  $\varphi_t$  and  $\varphi_z$  computed previously. The above conditions are applied at a pressure anti-node for each series term, therefore NPRES = 4 ( $z = z_e, \theta = 0^\circ$ ) for a  $\cos(m\theta)$  term and NPRES = 6 ( $z = z_e, \theta = 90^\circ$ ) for a  $\sin(m\theta)$  term.

For nozzles with phase shifts of  $\varphi = 90^\circ$  and  $\varphi = 270^\circ$  the quantity  $a_1^2 + a_2^2$  vanishes and Eqs. (D-8) become indeterminate. In these cases the amplitudes of the imaginary parts are given by:

$$AS(NJ + 1) = AC(NJ) \tag{D-11}$$

$$AC(NJ + 1) = AS(NJ)$$

which provides a good approximation to the nozzle admittance condition.

#### Integration of the Differential Equations

For purposes of numerical integration Eqs. (C-38) are written as an equivalent system of first order differential equations as follows:

$$\frac{dB_j}{dt} = B_j' \tag{D-12}$$

$$\frac{dB_j'}{dt} = f_j(B_p, B_p') \tag{D-13}$$

where the dependent variables are now  $B_j$  and  $B_j'$ . These equations are solved numerically using the fourth order Runge-Kutta method. Due to the presence of retarded variables in Eqs. (D-12) and (D-13) the formulas (see Ref. 21) used in the Runge-Kutta method must be slightly modified.

The appropriate formulas for applying the Runge-Kutta method to problems involving a time-delay are readily obtained by considering a single equation of the following form:

$$\frac{dx}{dt} = f(x,t) + g[x(t - \bar{\tau})] \tag{D-14}$$

Noting that at any step of the integration the value of  $x(t - \bar{\tau})$  has already been determined from previous steps, the function  $g$  can be considered to be a known function of time  $g(t)$ .

Since  $x(t)$  is computed only at discrete points  $x_n(t_n)$  it is desired that the retarded variable  $x(t_n - \bar{\tau})$  will coincide with such previously computed points. This can be accomplished by choosing the step-size  $\Delta t$  such that it divides the time-lag  $\bar{\tau}$  into  $k$  equal increments. Thus  $\bar{\tau} = k\Delta t$  and the Runge-Kutta formulas which apply to Eq. (D-14) can now be written as:

$$\begin{aligned}
 x_{n+1} &= x_n + \frac{1}{6}(k_1 + 2k_2 + 2k_3 + k_4) \\
 k_1 &= \{f(x_n, t_n) + g(x_{n-k})\}\Delta t \\
 k_2 &= \{f(x_n + k_1/2, t_n + \Delta t/2) + g(x_{n-k+\frac{1}{2}})\}\Delta t \quad (D-15) \\
 k_3 &= \{f(x_n + k_2/2, t_n + \Delta t/2) + g(x_{n-k+\frac{1}{2}})\}\Delta t \\
 k_4 &= \{f(x_n + k_3, t_n + \Delta t) + g(x_{n-k+1})\}\Delta t
 \end{aligned}$$

Equations (D-15) are readily extended to handle the system of equations given by Eqs. (D-12) and (D-13). It is seen from Eqs. (D-15) that  $k$  values of the dependent variables prior to the initial values are needed to start the integration.

Although the initial wave shape can be an arbitrary function of time, it is assumed that initially the mode-amplitudes are sinusoidal functions of time oscillating with the natural frequency  $\omega_j$ . Thus each mode-amplitude function is expressed in the following form:

$$B_j(t) = AS(J)\sin(\omega_j t) + AC(J)\cos(\omega_j t) \quad (D-16)$$

$$B'_j(t) = \omega_j \left[ AS(J) \cos(\omega_j t) - AC(J) \sin(\omega_j t) \right]$$

where  $-\bar{\tau} \leq t \leq 0$ .

In Program LCYC3D both the functions  $B_j(t)$  and the derivatives  $B'_j(t)$  are stored in the same array  $U(I,J)$ . The  $B_j(t)$  ( $N$  functions) are stored in the first half of the array ( $1 \leq J \leq N$ ), while the remaining space ( $N + 1 \leq J \leq 2N$ ) is used to store the values of  $B'_j(t)$ . Thus for a given value of  $j$  ( $1 \leq j \leq N$ ),  $B_j(t)$  is stored in  $U(I,J)$  and  $B'_j(t)$  is stored in  $U(I, J + N)$ . In addition the retarded variables  $B'_j(t - \bar{\tau})$  are stored in the array  $RV(J,K)$  as follows:

$$RV(J,1) = B'_j(t - \bar{\tau})$$

$$RV(J,2) = RV(J,3) = B'_j(t - \bar{\tau} + \Delta t/2) \quad (D-17)$$

$$RV(J,4) = B'_j(t - \bar{\tau} + \Delta t)$$

The values of  $B'_j(t - \bar{\tau} + \Delta t/2)$  are computed from  $B'_j(t - \bar{\tau})$ ,  $B'_j(t - \bar{\tau} + \Delta t)$ , and  $B'_j(t - \bar{\tau} + 2\Delta t)$  using a three-point interpolation.

#### Pressure and Axial Velocity Perturbations

From the calculated time dependence of the series terms Program LCYC3D computes the dimensionless pressure perturbation,  $p'$ , with the aid of Eqs. (D-4) through (D-6) and either Eq. (13) for  $NDROPS = 0$  or Eq. (A-6) for  $NDROPS = 1$ . The pressure is calculated at the injector face ( $z = 0$ ) and the nozzle entrance plane ( $z = z_e$ ) for three angular positions along the periphery of the chamber (i.e.,  $r = 1$ ;  $\theta = 0^\circ, 45^\circ, 90^\circ$ ). The results are stored in the array  $PRESS(NPRES)$  where  $NPRES$  gives the location according to Table D-3. The axial velocity perturbation at the nozzle entrance,  $u'_e$ , is calculated for  $\theta = 0^\circ, 45^\circ, 90^\circ$  using the relation  $u' = \varphi_z$  and Eq. (D-6), and the results are stored in  $AXVEL(K)$ , where  $K = NPRES - 3$ . In addition the quantity,  $Re[-\gamma Y \Phi_t]$ , is calculated at the nozzle entrance for  $\theta = 0^\circ$  and assigned to the variable  $YPHI$ . From Eq. (2) it is seen that  $YPHI$  is the axial velocity



at the nozzle entrance (i.e.,  $u'_e$ ) if the nozzle admittance condition is exactly satisfied. Since the solutions generated by Program LCYC3D are approximate, the difference between  $u'_e$  and YPHI is a measure of the accuracy of this approximation at the nozzle boundary.

#### Maximum and Minimum Values

In order to determine the transient behavior and limit-cycle amplitudes it is necessary to follow the growth or decay of the amplitudes of the series terms and the pressure perturbation. The maxima and minima of the principal series term (specified by JMODE) are assigned to the array UMAX(MAXNO) where MAXNO is a counter variable. For the pressure perturbation, maximum and minimum values at the location specified by NLOC are stored in PMAX(MAXP), and the corresponding times of maximum and minimum are stored in TIMAX(MAXP). Since the solutions are calculated only at discrete points, the maximum and minimum values are computed using a three-point interpolation scheme.

#### Calculation of Limit-Cycle Amplitude

A limit-cycle amplitude is calculated by specifying an initial disturbance and continuing the step-by-step integration of Eqs.(D-12) and (D-13) until a periodic solution is obtained; that is, the amplitude of the oscillation remains essentially constant. The test for convergence to a limit cycle is performed upon a single series term, usually the most important term in the series, in the following manner. After the first 500 integration steps, usually about 10 cycles for the 1T mode, the amplitude of the principal series term  $A_1$  is compared with its amplitude after 250 integration steps  $A_0$ . If the change in amplitude  $|A_1 - A_0|$  is greater than the maximum permissible change  $\epsilon$ , the calculations are continued and the change in amplitude during the next 250 integration steps is calculated. The process is repeated until  $|A_k - A_{k-1}| < \epsilon$  at which point the computation is terminated. The amplitudes used in the above calculations are determined by averaging the absolute values of UMAX(MAXNO) over the last two complete cycles for each 250 integration steps. A value of  $\epsilon = 0.001$  is used in Program LCYC3D which gives sufficient accuracy for most cases.

## Output

Printed Output. The printed output produced by Program LCYC3D consists of the five sections discussed below.

Section 1 is a restatement of the input from Program COEFFS3D. It includes the following information: (a) the ratio of specific heats (GAMMA), the mean flow Mach number at the nozzle entrance (UE), the dimensionless chamber length (ZE), the length of the combustion zone as a fraction of the chamber length (ZCOMB), and the number of series terms (real) NJMAX; (b) a statement regarding the presence or absence of the droplet momentum source; (c) the parameters which describe and identify each term in the series expansion; (d) the nozzle admittance (YR and YI) and the axial acoustic eigenvalue (EPS and ETA) for each series term; (e) the nonzero linear coefficients, C(KC, NJ, NP); and (f) the nonzero nonlinear coefficients, D(NJ, NP, NQ). The nonlinear coefficients are omitted from the output for NOUTCF = 1, and no coefficients are printed out for NOUTCF = 0.

Section 2 gives the coefficients needed for computation of the wall pressure waveforms; that is, the coefficients in the series for  $\varphi_t$ ,  $\varphi_\theta$ , and  $\varphi_z$ . These are given for each of the NJMAX series terms at each of the six locations specified by NPRES (see Table D-3).

Section 3 gives the initial amplitudes (AS(J) and AC(J)) of all series terms included in the assumed initial disturbance. This section also states whether the limit-cycle behavior is calculated and whether plots are produced.

Section 4 gives the time-dependent solutions for the following quantities: (a) the injector pressure perturbation at  $\theta = 0^\circ, 45^\circ, 90^\circ$ ; (b) the nozzle pressure perturbation at  $\theta = 0^\circ, 45^\circ, 90^\circ$ ; (c) the nozzle axial velocity perturbation at  $\theta = 0^\circ, 45^\circ, 90^\circ$ ; and (d) the nozzle boundary term,  $\text{Re}[-\gamma Y \Phi_t]$ , at  $\theta = 0^\circ$ . This output is given in two parts: (1) the initial values for  $-\bar{\tau} \leq t \leq 0$  and (2) the solutions for  $t_i \leq t \leq t_f$ , where  $t_i$  and  $t_f$  are determined by the input parameters TSTART and TQUIT (see discussion on Input). On the first page of each part a heading gives the interaction index,  $n$ , and the time-lag,  $\bar{\tau}$ , and the chamber parameters,  $\gamma$ ,  $\bar{u}_e$ , and  $L/D$ .

Section 5 gives the time history of the pressure amplitude (maximum and minimum values) for the chamber location specified by NLOC. This information

is printed as an array of number pairs giving the value of the pressure maximum or minimum (upper number) and the corresponding time of maximum or minimum (lower number). This information is useful in determining the growth (or decay) rate of the transient solutions, and it provides a check on the convergence of the solution to a limit-cycle.

Plotted Output. According to the values of NOUT and NFIRST the pressure and axial velocity waveforms given in Section 4 of the printed output may be plotted using a Calcomp plotter. The data over the dimensionless time interval for printed output,  $t_i \leq t \leq t_f$ , is plotted in sections of 10 units in length beginning at  $t = t_i$ . Thus for each quantity plotted, N plots are produced where N is the largest multiple of 10 contained in the interval  $t_i \leq t \leq t_f$ . The data left over (i.e., for  $t_i + 10N \leq t \leq t_f$ ) is not plotted. All quantities to be plotted for a given time interval are plotted before proceeding to the next time interval.

The data given in Section 5 of the printed output (pressure maxima only) is also plotted if NOUT > 0 and NOMIT = 0. The abscissa and ordinate ranges for this plot are not specified in the input, but are calculated such that all of the data falls within these ranges. This plot is always the last plot produced.

All of the above plots are scaled to fit on standard  $8\frac{1}{2}$ " x 11" paper and scissor-lines are plotted for trimming plots to this size. The data is plotted as individual points using a small circle symbol, and all of the values computed during the given time interval are plotted. Before the first plot is produced the identifying title (see Input) is printed.

Sample Output. The following sample output illustrates the printed and plotted output produced by Program LCYC3D for the sample input given in Table D-2.

Table D-4. Sample Output, Section 1.

GAMMA = 1.200      UE = .200      ZE = 1.00000      ZCOMB = 1.00      NJMAX = 10

DROPLET MOMENTUM SOURCE IS NEGLECTED

NAME	J	L	M	N	NS	SMN	JM(SMN)
A011	1	0	1	1	1	1.84118	.58187
B011	2	0	1	1	2	1.84118	.58187
A021	3	0	2	1	1	3.05424	.48650
B021	4	0	2	1	2	3.05424	.48650
B001	5	0	0	1	2	3.83171	-.40276

J	YR	YI	EPS	ETA
1	.01414	.01414	.08122	.19451
2	.01414	.01414	.08122	.19451
3	.01414	.01414	.10617	.25115
4	.01414	.01414	.10617	.25115
5	.01414	.01414	.11993	.28170

NUMBER OF COEFFICIENTS C(1,NJ,NP) IS 10

C(1, 1, 1) = 3.39060  
 C(1, 2, 2) = 3.39060  
 C(1, 3, 3) = 3.39060  
 C(1, 4, 4) = 3.39060  
 C(1, 5, 5) = 9.33021  
 C(1, 6, 6) = 9.33021  
 C(1, 7, 7) = 9.33021  
 C(1, 8, 8) = 9.33021  
 C(1, 9, 9) = 14.68491  
 C(1,10,10) = 14.68491

NUMBER OF COEFFICIENTS C(2,NJ,NP) IS 10

C(2, 1, 1) = .26153  
 C(2, 2, 2) = .26153  
 C(2, 3, 3) = .26153  
 C(2, 4, 4) = .26153  
 C(2, 5, 5) = .26457  
 C(2, 6, 6) = .26457  
 C(2, 7, 7) = .26457  
 C(2, 8, 8) = .26457  
 C(2, 9, 9) = .26654  
 C(2,10,10) = .26654

NUMBER OF COEFFICIENTS C(3,NJ,NP) IS 10

C(3, 1, 1) = .24000  
 C(3, 2, 2) = .24000  
 C(3, 3, 3) = .24000  
 C(3, 4, 4) = .24000  
 C(3, 5, 5) = .24000  
 C(3, 6, 6) = .24000  
 C(3, 7, 7) = .24000

Table D-4. (Continued)

C(3, 8, 8) = .24000  
 C(3, 9, 9) = .24000  
 C(3,10,10) = .24000

NUMBER OF COEFFICIENTS D(NJ, NP, NQ) IS 50

D( 1, 1, 7) = -1.73504  
 D( 1, 1, 9) = -2.33866  
 D( 1, 3, 5) = 1.73504  
 D( 1, 5, 3) = 1.49783  
 D( 1, 7, 1) = -1.49783  
 D( 1, 9, 1) = -1.96281  
 D( 2, 2, 8) = -1.73505  
 D( 2, 2,10) = -2.33867  
 D( 2, 4, 6) = 1.73505  
 D( 2, 6, 4) = 1.49784  
 D( 2, 8, 2) = -1.49784  
 D( 2,10, 2) = -1.96282  
 D( 3, 1, 5) = 1.73504  
 D( 3, 3, 7) = 1.73504  
 D( 3, 3, 9) = -2.33866  
 D( 3, 5, 1) = 1.49783  
 D( 3, 7, 3) = 1.49783  
 D( 3, 9, 3) = -1.96281  
 D( 4, 2, 6) = 1.73505  
 D( 4, 4, 8) = 1.73505  
 D( 4, 4,10) = -2.33867  
 D( 4, 6, 2) = 1.49784  
 D( 4, 8, 4) = 1.49784  
 D( 4,10, 4) = -1.96282  
 D( 5, 1, 3) = -1.13133  
 D( 5, 3, 1) = -1.13133  
 D( 5, 5, 9) = -3.07465  
 D( 5, 9, 5) = -2.81865  
 D( 6, 2, 4) = -1.13132  
 D( 6, 4, 2) = -1.13132  
 D( 6, 6,10) = -3.07469  
 D( 6,10, 6) = -2.81868  
 D( 7, 1, 1) = 1.13133  
 D( 7, 3, 3) = -1.13133  
 D( 7, 7, 9) = -3.07465  
 D( 7, 9, 7) = -2.81865  
 D( 8, 2, 2) = 1.13132  
 D( 8, 4, 4) = -1.13132  
 D( 8, 8,10) = -3.07469  
 D( 8,10, 8) = -2.81868  
 D( 9, 1, 1) = 1.04087  
 D( 9, 3, 3) = 1.04087  
 D( 9, 5, 5) = -.21090  
 D( 9, 7, 7) = -.21090  
 D( 9, 9, 9) = 4.18784  
 D(10, 2, 2) = 1.04087  
 D(10, 4, 4) = 1.04087  
 D(10, 6, 6) = -.21091  
 D(10, 8, 8) = -.21091  
 D(10,10,10) = 4.18793

Table D-5. Sample Output, Section 2.

COEFFICIENTS FOR COMPUTATION OF WALL PRESSURE WAVEFORMS

COEFFICIENTS IN SERIES FOR:					
J	Z	THETA (DEGREES)	TIME DERIVATIVE	THETA DERIVATIVE	AXIAL DERIVATIVE
1	.000	.0	.0000000	.5818700	.0000000
2	.000	.0	.0000000	.0000000	.0000000
3	.000	.0	.5818700	.0000000	.0000000
4	.000	.0	.0000000	.0000000	.0000000
5	.000	.0	.0000000	.9730000	.0000000
6	.000	.0	.0000000	.0000000	.0000000
7	.000	.0	.4865000	.0000000	.0000000
8	.000	.0	.0000000	.0000000	.0000000
9	.000	.0	-.4027600	.0000000	.0000000
10	.000	.0	.0000000	.0000000	.0000000
1	.000	45.0	.4114442	.4114442	.0000000
2	.000	45.0	.0000000	.0000000	.0000000
3	.000	45.0	.4114442	-.4114442	.0000000
4	.000	45.0	.0000000	.0000000	.0000000
5	.000	45.0	.4865000	-.0000000	.0000000
6	.000	45.0	.0000000	.0000000	.0000000
7	.000	45.0	-.0000000	-.9730000	.0000000
8	.000	45.0	.0000000	.0000000	.0000000
9	.000	45.0	-.4027600	.0000000	.0000000
10	.000	45.0	.0000000	.0000000	.0000000
1	.000	90.0	.5818700	-.0000000	.0000000
2	.000	90.0	.0000000	.0000000	.0000000
3	.000	90.0	-.0000000	-.5818700	.0000000
4	.000	90.0	.0000000	.0000000	.0000000
5	.000	90.0	-.0000000	-.9730000	.0000000
6	.000	90.0	.0000000	.0000000	.0000000
7	.000	90.0	-.4865000	.0000001	.0000000
8	.000	90.0	.0000000	.0000000	.0000000
9	.000	90.0	-.4027600	.0000000	.0000000
10	.000	90.0	.0000000	.0000000	.0000000
1	1.000	.0	.0000000	.5909575	.0000000
2	1.000	.0	.0000000	.0092403	.0000000
3	1.000	.0	.5909575	.0000000	.0181736
4	1.000	.0	.0092403	.0000000	.0185766
5	1.000	.0	.0000000	.9981959	.0000000
6	1.000	.0	.0000000	.0261690	.0000000
7	1.000	.0	.4990979	.0000000	.0251885
8	1.000	.0	.0130845	.0000000	.0263938
9	1.000	.0	-.4158379	.0000000	-.0261428
10	1.000	.0	-.0137546	.0000000	-.0278051
1	1.000	45.0	.4178700	.4178700	.0128507
2	1.000	45.0	.0065339	.0065339	.0131356
3	1.000	45.0	.4178700	-.4178700	.0128507

Table D-5. (Continued)

4	1.000	45.0	.0065339	-.0065339	.0131356
5	1.000	45.0	.4990979	-.0000000	.0251885
6	1.000	45.0	.0130845	-.0000000	.0263938
7	1.000	45.0	-.0000000	-.9981959	-.0000000
8	1.000	45.0	-.0000000	-.0261690	-.0000000
9	1.000	45.0	-.4158379	.0000000	-.0261428
10	1.000	45.0	-.0137546	.0000000	-.0278051
1	1.000	90.0	.5909575	-.0000000	.0181736
2	1.000	90.0	.0092403	-.0000000	.0185766
3	1.000	90.0	-.0000000	-.5909575	-.0000000
4	1.000	90.0	-.0000000	-.0092403	-.0000000
5	1.000	90.0	-.0000000	-.9981959	-.0000000
6	1.000	90.0	-.0000000	-.0261690	-.0000000
7	1.000	90.0	-.4990979	.0000001	-.0251885
8	1.000	90.0	-.0130845	.0000000	-.0263938
9	1.000	90.0	-.4158379	.0000000	-.0261428
10	1.000	90.0	-.0137546	.0000000	-.0278051

Table D-6. Sample Output, Section 3.

INITIAL CONDITIONS ARE OF THE FORM:

$$U(I,J) = AC(J)*COS(FREQ*T) + AS(J)*SIN(FREQ*T), * EXP(DAMP*T)$$

J	DAMPING	FREQUENCY	AC(J)	AS(J)
1	.00000000	1.84118000	.00000000	.30000000
2	.00000000	1.84118000	-.30278619	-.00209447
3	.00000000	1.84118000	.30000000	.00000000
4	.00000000	1.84118000	-.00209447	.30278619

THE LIMIT-CYCLE BEHAVIOR IS CALCULATED.

THIS RUN PRODUCES PLOTTED OUTPUT.

Table D-7. Sample Output, Section 4.

COMBUSTION PARAMETERS:		INTERACTION INDEX = .57486		TIME-LAG = 1.70000		LENGTH/DIAMETER = .50000					
MOTOR PARAMETERS:		GAMMA = 1.20000		EXIT MACH NUMBER = .20000							
INITIAL CONDITIONS											
STEP	TIME	0. DEG.	45. DEG.	90. DEG.	NOZZLE PRESSURE	0. DEG.	90. DEG.	NOZZLE AXIAL VELOCITY	YPHI		
-35	-1.70000	-.00446	.29088	.42934	.00294	.30085	.43542	-.00548	.00006	.00556	-.00557
-34	-1.65143	-.03845	.26129	.42696	-.03161	.27126	.43380	-.00595	-.00064	.00505	-.00605
-33	-1.60286	-.07144	.22989	.42083	-.06520	.23977	.42837	-.00638	-.00133	.00450	-.00648
-32	-1.55429	-.10320	.19702	.41103	-.09758	.20673	.41918	-.00676	-.00201	.00391	-.00685
-31	-1.50571	-.13352	.16303	.39768	-.12854	.17250	.40636	-.00708	-.00268	.00329	-.00718
-30	-1.45714	-.16221	.12826	.38093	-.15788	.13741	.39006	-.00734	-.00332	.00265	-.00744
-29	-1.40857	-.18912	.09306	.36100	-.18543	.10182	.37048	-.00755	-.00394	.00198	-.00765
-28	-1.36000	-.21410	.05775	.33812	-.21107	.06606	.34786	-.00770	-.00453	.00130	-.00779
-27	-1.31143	-.23704	.02265	.31256	-.23466	.03047	.32246	-.00778	-.00508	.00060	-.00788
-26	-1.26286	-.25785	-.01193	.28461	-.25611	-.00465	.29459	-.00781	-.00559	-.00009	-.00790
-25	-1.21429	-.27645	-.04572	.25460	-.27936	-.03901	.26456	-.00777	-.00605	-.00079	-.00785
-24	-1.16571	-.29280	-.07847	.22285	-.29234	-.07236	.23270	-.00766	-.00647	-.00148	-.00775
-23	-1.11714	-.30685	-.10993	.18970	-.30700	-.10445	.19937	-.00750	-.00683	-.00216	-.00758
-22	-1.06857	-.31856	-.13991	.15552	-.31932	-.13507	.16492	-.00728	-.00714	-.00282	-.00735
-21	-1.02000	-.32792	-.16823	.12082	-.32927	-.16403	.12969	-.00700	-.00739	-.00346	-.00706
-20	-.97143	-.33491	-.19472	.08537	-.33684	-.19118	.09404	-.00666	-.00759	-.00407	-.00672
-19	-.92286	-.33953	-.21926	.05008	-.34202	-.21638	.05829	-.00627	-.00772	-.00465	-.00632
-18	-.87429	-.34176	-.24175	.01507	-.34480	-.23951	.02278	-.00583	-.00779	-.00519	-.00587
-17	-.82571	-.34160	-.26209	-.01936	-.34319	-.26049	-.01220	-.00534	-.00780	-.00569	-.00538
-16	-.77714	-.33906	-.28021	-.05294	-.34317	-.27925	-.04636	-.00481	-.00775	-.00614	-.00484
-15	-.72857	-.33414	-.29606	-.08543	-.33875	-.29572	-.07946	-.00425	-.00763	-.00655	-.00426
-14	-.68000	-.32684	-.30960	-.11659	-.33194	-.30908	-.11124	-.00364	-.00746	-.00690	-.00365
-13	-.63143	-.31718	-.32080	-.14622	-.32273	-.32169	-.14152	-.00301	-.00722	-.00720	-.00301
-12	-.58286	-.30516	-.32964	-.17415	-.31115	-.33112	-.17010	-.00236	-.00693	-.00744	-.00235
-11	-.53429	-.29081	-.33612	-.20023	-.29721	-.33817	-.19683	-.00168	-.00658	-.00762	-.00167
-10	-.48571	-.27417	-.34021	-.22334	-.28094	-.34283	-.22159	-.00100	-.00618	-.00774	-.00097
-9	-.43714	-.25527	-.34193	-.24636	-.26237	-.34509	-.24426	-.00030	-.00530	-.00780	-.00027
-8	-.38857	-.23418	-.34125	-.26622	-.24157	-.34495	-.26477	-.00040	-.00523	-.00780	-.00044
-7	-.34000	-.21097	-.33819	-.28385	-.21860	-.34241	-.28303	.00109	-.00469	-.00773	.00114
-6	-.29143	-.18574	-.33275	-.29920	-.19355	-.33747	-.29900	.00178	-.00412	-.00760	.00183
-5	-.24286	-.15859	-.32494	-.31223	-.16653	-.33014	-.31265	.00245	-.00351	-.00741	.00251
-4	-.19429	-.12968	-.31476	-.32293	-.13767	-.32041	-.32394	.00310	-.00287	-.00716	.00317
-3	-.14571	-.09916	-.30223	-.33126	-.10714	-.30832	-.33286	.00373	-.00221	-.00686	.00380
-2	-.09714	-.06723	-.28739	-.33721	-.07512	-.29386	-.33939	.00433	-.00154	-.00650	.00441
-1	-.04857	-.03410	-.27025	-.34079	-.04183	-.27709	-.34353	.00469	-.00085	-.00609	.00497
0	.00000	.00000	-.25087	-.34198	-.00749	-.25803	-.34527	.00541	-.00015	-.00562	.00550



Table D-7. (Continued)

STEP	TIME	COMBUSTION PARAMETERS:		INTERACTION INDEX = .57486		EXIT MACH NUMBER = .20000		LENGTH/DIAMETER = .50000		YPHI	
		0. DEG.	45. DEG.	90. DEG.	0. DEG.	45. DEG.	90. DEG.	0. DEG.	45. DEG.		90. DEG.
3006	146.00571	-12500	.1759	.48179	-.11918	.18709	.48937	-.06618	-.00133	.00429	-.00790
3007	146.05428	-114707	.13466	.46189	-.14184	.14395	.47008	-.00654	-.00200	.00372	-.00800
3008	146.10286	-116640	.09290	.43622	-.16178	.10189	.44492	-.00684	-.00265	.00312	-.00800
3009	146.15143	-118316	.05286	.40547	-.17917	.06150	.41458	-.00709	-.00329	.00248	-.00790
3010	146.20000	-119756	.01498	.37044	-.19421	.02321	.37985	-.00727	-.00389	.00183	-.00770
3011	146.24857	-120984	-.02038	.33200	-.20714	-.01261	.34161	-.00739	-.00446	.00116	-.00743
3012	146.29714	-122024	-.05300	.29104	-.21820	-.04573	.30075	-.00745	-.00499	.00048	-.00710
3013	146.34571	-122903	-.08273	.24846	-.22764	-.07599	.25816	-.00745	-.00548	-.00021	-.00671
3014	146.39428	-123645	-.10952	.20511	-.23571	-.10334	.21472	-.00739	-.00593	-.00090	-.00629
3015	146.44286	-124273	-.13339	.16179	-.24265	-.12779	.17123	-.00726	-.00632	-.00157	-.00583
3016	146.49143	-124810	-.15444	.11923	-.24866	-.14944	.12842	-.00708	-.00666	-.00224	-.00537
3017	146.54000	-125273	-.17281	.07804	-.25393	-.16842	.08691	-.00693	-.00694	-.00289	-.00490
3018	146.58857	-125678	-.18868	.03874	-.25860	-.18492	.04724	-.00653	-.00716	-.00351	-.00443
3019	146.63714	-126036	-.20227	.00175	-.26277	-.19316	.00982	-.00618	-.00732	-.00410	-.00399
3020	146.68571	-126352	-.21384	-.03263	-.26658	-.21138	-.02504	-.00577	-.00742	-.00466	-.00356
3021	146.73428	-126627	-.22362	-.06420	-.26980	-.22181	-.05712	-.00532	-.00746	-.00518	-.00316
3022	146.78286	-126850	-.23188	-.09286	-.27263	-.23073	-.08631	-.00483	-.00744	-.00565	-.00279
3023	146.83143	-127038	-.23885	-.11857	-.27490	-.23836	-.11260	-.00430	-.00735	-.00608	-.00244
3024	146.88000	-127152	-.24477	-.14140	-.27649	-.24493	-.13601	-.00374	-.00720	-.00645	-.00213
3025	146.92857	-127183	-.24985	-.16144	-.27721	-.25065	-.15666	-.00314	-.00699	-.00677	-.00183
3026	146.97714	-127111	-.25426	-.17887	-.27686	-.25568	-.17472	-.00252	-.00673	-.00703	-.00156
3027	147.02571	-126914	-.25813	-.19388	-.27522	-.26016	-.19036	-.00189	-.00641	-.00723	-.00130
3028	147.07428	-126565	-.26154	-.20671	-.27203	-.26474	-.20383	-.00124	-.00603	-.00737	-.00104
3029	147.12286	-126030	-.26456	-.21759	-.26702	-.26774	-.20383	-.00058	-.00561	-.00744	-.00079
3030	147.17143	-125300	-.26716	-.22679	-.25993	-.27088	-.22522	-.00009	-.00515	-.00746	-.00052
3031	147.22000	-124347	-.26929	-.23455	-.25048	-.27352	-.23364	-.00075	-.00464	-.00741	-.00023
3032	147.26857	-123120	-.27086	-.24111	-.23943	-.27555	-.24056	-.00141	-.00410	-.00730	-.00008
3033	147.31714	-121630	-.27172	-.24671	-.22354	-.27684	-.24710	-.00205	-.00352	-.00713	-.00042
3034	147.36571	-119830	-.27168	-.25152	-.20559	-.27720	-.25255	-.00268	-.00292	-.00690	-.00080
3035	147.41428	-117713	-.27054	-.25572	-.18441	-.27641	-.25737	-.00328	-.00229	-.00662	-.00121
3036	147.46285	-.15265	-.26804	-.25941	-.15907	-.27423	-.26167	-.00386	-.00165	-.00628	-.00167
3037	147.51143	-.12481	-.26394	-.26268	-.13192	-.27011	-.26552	-.00441	-.00100	-.00589	-.0217
3038	147.56000	-.09362	-.25796	-.26555	-.10055	-.26467	-.26893	-.00492	-.00033	-.00545	-.00270
3039	147.60857	-.05917	-.24984	-.26799	-.06585	-.25675	-.27190	-.00540	-.00033	-.00497	-.00327
3040	147.65714	-.02164	-.23932	-.26994	-.02801	-.24638	-.27433	-.00583	-.00099	-.00445	-.00386
3041	147.70571	.01867	-.22614	-.27126	.01268	-.23322	-.27612	-.00621	-.00164	-.00399	-.00447
3042	147.75428	.05994	-.21007	-.26994	-.02801	-.23322	-.27709	-.00655	-.00228	-.00350	-.00509
3043	147.80285	.10594	-.19094	-.27140	.00995	-.19822	-.27705	-.00683	-.00290	-.00269	-.00570
3044	147.85143	.15176	-.16857	-.26979	.14738	-.17583	-.27579	-.00706	-.00350	-.00206	-.00629
3045	147.90000	.19811	-.14287	-.26674	.19442	-.15005	-.27304	-.00723	-.00407	-.00141	-.00685
3046	147.94857	.24418	-.11380	-.26194	.24125	-.12094	-.26855	-.00734	-.00460	-.00075	-.00736
3047	147.99714	.28908	-.08140	-.25526	.28698	-.08825	-.26204	-.00739	-.00510	-.00009	-.00780
3048	148.04571	.33190	-.04580	-.24629	.33068	-.05238	-.25326	-.00739	-.00556	-.00057	-.00818
3049	148.09428	.37171	-.00721	-.23482	.37141	-.01346	-.24194	-.00732	-.00597	-.00023	-.00846

Table D-8. Sample Output, Section 5.

PRESSURE MAXIMA AND MINIMA AT: Z = .00 THETA = .0							
VALUES COMPUTED: 94							
.456418	-.308270	.560628	-.272996	.478533	-.308486	.542703	-.252604
.771543	2.863856	4.172075	5.603093	7.544092	9.446675	10.853099	12.786936
.510174	-.294000	.515242	-.268418	.523881	-.279236	.506445	-.277079
14.257257	16.063277	17.564400	19.537089	20.950593	22.744107	24.284235	26.215260
.522925	-.271794	.507847	-.278825	.517217	-.271253	.511007	-.277434
27.645648	29.485428	30.999033	32.887355	34.347683	36.223408	37.707680	39.573612
.512651	-.273096	.512507	-.275527	.510428	-.274546	.512173	-.274260
41.054779	42.940316	44.413538	46.276354	47.763727	49.647243	51.119364	52.988021
.509667	-.274897	.510385	-.273707	.509343	-.274477	.509485	-.273529
54.472655	56.351470	57.826298	59.701087	61.181129	63.056576	64.534305	66.411903
.508919	-.273837	.508374	-.273437	.508277	-.273341	.507590	-.273339
67.889316	69.763511	71.242904	73.120358	74.597562	76.471918	77.951710	79.827781
.507531	-.273099	.507004	-.273171	.506817	-.272970	.506484	-.272988
81.306071	83.180643	84.660571	86.534866	88.014882	89.888966	91.369514	93.242868
.506195	-.272868	.505966	-.272806	.505655	-.272734	.505445	-.272628
94.723948	96.597583	98.078606	99.951679	101.433208	103.306509	104.787890	106.660972
.505162	-.272564	.504934	-.272457	.504692	-.272387	.504466	-.272298
108.142635	110.015746	111.497398	113.370504	114.852245	116.725281	118.207081	120.080224
.504254	-.272226	.504037	-.272157	.503844	-.272090	.503647	-.272062
121.561975	123.435121	124.916878	126.790210	128.271814	130.145315	131.626776	133.500187
.503467	-.272003	.503289	-.271953	.503120	-.271899	.502957	-.271849
134.981756	136.854771	138.336773	140.209436	141.691811	143.564207	145.046881	146.919048
.502798	-.271799	.502646	-.271749	.502497	-.271700	.502347	-.271649
148.401972	150.273991	151.757095	153.629004	155.112246	156.984108		

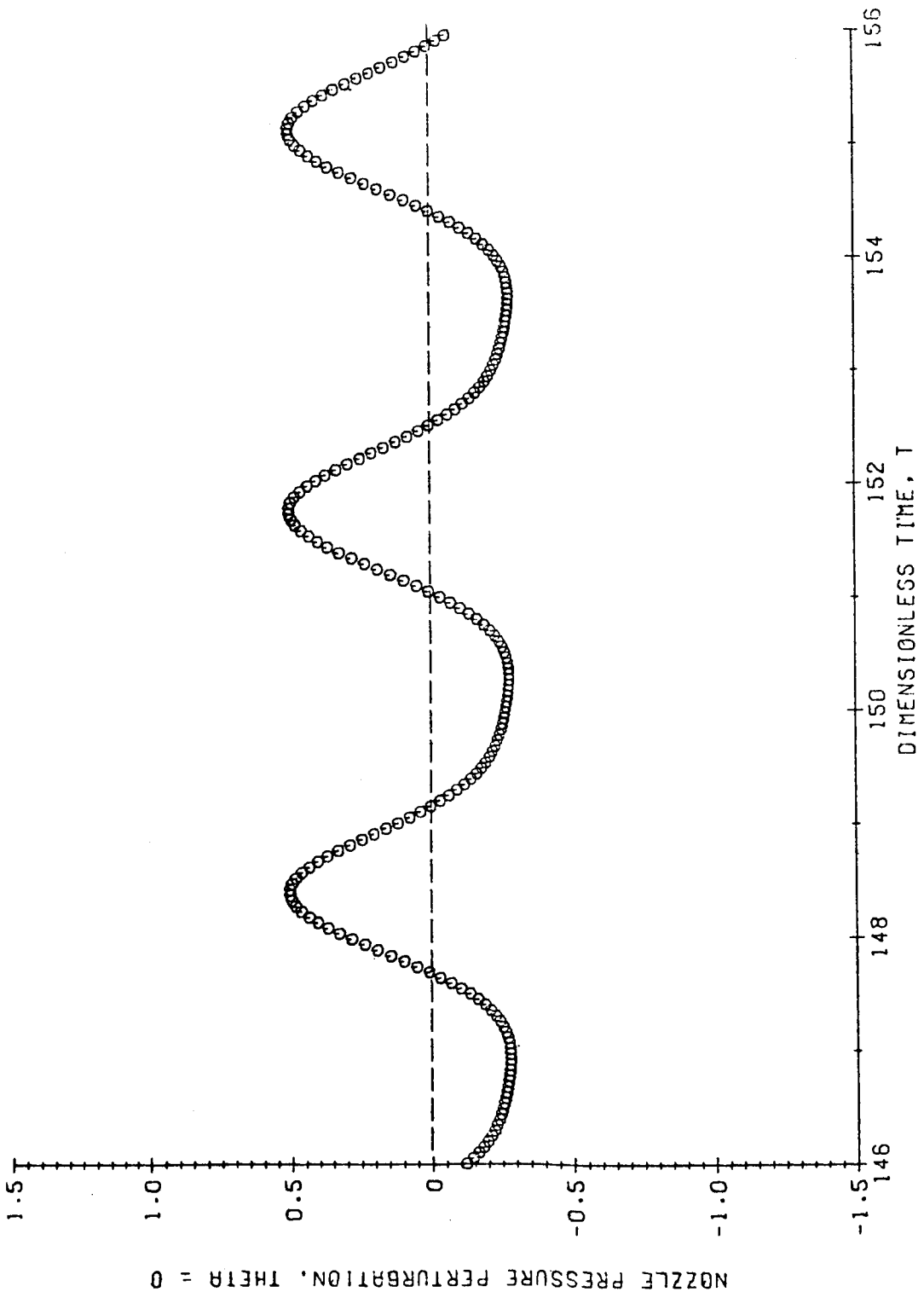


Figure D-2. Sample Pressure Plot.

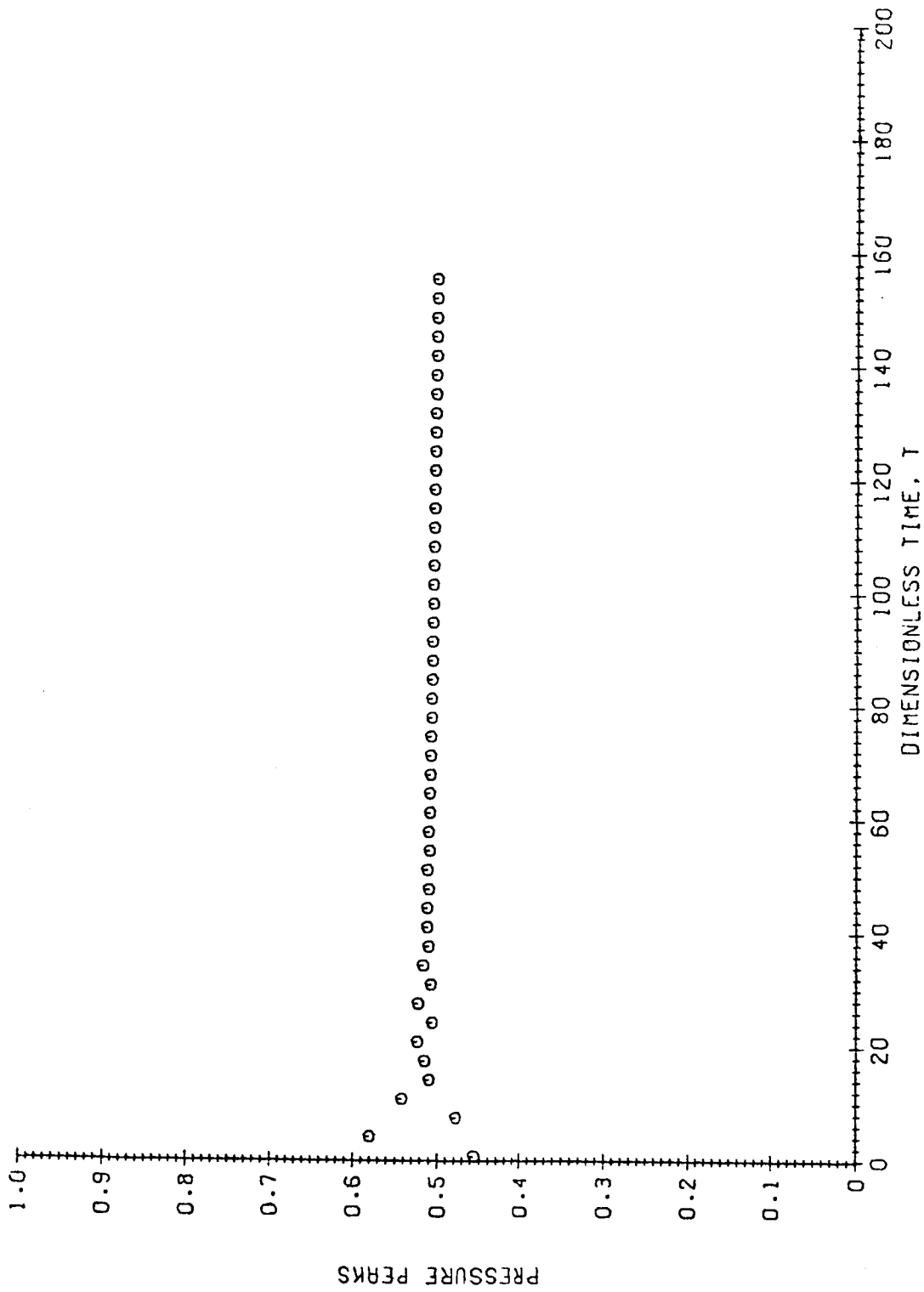


Figure D-3. Sample Amplitude Plot.

FORTTRAN Listing

```
C ***** PROGRAM LCYC3D *****
C
C     THIS PROGRAM CALCULATES THE NONLINEAR BEHAVIOR OF
C     TRANSVERSE, AXIAL, OR COMBINED LONGITUDINAL-TRANSVERSE
C     INSTABILITIES IN A CYLINDRICAL COMBUSTION CHAMBER WITH
C     UNIFORM PROPELLANT INJECTION, DISTRIBUTED COMBUSTION
C     PROCESS, AND A CONVENTIONAL NOZZLE. THE COMBUSTION PROCESS
C     IS DESCRIBED BY CROCCO'S TIME-LAG MODEL. BOTH TRANSIENT
C     AND LIMIT-CYCLE SOLUTIONS ARE CALCULATED.
C
C     THE FOLLOWING INPUTS ARE REQUIRED:
C
C     (1) THE CONTROL NUMBER, NOUTCF.
C     (2) THE COEFFICIENTS FROM PROGRAM COEFFS3D.
C     (3) THE DATA DECK.
C
C     NOUTCF DETERMINES PRINTOUT OF COEFFICIENTS.
C     IF NOUTCF = 0 COEFFICIENTS ARE NOT PRINTED OUT.
C     IF NOUTCF = 1 LINEAR COEFFICIENTS ONLY ARE PRINTED OUT.
C     IF NOUTCF = 2 ALL COEFFICIENTS ARE PRINTED OUT.
C
C     THE DATA DECK CONSISTS OF THE FOLLOWING CARDS:
C
C     FIRST CARD:
C
C     EN IS THE INTERACTION INDEX.
C     TAU IS THE TIME LAG.
C     H IS THE INTEGRATION STEP SIZE.
C     TSTART IS THE TIME AT WHICH OUTPUT STARTS.
C     TQUIT IS THE TIME AT WHICH COMPUTATIONS ARE TERMINATED.
C
C     SECOND CARD:
C
C     NTEST IS TASK CONTROL NUMBER:
C     IF NTEST = 0 COMPUTE TRANSIENT BEHAVIOR.
C     IF NTEST = 1 COMPUTE THE LIMIT-CYCLE BEHAVIOR.
C     JMODE IS THE MODE-AMPLITUDE USED TO TEST FOR LIMIT-CYCLES.
C     NLOC DETERMINES THE LOCATION OF THE WALL PRESSURE MAXIMA
C     AND MINIMA:
C     IF NLOC = 1 LOCATION IS Z = 0, THETA = 0 DEGREES.
C     IF NLOC = 2 LOCATION IS Z = 0, THETA = 45 DEGREES.
C     IF NLOC = 3 LOCATION IS Z = 0, THETA = 90 DEGREES.
C     NTERMS IS THE NUMBER OF TERMS GIVEN INITIAL VALUES.
C     NPZ DETERMINES HOW SECONDARY STABILITY ZONES (PHANTOM
C     ZONES) ARE HANDLED.
C     IF NPZ = 0 PHANTOM ZONES ARE RETAINED.
C     IF NPZ = 1 PHANTOM ZONES ARE ELIMINATED.
C     NOUT IS THE OUTPUT CONTROL NUMBER.
C     IF NOUT = 0 PRINTED OUTPUT ONLY.
C     IF NOUT > 0 BOTH PRINTED AND PLOTTED OUTPUT, NOUT
```



7 ITP/'PRESSURE PEAKS'/

C

LAST = 250  
ERR = 0.001  
TDEL = 10.0  
NPT = 0  
AA(1) = 0.0  
AA(2) = 0.5  
AA(3) = 0.5  
AA(4) = 1.0  
PI = 3.1415927  
READ (5,5003) NOUTCF

C

C

C

C

C

C

C

C

C

\*\*\*\*\* COEFFICIENT INPUT SECTION \*\*\*\*\*

THIS VERSION OF LCYC3D READS THE COEFFICIENT DATA FROM  
A FASTRAND FILE GENERATED BY PROGRAM COEFFS3D. TO READ  
THIS DATA FROM CARDS, USE READ (5,XXXX) INSTEAD OF  
READ (9,XXXX) IN THIS SECTION.

INPUT OF MOTOR PARAMETERS AND NUMBER OF TERMS.  
READ (9,5001) GAMMA, UE, ZE, ZCOMB, NDROPS, NJMAX  
WRITE (6,6001) GAMMA, UE, ZE, ZCOMB, NJMAX  
IF (NDROPS .EQ. 0) WRITE (6,6030)  
IF (NDROPS .EQ. 1) WRITE (6,6031)  
NU = 2 \* NJMAX  
JMX = NJMAX/2  
RLD = 0.5 \* ZE

C

WRITE (6,6002)

C

C

C

INPUT OF DESCRIPTION OF SERIES EXPANSION.

DO 10 K = 1, JMX  
READ (9,5002) NJ, L(NJ), M(NJ), N(NJ), NS(NJ), S(NJ), SJ(NJ),  
1 NAME(NJ)  
WRITE (6,6003) NAME(NJ), NJ, L(NJ), M(NJ), N(NJ), NS(NJ),  
1 S(NJ), SJ(NJ)

10 CONTINUE

C

WRITE (6,6010)  
DO 15 K = 1, JMX  
READ (9,5010) J, YNOZ(J), B(J)  
WRITE (6,6015) J, YNOZ(J), B(J)  
NJ = (2 \* J) - 1  
YR(NJ) = REAL(YNOZ(J))  
YI(NJ) = AIMAG(YNOZ(J))  
YR(NJ+1) = YR(NJ)  
YI(NJ+1) = YI(NJ)

15 CONTINUE

C

```

C   ZERO LINEAR COEFFICIENT ARRAYS.
    DO 20 KC = 1, 3
    DO 20 NJ = 1, 20
    DO 20 NP = 1, 20
    C(KC,NJ,NP) = 0.0
    CP(KC,NJ,NP) = 0.0
20  CONTINUE

C
C   ZERO NONLINEAR COEFFICIENT ARRAY.
    DO 30 NJ = 1, 20
    DO 30 NPQ = 1, 400
    D(NJ,NPQ) = 0.0
30  CONTINUE

C
C   INPUT OF LINEAR COEFFICIENTS.
    DO 40 KC = 1, 3
    READ (9,5003) KMAX
    IF (NOUTCF .GT. 0) WRITE (6,6004) KC, KMAX
    IF (KMAX .EQ. 0) GO TO 40
    DO 45 K = 1, KMAX
    READ (9,5004) NJ, NP, CP(KC,NJ,NP)
    IF (NOUTCF .GT. 0) WRITE (6,6005) KC, NJ, NP, CP(KC,NJ,NP)
45  CONTINUE
40  CONTINUE

C
C
C   INPUT OF NONLINEAR COEFFICIENTS.
    READ (9,5003) NLMAX
    IF (NOUTCF .EQ. 2) WRITE (6,6006) NLMAX
    IF (NLMAX .EQ. 0) GO TO 50
    DO 52 NJ = 1, 20
    KPQMAX(NJ) = 0
52  CONTINUE
    DO 55 K = 1, NLMAX
    READ (9,5005) NJ, NP, NQ, DT
    IF (NOUTCF .EQ. 2) WRITE (6,6007) NJ, NP, NQ, DT
    KPQMAX(NJ) = KPQMAX(NJ) + 1
    KPQ = KPQMAX(NJ)
    IDP(NJ,KPQ) = NP
    IDQ(NJ,KPQ) = NQ
    D(NJ,KPQ) = DT
55  CONTINUE
50  CONTINUE

C
C
C   ***** PRESSURE COEFFICIENT SECTION *****
C
C   CALCULATE SPATIAL COORDINATES FOR PRESSURE COMPUTATION.
    DO 51 NPRES = 1, 3
    Z(NPRES) = 0.0
    RTHETA = NPRES - 1

```



```

    ANGLE(NPRES) = RTHETA * 45.0
    THETA(NPRES) = RTHETA * PI/4.0
    Z(NPRES + 3) = ZE
    ANGLE(NPRES + 3) = ANGLE(NPRES)
    THETA(NPRES + 3) = THETA(NPRES)
51 CONTINUE
C
C   CALCULATE COEFFICIENTS FOR PRESSURE TIME HISTORIES.
DO 53 NPRES = 1, 6
DO 53 J = 1, JMX
NP = (2 * J) - 1
Z1 = Z(NPRES)
ANG = THETA(NPRES)
CALL PHICFS(J,Z1,ANG,C1,C2,C3)
IF (NPRES .EQ. 4) CPHIT(J) = C1
CFT(NPRES,NP) = REAL(C1)
CFT(NPRES,NP+1) = -AIMAG(C1)
CFTH(NPRES,NP) = REAL(C2)
CFTH(NPRES,NP+1) = -AIMAG(C2)
CFZ(NPRES,NP) = REAL(C3)
CFZ(NPRES,NP+1) = -AIMAG(C3)
53 CONTINUE
C
C   OUTPUT OF COEFFICIENTS FOR PRESSURE TIME HISTORIES.
WRITE (6,6020)
DO 56 NPRES = 1, 6
WRITE (6,6014)
DO 56 J = 1, NJMAX
WRITE (6,6021)
1          J, Z(NPRES), ANGLE(NPRES),
          CFT(NPRES,J), CFTH(NPRES,J), CFZ(NPRES,J)
56 CONTINUE
C
C   ***** DATA INPUT SECTION *****
C
C   READ (5,5000) TITLE
C
C   ZERO INITIAL VALUE AND FREQUENCY ARRAYS.
5 DO 57 K = 1, NJMAX
AS(K) = 0.0
AC(K) = 0.0
FRQ1(K) = 0.0
57 CONTINUE
C
C
C   READ COMBUSTION AND CONTROL PARAMETERS.
READ (5,5006, END = 300) EN, TAU, H, TSTART, TQUIT
C
C   READ CONTROL NUMBERS.
READ (5,5008) NTEST, JMODE, NLOC, NTERMS, NPZ, NOUT
JMODE = (2 * JMODE) - 1

```

```

JPMODE = JMODE + NJMAX
IF (NOUT .GT. 0) NPT = 1
C
C
IF (NOUT .EQ. 0) GO TO 9
C
READ DATA FOR SETTING UP PLOTS.
READ (5,5009) YHI(1), YHI(5), YLAB(1), YLAB(5)
READ (5,5008) ITICY(1), ITICY(5), NFIRST, NOMIT
C
C
***** INITIAL AMPLITUDES SECTION *****
C
9 DO 58 K = 1, NTERMS
C
INPUT INITIAL AMPLITUDES FOR F-FUNCTIONS.
READ (5,5007) J, AST, ACT
NJ = (2 * J) - 1
AS(NJ) = AST
AC(NJ) = ACT
C
C
CALCULATE FREQUENCY AND DAMPING.
RL = L(J)
AX = RL * PI/ZE
AXSQ = AX * AX
SSQ = S(J) * S(J)
FRQ1(NJ) = SQRT(SSQ + AXSQ)
DMP1(NJ) = 0.0
FRQ1(NJ+1) = FRQ1(NJ)
DMP1(NJ+1) = DMP1(NJ)
C
C
CALCULATE INITIAL AMPLITUDES FOR G-FUNCTIONS.
C
IF (FRQ1(NJ)) 58, 58, 581
581 GYRU = GAMMA*YR(NJ)*UE
GYIF = GAMMA*YI(NJ)*FRQ1(NJ)
GYRF = GAMMA*YR(NJ)*FRQ1(NJ)
GYIU = GAMMA*YI(NJ)*UE
C
NPRES = 4
IF (NS(J) .EQ. 1) NPRES = 6
C
A1 = (1.0 + GYRU)*CFZ(NPRES,NJ+1)
1 - GYIF*CFT(NPRES,NJ+1)
A2 = GYRF*CFT(NPRES,NJ+1) + GYIU*CFZ(NPRES,NJ+1)
A3 = -(1.0 + GYRU)*CFZ(NPRES,NJ) + GYIF*CFT(NPRES,NJ)
A4 = GYRF*CFT(NPRES,NJ) + GYIU*CFZ(NPRES,NJ)
C
DET = A1*A1 + A2*A2
IF (DET .LT. 0.00001) GO TO 583
R1 = A3*AC(NJ) - A4*AS(NJ)
R2 = -A4*AC(NJ) - A3*AS(NJ)

```

```

C      AC(NJ+1) = (R1*A1 + R2*A2)/DET
      AS(NJ+1) = -(R2*A1 - R1*A2)/DET
      GO TO 58
583 AC(NJ+1) = -AS(NJ)
      AS(NJ+1) = AC(NJ)
C
C      58 CONTINUE
C
C      OUTPUT OF INITIAL AMPLITUDES.
C      WRITE (6,6016)
      DO 590 J = 1, NJMAX
      IF (AS(J)) 591, 592, 591
592 IF (AC(J)) 591, 590, 591
591 WRITE (6,6017) J, DMP1(J), FRQ1(J), AC(J), AS(J)
590 CONTINUE
      IF (NTEST .EQ. 0) WRITE (6,6025)
      IF (NTEST .EQ. 1) WRITE (6,6026)
      IF (NPZ .EQ. 1) WRITE (6,6028)
      IF (NOUT .GE. 1) WRITE (6,6027)
C
C      ***** LINEAR COEFFICIENTS SECTION *****
C
      DO 59 KC = 1, 3
      DO 59 NJ = 1, 10
      KPMAX(KC,NJ) = 0
59 CONTINUE
C
      IF (NPZ .EQ. 0) GO TO 605
      DO 602 J = 1, JMX
      NJ = (2 * J) - 1
      RL = L(J)
      AX = RL * PI/ZE
      AXSQ = AX * AX
      SSQ = S(J) * S(J)
      OMEGA = SQRT(SSQ + AXSQ)
      TAUCUT(NJ) = 2.0 * PI/OMEGA
      TAUCUT(NJ+1) = TAUCUT(NJ)
602 CONTINUE
C
      DO 604 NJ = 1, NJMAX
      DO 604 NP = 1, NJMAX
      IF (TAU .GT. TAUCUT(NP)) CP(3,NJ,NP) = 0.0
604 CONTINUE
C
C      COMPUTE LINEAR COEFFICIENTS FOR GIVEN VALUES OF EN AND TAU.
605 DO 60 NJ = 1, NJMAX
      DO 60 NP = 1, NJMAX
      CT = CP(1,NJ,NP)

```

```

        IF (CT) 61, 62, 61
61  KPMAX(1,NJ) = KPMAX(1,NJ) + 1
    KP = KPMAX(1,NJ)
    IC(1,NJ,KP) = NP
    C(1,NJ,KP) = CT
62  CT = CP(2,NJ,NP) - EN*CP(3,NJ,NP)
    IF (CT) 63, 64, 63
63  KPMAX(2,NJ) = KPMAX(2,NJ) + 1
    KP = KPMAX(2,NJ)
    IC(2,NJ,KP) = NP
    C(2,NJ,KP) = CT
64  CT = EN * CP(3,NJ,NP)
    IF (CT) 65, 60, 65
65  KPMAX(3,NJ) = KPMAX(3,NJ) + 1
    KP = KPMAX(3,NJ)
    IC(3,NJ,KP) = NP
    C(3,NJ,KP) = CT
60  CONTINUE

```

C  
C  
C

```

***** STEP-SIZE COMPUTATION *****

```

```

NDIV = 1.0 + TAU/H
RN = NDIV
H = TAU/RN
H6 = H/6.0

```

C  
C  
C

```

***** INITIAL VALUES SECTION *****

```

```

WRITE (6,6008) EN, TAU, GAMMA, UE, RLD
WRITE (6,6009)
WRITE (6,6022) (ANGLE(J), J = 1,6), (ANGLE(J), J = 1,3)
WRITE (6,6012)
NP1 = NDIV + 1
DO 70 I = 1, NP1
NSTEP = I - NP1
RSTEP = NSTEP
TIME = RSTEP * H
TI(I) = TIME
DO 75 J = 1, NJMAX
JP = J + NJMAX
IF (AC(J)) 751, 753, 751
753 IF (AS(J)) 751, 752, 751
752 U(I,J) = 0.0
    U(I,JP) = 0.0
    GO TO 75
751 ARG = FRQ1(J) * TIME
    FSIN = SIN(ARG)
    FCOS = COS(ARG)
    FEXP = EXP(DMP1(J)*TIME)
    U(I,J) = (AS(J)*FSIN + AC(J)*FCOS) * FEXP

```

```

      U(I,JP) = ((AS(J) * FCOS) - (AC(J) * FSIN)) * FRQ1(J) * FEXP
      1      + DMP1(J) * U(I,J)
75 CONTINUE
C   CALCULATE INITIAL VALUES OF PRESSURE AND VELOCITY.
      DO 704 NPRES = 1, 6
      DO 702 J = 1, NJMAX
      COEF(1,J) = CFT(NPRES,J)
      COEF(2,J) = CFTH(NPRES,J)
      COEF(3,J) = CFZ(NPRES,J)
702 CONTINUE
      DO 703 J = 1, NU
      Y(J) = U(I,J)
703 CONTINUE
      UBAR = 0.0
      IF (NPRES .GT. 3) UBAR = UE
      UMS = 0.0
      IF ((NDROPS.EQ.1) .AND. (NPRES.LT.4)) UMS = UE/(ZE*ZCOMB)
      CALL PRSVEL(UBAR,UMS,Y,P,VTH,VZ)
      PRESS(NPRES) = P
      IF (NPRES .GT. 3) AXVEL(NPRES - 3) = VZ
704 CONTINUE
      PRS(1) = PRESS(NLOC)
C
C   CALCULATE INITIAL VALUES OF NOZZLE B.C.
      CSUM = (0.0,0.0)
      DO 710 J = 1, JMX
      JP = NJMAX + (2 * J) - 1
      FT = Y(JP)
      GT = Y(JP+1)
      A = CMPLX(FT,GT)
      CSUM = CSUM + YNOZ(J) * CPHIT(J) * A
710 CONTINUE
      SUM = REAL(CSUM)
      YPHI = -GAMMA * SUM
      WRITE (6,6011) NSTEP, TIME, (PRESS(J), J = 1,6),
      1      (AXVEL(J), J = 1,3), YPHI
70 CONTINUE
C
      WRITE (6,6008) EN, TAU, GAMMA, UE, RLD
      WRITE (6,6022) (ANGLE(J), J = 1,6), (ANGLE(J), J = 1,3)
C
C   ***** INITIALIZE CONTROL NUMBERS *****
C
      LINE = 8
      K = 0
      MAXNO = 0
      MAXP = 0
      IF (NOUT .EQ. 0) GO TO 100
      JPLOT = 0
      TMIN = TSTART

```

```

TMAX = TSTART + TDEL
YLO(1) = -YHI(1)
DO 90 J = 2,4
YHI(J) = YHI(1)
YLO(J) = YLO(1)
YLAB(J) = YLAB(1)
ITICY(J) = ITICY(1)
90 CONTINUE
YLO(5) = -YHI(5)
YHI(6) = YHI(5)
YLO(6) = YLO(5)
YLAB(6) = YLAB(5)
ITICY(6) = ITICY(5)
C
C ***** NUMERICAL CALCULATIONS SECTION *****
C
100 I = NP1
C
C RUNGE-KUTTA INTEGRATION SCHEME.
105 NSTEP = (I - NP1 + (LAST - NP1) * K)
RSTEP = NSTEP
TIME = RSTEP * H
TI(I) = TIME
DO 110 J = 1, NJMAX
JP = J + NJMAX
RV(J,1) = U(I-NDIV,JP)
RV(J,4) = U(I-NDIV+1,JP)
RV(J,2) = 0.375*RV(J,1) + 0.75*RV(J,4) - 0.125*U(I-NDIV+2,JP)
RV(J,3) = RV(J,2)
110 CONTINUE
DO 120 J = 1, NU
Y(J) = U(I,J)
120 CONTINUE
CALL RHS(NU,1,Y,YP)
DO 130 J = 1, NU
FZ(1,J) = YP(J)
130 CONTINUE
DO 140 II = 2,4
DO 144 J = 1, NU
UZ(J) = Y(J) + AA(II) * H * FZ(II-1,J)
144 CONTINUE
CALL RHS(NU,II,UZ,YP)
DO 148 J = 1, NU
FZ(II,J) = YP(J)
148 CONTINUE
140 CONTINUE
DO 150 J = 1, NU
U(I+1,J) = Y(J) + (FZ(1,J)+2.0*(FZ(2,J)+FZ(3,J)) + FZ(4,J)) * H6
150 CONTINUE
C

```

```

C      CALCULATE PRESSURE TIME HISTORIES.
      DO 154 NPRES = 1, 6
      DO 152 J = 1, NJMAX
      COEF(1,J) = CFT(NPRES,J)
      COEF(2,J) = CFTH(NPRES,J)
      COEF(3,J) = CFZ(NPRES,J)
152  CONTINUE
      UBAR = 0.0
      IF (NPRES .GT. 3) UBAR = UE
      UMS = 0.0
      IF ((NDROPS.EQ.1) .AND. (NPRES.LT.4)) UMS = UE/(ZL*ZCOMB)
      CALL PRSVEL(UBAR,UMS,Y,P,VTH,VZ)
      PRESS(NPRES) = P
      IF (NPRES .GT. 3) AXVEL(NPRES - 3) = VZ
154  CONTINUE
      PRS(I) = PRESS(NLOC)

C
C      CALCULATE VALUES OF NOZZLE B.C.
      CSUM = (0.0,0.0)
      DO 650 J = 1, JMX
      JP = NJMAX + (2 * J) - 1
      FT = Y(JP)
      GT = Y(JP+1)
      A = CMFLX(FT,GT)
      CSUM = CSUM + YNOZ(J) * CPHIT(J) * A
650  CONTINUE
      SUM = REAL(CSUM)
      YPHI = -GAMMA * SUM

C
C
C      DETERMINE MAXIMA AND MINIMA OF PRINCIPAL MODE-AMPLITUDE
C      FUNCTION FOR USE IN DETERMINING LIMIT-CYCLE BEHAVIOR.
      IF (U(I,JPMODE) * U(I+1,JPMODE)) 170, 170, 160
170  PDEN = U(I,JPMODE) - U(I+1,JPMODE)
      IF (PDEN) 171, 160, 171
171  PP = U(I,JPMODE)/PDEN
      PA = (PP - 1.0) * PP * 0.5
      PB = 1.0 - (PP * PP)
      PC = (PP + 1.0) * PP * 0.5
      MAXNO = MAXNO + 1
      UMAX(MAXNO) = PA*U(I-1,JMODE) + PB*U(I,JMODE) + PC*U(I+1,JMODE)
      IF (MAXNO .GE. 500) GO TO 250
160  CONTINUE

C
C      DETERMINE MAXIMUM AND MINIMUM PRESSURE AT LOCATION SPECIFIED
C      BY NLOC.
      DPL = PRS(I) - PRS(I-1)
      DPS = PRS(I-1) - PRS(I-2)
      IF (DPL*DPS) 173, 173, 175
173  PNUM = PRS(I-2) - PRS(I)

```

```

      PDEN = 2.0 * (PRS(I-2) + PRS(I) - 2.0*PRS(I-1))
      IF (PDEN) 174, 175, 174
174  PP = PNUM/PDEN
      FA = (PF - 1.0) * PP * 0.5
      PB = 1.0 - (PF * PP)
      FC = (PF + 1.0) * PP * 0.5
      MAXP = MAXP + 1
      PMAX(MAXP) = PA*PRS(I-2) + FB*PRS(I-1) + FC*PRS(I)
      TIMAX(MAXP) = TI(I-1) + PP*H
      IF (MAXP .GE. 500) GO TO 250
175  CONTINUE
C
      IF (NTEST .EQ. 1) GO TO 155
      IF (TIME .LT. TSTART) GO TO 155
      IF ((NOUT .EQ. 0) .OR. (NOUT .GT. 6)) GO TO 156
C
C ***** TIME HISTORY PLOTTING SECTION *****
C
      IF (TMAX .GT. TQUIT) GO TO 156
      IF ((TIME .GT. TMAX) .OR. (JPLOT .GE. 500)) GO TO 1000
C
      JPLOT = JPLOT + 1
C
C FILL TIME ARRAY FOR PLOTTING.
      TPLOT(JPLOT) = TIME
C
C FILL INJECTOR PRESSURE ARRAYS FOR PLOTTING (THETA = 0, 45, 90)
      DO 1001 J = 1, 3
      YPLOT(J, JPLOT) = PRESS(J)
1001 CONTINUE
C
C FILL NOZZLE PRESSURE ARRAY FOR PLOTTING (THETA = 0)
      YPLOT(4, JPLOT) = PRESS(4)
C
C FILL NOZZLE AXIAL VELOCITY ARRAY FOR PLOTTING (THETA = 0)
      YPLOT(5, JPLOT) = AXVEL(1)
C
C FILL NOZZLE B.C. ARRAY FOR PLOTTING (THETA = 0).
      YPLOT(6, JPLOT) = YPHI
C
      GO TO 156
C
1000 NUM = JPLOT
C
C PLOT TIME HISTORIES.
C
      DO 1020 NPLOT = NFIRST, NOUT
      JPLOT = 0
C

```



```

C   ASSIGN PLOTTING PARAMETERS.
    YMIN = YLO(NPLOT)
    YMAX = YHI(NPLOT)
    NTICY = ITICY(NPLOT)
    DELY = YLAB(NPLOT)

C
C   ELIMINATE POINTS THAT ARE OUT OF THE ORDINATE RANGE.
    DO 1010 J = 1, NUM
    IF ((YPLOT(NPLOT,J) .LT. YMIN) .OR. (YPLOT(NPLOT,J) .GT. YMAX))
1   GO TO 1010
    JPLOT = JFLOT + 1
    DUMMYT(JPLOT) = TFLOT(J)
    DUMMYY(JPLOT) = YPLOT(NPLOT,J)
1010 CONTINUE

C
    IF (JPLOT .EQ. 0) GO TO 1020
    GO TO (1011,1012,1013,1014,1015,1016), NPLOT

C
C   PLOT INJECTOR PRESSURE AT THETA = 0 DEGREES.
1011 CALL GRAPHS(IBUF,3000,4,JPLOT,11,NTICY,TMAX,YMAX,TMIN,YMIN,
1   ITT,ITY1,21,41,DUMMYT,DUMMYY,2.0,DELY,TITLE)
    GO TO 1020

C
C   PLOT INJECTOR PRESSURE AT THETA = 45 DEGREES.
1012 IF (M(JMODE) .EQ. 0) GO TO 1020
    CALL GRAPHS(IBUF,3000,4,JPLOT,11,NTICY,TMAX,YMAX,TMIN,YMIN,
1   ITT,ITY2,21,42,DUMMYT,DUMMYY,2.0,DELY,TITLE)
    GO TO 1020

C
C   PLOT INJECTOR PRESSURE AT THETA = 90 DEGREES.
1013 IF (M(JMODE) .EQ. 0) GO TO 1020
    CALL GRAPHS(IBUF,3000,4,JPLOT,11,NTICY,TMAX,YMAX,TMIN,YMIN,
1   ITT,ITY3,21,42,DUMMYT,DUMMYY,2.0,DELY,TITLE)
    GO TO 1020

C
C   PLOT NOZZLE PRESSURE AT THETA = 0 DEGREES.
1014 CALL GRAPHS(IBUF,3000,4,JPLOT,11,NTICY,TMAX,YMAX,TMIN,YMIN,
1   ITT,ITY4,21,39,DUMMYT,DUMMYY,2.0,DELY,TITLE)
    GO TO 1020

C
C   PLOT NOZZLE AXIAL VELOCITY AT THETA = 0 DEGREES.
1015 CALL GRAPHS(IBUF,3000,4,JPLOT,11,NTICY,TMAX,YMAX,TMIN,YMIN,
1   ITT,ITY5,21,32,DUMMYT,DUMMYY,2.0,DELY,TITLE)
    GO TO 1020

C
C   PLOT NOZZLE B.C. AT THETA = 0 DEGREES.
1016 CALL GRAPHS(IBUF,3000,4,JPLOT,11,NTICY,TMAX,YMAX,TMIN,YMIN,
1   ITT,ITY6,21,44,DUMMYT,DUMMYY,2.0,DELY,TITLE)
C
1020 CONTINUE

```

```

C
C REASSIGN PLOTTING PARAMETERS FOR NEXT SET OF PLOTS.
  JPLOT = 0
  TMIN = TMAX
  TMAX = TMAX + TDEL
C
C ***** TIME HISTORY PRINTED OUTPUT SECTION *****
C
156 WRITE (6,6011) NSTEP, TIME, (PRESS(J), J = 1,6),
  1 (AXVEL(J), J = 1,3), YFHI
  LINE = LINE + 1
157 IF (TIME .GT. TQUIT) GO TO 250
  IF (LINE .LT. 52) GO TO 155
  WRITE (6,6013)
  WRITE (6,6022) (ANGLE(J), J = 1,6), (ANGLE(J), J = 1,3)
  LINE = 4
C
155 I = I + 1
  IF (I .LT. LAST) GO TO 105
C
C ***** LIMIT-CYCLE SECTION *****
C
C TEST FOR LIMIT CYCLE.
  K = K + 1
  IF ((NTEST .EQ. 0) .OR. (MAXNO .LT. 80)) GO TO 190
  UTOT = 0.0
  DO 180 J = 0, 3
    JMAX = MAXNO - J
    UTOT = UTOT + ABS(UMAX(JMAX))
180 CONTINUE
  UAVG(K) = UTOT/4.0
  IF (K .EQ. 1) GO TO 190
  CHANGE = UAVG(K) - UAVG(K-1)
  ABSCHG = ABS(CHANGE/UAVG(K))
  IF (ABSCHG .GT. ERR) GO TO 190
  TM = TIME/2.0
  ITM = TM
  ITM = 2*ITM + 2
  TM = ITM
  TSTART = TM + TSTART
  TQUIT = TM + TQUIT
  TMIN = TSTART
  TMAX = TSTART + TDEL
  NTEST = 0
C
C RE-ASSIGN ARRAYS.
190 DO 200 I = 1, NP1
  ILAST = LAST - NP1 + I
  PRS(I) = PRS(ILAST)
  TI(I) = TI(ILAST)

```

```

DO 200 J = 1, NU
U(I,J) = U(ILAST,J)
200 CONTINUE
GO TO 100

C
C
C ***** PRESSURE MAXIMA AND MINIMA PRINTOUT *****
C
250 WRITE (6,6023) Z(NLOC), ANGLE(NLOC), MAXP
LINE = 4
DO 255 JST = 1, MAXP, 8
JSTART = JST
JSTOP = JST + 7
IF (JSTOP .GT. MAXP) JSTOP = MAXP
WRITE (6,6024) (PMAX(J), J = JSTART, JSTOP)
WRITE (6,6024) (TIMAX(J), J = JSTART, JSTOP)
WRITE (6,6014)
LINE = LINE + 3
IF (LINE .LT. 52) GO TO 255
LINE = 0
WRITE (6,6013)
255 CONTINUE
IF ((NOUT .EQ. 0) .OR. (NOMIT .EQ. 1)) GO TO 5

C
C ***** PRESSURE MAXIMA PLOTTING SECTION *****
C
DETERMINE LARGEST VALUE OF FMAX.
AMPMAX = 0.0
DO 260 J = 1, MAXP
IF (PMAX(J) .LT. AMPMAX) GO TO 260
AMPMAX = FMAX(J)
260 CONTINUE

C
C RANGE OF PLOT AND COORDINATE LABELING.
ITM = AMPMAX + 1.0
AMPMAX = ITM
ITM = 1.0 + TIMAX(MAXP)/50.0
TMAX = ITM * 50
DELX = TMAX/10.0
DELY = AMPMAX/10.0

C
C ELIMINATE NEGATIVE VALUES.
JFLOT = 0
DO 262 J = 1, MAXP
IF (PMAX(J)) 262, 264, 264
264 JFLOT = JFLOT + 1
DUMMYT(JFLOT) = TIMAX(J)
DUMMYY(JFLOT) = FMAX(J)
262 CONTINUE

C

```

```

C      PLOT VALUES.
      CALL GRAPHS(1BUF, 3000, 4, JPLOT, 101, 101, TMAX, AMPMAX, 0.0, 0.0,
1          ITT, ITP, 21, 14, DUMMYT, DUMMY, DELX, DELY, TITLE)
C
      GO TO 5
C
      TURN OFF PLOTTING ROUTINE.
300 IF (NPT.EQ. 1) CALL SHPARG
C
      ***** READ FORMAT SPECIFICATIONS *****
C
5000 FORMAT (12A6)
5001 FORMAT (4F10.0, 2I5)
5002 FORMAT (5I5, 2F10.5, 1X, A4)
5003 FORMAT (I5)
5004 FORMAT (2I5, F15.6)
5005 FORMAT (3I5, F15.6)
5006 FORMAT (5F10.0)
5007 FORMAT (I5, 2F10.0)
5008 FORMAT (7I5)
5009 FORMAT (7F10.0)
5010 FORMAT (I5, 4F10.5)
C
      ***** WRITE FORMAT SPECIFICATIONS *****
C
6001 FORMAT (1H1, 9H GAMMA = , F5.3, 5X, 5HUE = , F5.3,
1          5X, 5HZE = , F8.5, 5X, 8HZCOMB = , F5.2,
2          5X, 8HNJMAX = , I2//)
6002 FORMAT (2X, 29HNAME      J      L      M      N      NS, 7X, 3HSMN, 3X,
1          7HJM(SMN)//)
6003 FORMAT (2X, A4, 5I5, 2F10.5)
6004 FORMAT (1H0, 26H NUMBER OF COEFFICIENTS C(, I1, 10H, NJ, NP) IS, I5//)
6005 FORMAT (2X, 2HC(, I1, 1H, , I2, 1H, , I2, 4H) = , F10.5)
6006 FORMAT (1H0, 38H NUMBER OF COEFFICIENTS D(NJ, NP, NQ) IS, I5//)
6007 FORMAT (2X, 2HD(, I2, 1H, , I2, 1H, , I2, 4H) = , F10.5)
6008 FORMAT(1H1, 45H COMBUSTION PARAMETERS: INTERACTION INDEX = , F7.5,
1          12X, 11HTIME-LAG = , F7.5/2X, 17HMOTOR PARAMETERS:, 19X,
2          8HGAMMA = , F7.5, 23H      EXIT MACH NUMBER = , F7.5,
3          22H      LENGTH/DIAMETER = , F7.5//)
6009 FORMAT (2X, 18HINITIAL CONDITIONS//)
6010 FORMAT (1H0, 5X, 1HJ, 8X, 2HYR, 8X, 2HYI, 7X, 3HEPS, 7X, 3HETA//)
6011 FORMAT (2X, I5, F12.5, 10F10.5)
6012 FORMAT (1H0)
6013 FORMAT (1H1)
6014 FORMAT (1H )
6015 FORMAT (2X, I5, 4F10.5)
6016 FORMAT (1H1, 36H INITIAL CONDITIONS ARE OF THE FORM://
1          2X, 49HU(I, J) = AC(J)*COS(FREQ*T) + AS(J)*SIN(FREQ*T)),
2          14H * EXP(DAMP*T)//6X, 1HJ, 8X, 7HDAMPING,
3          6X, 9HFREQUENCY, 10X, 5HAC(J), 10X, 5HAS(J)//)

```

```

6017 FORMAT (2X, I5, 4F15.8/)
6020 FORMAT (1H1, 46H COEFFICIENTS FOR COMPUTATION OF WALL PRESSURE,
1      10H WAVEFORMS///43X, 27HCOEFFICIENTS IN SERIES FOR://
2      22X, 5HTHETA, 10X, 4HTIME, 10X, 5HTHETA, 10X, 5HAXIAL/
3      6X, 1HJ, 9X, 1HZ, 3X, 9H(DEGREES), 5X, 10HDERIVATIVE,
4      5X, 10HDERIVATIVE, 5X, 10HDERIVATIVE//)
6021 FORMAT (2X, I5, F10.3, F12.1, 3F15.7)
6022 FORMAT (26X, 17HINJECTOR PRESSURE, 14X, 15HNOZZLE PRESSURE,
1      12X, 21HNOZZLE AXIAL VELOCITY/3X, 4HSTEP, 8X, 4HTIME,
2      F5.0, 5H DEG., F5.0, 5H DEG., F5.0, 5H DEG.,
3      F5.0, 5H DEG., F5.0, 5H DEG., F5.0, 5H DEG.,
4      F5.0, 5H DEG., F5.0, 5H DEG., F5.0, 5H DEG., 6X, 4HYPHI//)
6023 FORMAT (1H1, 38H PRESSURE MAXIMA AND MINIMA AT:  Z = , F5.2,
1      11H THETA = , F4.1/19H VALUES COMPUTED: , I3//)
6024 FORMAT (1H , 7X, 8F13.6)
6025 FORMAT (2X//2X, 37HTHE TRANSIENT BEHAVIOR IS CALCULATED.)
6026 FORMAT (2X//2X, 39HTHE LIMIT-CYCLE BEHAVIOR IS CALCULATED.)
6027 FORMAT (2X//2X, 33HTHIS RUN PRODUCES PLOTTED OUTPUT.)
6028 FORMAT (2X//2X, 'THE PHANTOM ZONES ARE ELIMINATED.')
6030 FORMAT (2X, 'DROPLET MOMENTUM SOURCE IS NEGLECTED'//)
6031 FORMAT (2X, 'DROPLET MOMENTUM SOURCE IS INCLUDED'//)
      END

```

```

SUBROUTINE PHICFS(NP,Z,THETA,CT,CTH,CZ)
C
C THIS SUBROUTINE COMPUTES THE COEFFICIENTS NEEDED TO
C CALCULATE THE WALL PRESSURE PERTURBATION.
C
C NP IS THE INDEX OF THE COMPLEX SERIES TERM.
C Z IS THE AXIAL LOCATION.
C THETA IS THE AZIMUTHAL LOCATION.
C CT IS THE COEFFICIENT IN THE SERIES FOR THE TIME DERIVATIVE OF
C THE VELOCITY POTENTIAL.
C CTH IS THE COEFFICIENT IN THE SERIES FOR THE THETA DERIVATIVE
C OF THE VELOCITY POTENTIAL.
C CZ IS THE COEFFICIENT IN THE SERIES FOR THE AXIAL DERIVATIVE
C OF THE VELOCITY POTENTIAL.
C
COMPLEX CI, CZ, CAXI, CAXIZ, CRAD, CAZI, CAZITH,
1 COMMON B(10), CT, CTH, CZ
C COMMON /BLK2/ M(10), NS(10), SJ(10), B

CI = (0.0,1.0)
CZ = CMPLX(Z,0.0)
CAXI = CCOSH(CI * B(NP) * CZ)
CAXIZ = CI * B(NP) * CSINH(CI * B(NP) * CZ)
CRAD = CMPLX(SJ(NP),0.0)
EM = M(NP)
ARG = EM * THETA
FSIN = SIN(ARG)
FCOS = COS(ARG)
AZI = FCOS
IF (NS(NP) .EQ. 1) AZI = FSIN
AZITH = EM * FCOS
IF (NS(NP) .EQ. 2) AZITH = -EM * FSIN
CAZI = CMPLX(AZI,0.0)
CAZITH = CMPLX(AZITH,0.0)
C
CT = CAZI * CAXI * CRAD
CTH = CAZITH * CAXI * CRAD
CZ = CAZI * CAXIZ * CRAD
C
RETURN
END

```

```

SUBROUTINE PRSVEL(UBAR, UMS, Y, P, VTH, VZ)
C
C THIS SUBROUTINE COMPUTES THE WALL PRESSURE AND VELOCITY.
C
C UBAR IS THE LOCAL AXIAL STEADY STATE MACH NUMBER.
C UMS IS THE DERIVATIVE OF THE MACH NUMBER FOR THE CASE
C WHEN DROPLET MOMENTUM SOURCES ARE INCLUDED.
C Y IS THE ARRAY CONTAINING VALUES OF THE MODE-AMPLITUDE
C FUNCTIONS AND THEIR DERIVATIVES.
C P IS THE VALUE OF THE WALL PRESSURE PERTURBATION.
C VTH IS THE TANGENTIAL COMPONENT OF VELOCITY AT THE WALL.
C VZ IS THE AXIAL COMPONENT OF VELOCITY AT THE WALL.
C
C DIMENSION Y(40), SUM(4), SUMSQ(3)
C COMMON /BLK3/ NJMAX, NLMAX, GAMMA, COEF(3,20)
C
C DO 10 I = 1, 4
C SUM(I) = 0.0
10 CONTINUE
C
C DO 20 I = 1, 4
C DO 20 J = 1, NJMAX
C JY = J
C IF (I .EQ. 1) JY = J + NJMAX
C II = I
C IF (I .EQ. 4) II = 1
C SUM(I) = SUM(I) + Y(JY) * COEF(II,J)
20 CONTINUE
C
C PLIN = SUM(1) + UBAR*SUM(3) + UMS*SUM(4)
C PNL = 0.0
C IF (NLMAX .EQ. 0) GO TO 40
C DO 30 I = 1, 3
C SUMSQ(I) = SUM(I) * SUM(I)
30 CONTINUE
C PNL = 0.5 * (SUMSQ(2) + SUMSQ(3) - SUMSQ(1))
C
C 40 P = -GAMMA * (PLIN + PNL)
C VTH = SUM(2)
C VZ = SUM(3)
C
C RETURN
C END

```

```

SUBROUTINE RHS(NU,II,U,UP)
C
DIMENSION      U(NU), UP(NU)
COMMON         RV(20,4), C(3,20,20), D(20,400),
1             KPMAX(3,20), IC(3,20,20), KPGMAX(20),
2             IDP(20,400), IDQ(20,400)
COMMON         /BLK3/  NJMAX, NLMAX, GAMMA, COEF(3,20)
C
DO 10 NJ = 1, NJMAX
NJP = NJ + NJMAX
UP(NJ) = U(NJP)
SL1 = 0.0
SL2 = 0.0
SL3 = 0.0
SNL = 0.0
MAX = KPMAX(1,NJ)
IF (MAX .EQ. 0) GO TO 25
DO 20 KP = 1, MAX
NP = IC(1,NJ,KP)
SL1 = SL1 + (C(1,NJ,KP) * U(NP))
20 CONTINUE
25 MAX = KPMAX(2,NJ)
IF (MAX .EQ. 0) GO TO 35
DO 30 KP = 1, MAX
NPP = IC(2,NJ,KP) + NJMAX
SL2 = SL2 + (C(2,NJ,KP) * U(NPP))
30 CONTINUE
35 MAX = KPMAX(3,NJ)
IF (MAX .EQ. 0) GO TO 45
DO 40 KP = 1, MAX
NP = IC(3,NJ,KP)
SL3 = SL3 + (C(3,NJ,KP) * RV(NP,II))
40 CONTINUE
45 IF (NLMAX .EQ. 0) GO TO 55
MAX = KPGMAX(NJ)
IF (MAX .EQ. 0) GO TO 55
DO 50 KPG = 1, MAX
NP = IDP(NJ,KPG)
NQP = IDQ(NJ,KPG) + NJMAX
SNL = SNL + (D(NJ,KPG) * U(NP) * U(NQP))
50 CONTINUE
55 UP(NJP) = -(SL1 + SL2 + SL3 + SNL)
10 CONTINUE
RETURN
END

```



COMPILER (FLD=ABS)  
 SUBROUTINE GRAPH8(IBUF,NLOC,LDEV,NTOT,NTICK,NTICY,  
 1 XMAX,YMAX,XMIN,YMIN,ITITLX,ITITLY,LTITLX,LTITLY,XARRAY,  
 2 YARRAY,DELX,DELY,TITLE)

C IDENTIFIER	MEANING	TYPE
C IBUF:	ADDRESS OF BUFFER AREA FOR PLOT OUTPUT	INTEGER
C NLOC:	NUMBER OF LOCATIONS IN BUFFER AREA (>=2000)	INTEGER
C LDEV:	LOGICAL DEVICE NUMBER FOR PLOT	INTEGER
C NTOT:	NUMBER OF POINTS TO BE PLOTTED	INTEGER
C NTICK:	NUMBER OF TIC MARKS ON ABSCISSA (>=2)	INTEGER
C NTICY:	NUMBER OF TIC MARKS ON ORDINATE (>=2)	INTEGER
C XMAX:	UPPER LIMIT OF ABSCISSA DOMAIN	REAL
C YMAX:	UPPER LIMIT OF ORDINATE RANGE	REAL
C XMIN:	LOWER LIMIT OF ABSCISSA DOMAIN	REAL
C YMIN:	LOWER LIMIT OF ORDINATE RANGE	REAL
C ITITLX:	ABSCISSA LABEL	FIELDATA ARRAY
C ITITLY:	ORDINATE LABEL	FIELDATA ARRAY
C LTITLX:	NUMBER OF CHARACTERS IN ITITLX	INTEGER
C LTITLY:	NUMBER OF CHARACTERS IN ITITLY	INTEGER
C XARRAY:	ABSCISSA POINTS IN TERMS OF XMIN-XMAX COORD'S	REAL ARRAY
C YARRAY:	ORDINATE POINTS IN TERMS OF YMIN-YMAX COORD'S	REAL ARRAY
C DELX:	INTERVALS OF ABSCISSA TIC MARK LABELING IN TERMS OF XMIN-XMAX COORDINATES	REAL
C DELY:	INTERVALS OF ORDINATE TIC MARK LABELING IN TERMS OF YMIN-YMAX COORDINATES	REAL
C TITLE:	LABEL FOR THE WHOLE RUN	FIELDATA ARRAY

DIMENSION IBUF(NLOC),XARRAY(NTOT),YARRAY(NTOT),ITITLX(1),  
 1 ITITLY(1),YDIT(100)  
 DIMENSION TITLE(1)

FIXED BASIC PARAMETERS

LOGICAL ZERO  
 DEFINE ZERO=NDEC.LT.0.AND.ABS(FPN).LT.5  
 1 .OR.NDEC.GT.0.AND.ABS(FPN).LT.5.\*10.\*\*(-NDEC-1)  
 DEFINE DNDEC=NDEC-FLD(0,36,ZERO)\*NDEC-FLD(0,36,ZERO)  
 DEFINE IFIX(FARG)=INT(FARG+.5)  
 DATA J/1/  
 DATA HEIGHT/.105/  
 DATA INTEG/1/  
 DATA ABSCIS/8./  
 DATA ORDINA/6./  
 DATA ICODE/-1/

```
DATA TOPMAR/1./
DATA BOTMAR/1.5/
REAL LEFMAR
DATA LEFMAR/1.9/
DATA RYTMAR/1.1/
DATA FACT/1./
DATA MAXIS/1/
DATA MLINE/1/
DATA HTLAB/.105/
```

```
C -----
C
C 19 INITIAL COMPUTATION OF DERIVED PARAMETERS
C AND INITIAL PLOTS CALL
C 20 SKIPS PRELIMINARIES FOR 2ND AND SUBSEQUENT CALLS
C -----
C
```

```
GO TO (19,20),J
19 YDIT(1) = 3./19.
TICKLE = HEIGHT/2.
ROTFAC = - 3./14. * HEIGHT - 4./7. * HEIGHT
STARTL = 6 * HEIGHT + ROTFAC + TICKLE
SEPLAB = STARTL + 1.5 * HEIGHT
SYMBLH = 0.070
REAL LABSEP
LABSEP = 4. * HEIGHT
ASTART = 2. * HEIGHT
DO 1 I = 2,100
1 YDIT(I) = YDIT(I - 1) + (2 * MOD(I,2) + 1)/19.
YDIT(100) = YDIT(100) + .5
CALL PLOTS(IBUF,NLOC,LDEV)
CALL FACTOR(1.)
J = 2
CALL SYMBOL (HEIGHT,36 * HEIGHT + 5.5,HEIGHT,TITLE,270.,72)
CALL PLOT(1., - .5, - 3)
3 DO 2 I = 1,100
2 CALL PLOT(0.,YDIT(I),3 - MOD(I,2))
DO 33 I = 1,100
33 YDIT(I) = YDIT(I) - ABSCIS - RYTMAR
```

```
C -----
C
C RESET ORIGIN
C -----
C
```

```
XPAGE = BOTMAR + ORDINA
GO TO 2019
20 XPAGE = BOTMAR + ORDINA + TOPMAR
2019 CALL WHERE(RXPAGE,RYPAGE,FACT)
YPAGE = RYPAGE - LEFMAR
CALL PLOT(XPAGE,YPAGE, - 3)
CALL FACTOR(FACT)
```

```

C -----
C
C   DRAW AXES AND LABELING MAXIS TIMES
C
C -----
100  DO 100 I = 1,MAXIS
      CALL MYAXIS
C -----
C
C   DRAW POINTS, OPTIONAL CENTERLINE, AND PAGE SCISSORLINE
C   MLINE TIMES
C
C -----
200  DO 200 I = 1,MLINE
      CALL MYLINE
      RETURN
C -----
C
C   ENTRY POINT SHPARG
C   TERMINATE PLOTTING SEQUENCE
C
C -----
      ENTRY SHPARG
      CALL WHERE(RXPAGE,RYPAGE,1)
      CALL PLOT(RXPAGE,RYPAGE,999)
      RETURN
C -----
C
C   SUBROUTINE MYAXIS (INTERNAL)
C
C -----
      SUBROUTINE MYAXIS
      STARTL = 6 * HEIGHT + ROTFAC + TICKLE
      IMAX = IFIX((YMAX - YMIN)/DELY)
      TICSEP = ORDINA/(ABS(NTICY) - 1)
      CALL DENDEC(YMAX,DELY,NDEC)
      K = 1
      N = (ABS(NTICY)/IMAX) - 1 + MOD(ABS(NTICY),2)
      DO 9 I = 0,IMAX
      GO TO (11,12),K
11   IF(2 * I.LT.IMAX)GO TO 12
      CALL AXLAB(0.,ITITLY,LTITLY,HTLAB)
      K = 2
12   FPN = YMAX - I * DELY
      IF(ZERO)FPN = 0.
      TMID = 1.
      XPAGE = - I * ORDINA/IMAX - .5 * HEIGHT
      IF(FPN)113,122,118
113  IF(NDEC - 2)115,114,112
114  YPAGE = STARTL

```

```

GO TO 112
115 IF(NDEC - 1)117,116,112
116 YPAGE = STARTL - HEIGHT
GO TO 112
117 IF(ABS(FPN) - 100.)119,116,116
119 IF(ABS(FPN) - 10.)120,121,121
120 YPAGE = STARTL - 3 * HEIGHT
GO TO 112
121 YPAGE = STARTL - 2 * HEIGHT
GO TO 112
122 YPAGE = STARTL - 4 * HEIGHT
GO TO 112
118 IF(NDEC - 2)123,116,112
123 IF(NDEC - 1)125,124,112
124 IF(FPN - 10.)121,116,116
125 IF(FPN - 10.)122,120,126
126 IF(FPN - 100.)120,121,127
127 IF(FPN - 1000.)121,116,128
128 IF(FPN - 10000.)116,114,114
112 NNDEC = DNDEC
CALL NUMBER(XPAGE,YPAGE,HEIGHT,FPN,270.,NNDEC)
XPAGE = - I * (ORDINA/IMAX)
DO 10 JJ = 1,N
YPAGE = TICKLE * TMID
CALL PLOT(XPAGE,YPAGE,3)
YPAGE = YPAGE * ( - 1 + I/IMAX * .5)
CALL PLOT(XPAGE,YPAGE,2)
IF(I/IMAX)110,110,9
110 YPAGE = 0
CALL PLOT(XPAGE,YPAGE,3)
XPAGE = XPAGE - TICSEP
CALL PLOT(XPAGE,YPAGE,2)
TMID = .5
10 CONTINUE
9 CONTINUE
K = 1
IMAX = IFIX((XMAX - XMIN)/DELX)
TICSEP = ABSCIS/(NTICX - 1)
XPAGE = - ASTART - ORDINA
CALL DENDEC(XMAX,DELX,NDEC)
DO 28 I = 0,IMAX
STARTL = - I * ABSCIS/IMAX
GO TO (24,25),K
24 IF(2 * I.LT.IMAX)GO TO 25
CALL AXLAB(270.,ITITLX,LTITLX,HTLAB)
K = 2
XPAGE = - ASTART - ORDINA
25 FPN = XMIN + I * DELX
IF(ZERO)FPN = 0.
IF(FPN)813,822,818
813 IF(NDEC - 2)815,811,23
814 YPAGE = STARTL + 16./7. * HEIGHT
GO TO 23
815 IF(NDEC - 1)817,816,23

```

```

816 YPAGE = STARTL + 25./14. * HEIGHT
GO TO 23
817 IF(ABS(FPN) - 100.)819,816,816
819 IF(ABS(FPN) - 10.)820,821,821
820 YPAGE = STARTL + 11./14. * HEIGHT
GO TO 23
821 YPAGE = STARTL + 9./7. * HEIGHT
GO TO 23
822 YPAGE = STARTL + 2./7. * HEIGHT
GO TO 23
818 IF(NDEC - 2)823,816,23
823 IF(NDEC - 1)825,824,23
824 IF(FPN - 10.)821,816,816
825 IF(FPN - 10.)822,820,826
826 IF(FPN - 100.)820,821,827
827 IF(FPN - 1000.)821,816,828
828 IF(FPN - 10000.)816,814,814
23 NNDEC = DNDEC
28 CALL NUMBER(XPAGE,YPAGE,HEIGHT,FPN,270.,NNDEC)
N = (NTICKX/IMAX) - 1 + MOD(NTICKX,2)
DO 26 I = IMAX,0, - 1
  TMID = 1.
  YPAGE = - I * ABSCIS/IMAX
  DO 27 JJ = 1,N
    XPAGE = - ORDINA - TICKLE * TMID
    CALL PLOT(XPAGE,YPAGE,3)
    XPAGE = XPAGE + (TICKLE + FLD(0,36,I.NE.0) * TICKLE) * TMID
    CALL PLOT(XPAGE,YPAGE,2)
    IF(I)111,26,111
111 XPAGE = - ORDINA
    CALL PLOT(XPAGE,YPAGE,3)
    YPAGE = YPAGE + TICSEP
    CALL PLOT(XPAGE,YPAGE,2)
    TMID = .5
27 CONTINUE
26 CONTINUE
RETURN
C -----
C
C SUBROUTINE MYLINE (INTERNAL)
C -----
C
SUBROUTINE MYLINE
ITOP = IFIX((ABSCIS + RYTMAR + .5)/11. * 99.)
IBOT = IFIX(RYTMAR/11. * 99.)
DO 17 I = 1,NTOT
  XPAGE = (YARRAY(I) - YMAX)/(YMAX - YMIN) * ORDINA
  YPAGE = (XMIN - XARRAY(I))/(XMAX - XMIN) * ABSCIS
17 CALL SYMBOL(XPAGE,YPAGE,SYMBLH,INTEG,270.,ICODE)
IF(NTICY.GE.0)GO TO 22
XPAGE = - ORDINA/2.
YPAGE = - ABSCIS
CALL PLOT(XPAGE,YPAGE,3)
DO 18 I = IBOT,ITOP

```

```

18 CALL PLOT(XPAGE,YDIT(I),3 - MOD(I,2))
22 XPAGE = TOPMAR
   YPAGE = - ABSCIS - RYTMAR - .5
   CALL PLOT(XPAGE,YPAGE,3)
   DO 21 I = 1,100
21 CALL PLOT(XPAGE,YDIT(I),3 - MOD(I,2))
   RETURN

```

```

C -----
C
C SUBROUTINE AXLAB (INTERNAL)
C
C -----

```

```

SUBROUTINE AXLAB(ANGLE,IBCD,NCHARX,HEIGHT)
DIMENSION IBCD(7)
LOGICAL S
INTEGER QSQ/' S'/
K = 2
NCHAR = NCHARX
S = .FALSE.
IF(ABS(ANGLE).GT..1)GO TO 30
XPAGE = - ORDINA/2. - NCHAR * HEIGHT/2
YPAGE = SEPLAB
GO TO 31
30 XPAGE = - ORDINA - LABSEP
   YPAGE = - ABSCIS/2. + NCHAR * HEIGHT/2
31 LSTART = 6 * MOD(NCHAR,6) - 12
   IF(LSTART.EQ. - 12)LSTART = 24
   LOOK = NCHAR/6 + 1.1
   IF(LSTART.EQ. - 6)GO TO 13
   IF(FLD(0,12,'S').EQ.FLD(LSTART,12,IBCD(LOOK)))GO TO 15
   GO TO 14
13 IF(FLD(0,6,'').NE.FLD(30,6,IBCD(LOOK - 1)))GO TO 14
   IF(FLD(0,6,'S').NE.FLD(0,6,IBCD(LOOK)))GO TO 14
15 NCHAR = NCHAR - 1
   S = .TRUE.
14 CALL SYMBOL(XPAGE,YPAGE,HEIGHT,IBCD,ANGLE,NCHAR)
   IF(S)CALL SYMBOL(999.,999.,2 * HEIGHT/3, QSQ, ANGLE, 2)
   RETURN

```

```

C -----
C
C SUBROUTINE DENDEC (INTERNAL)
C
C -----

```

```

SUBROUTINE DENDEC(QMAX,DELQ,NDEC)
IF(INT(ABS(QMAX)).GE.10)GO TO 5
IF(AMOD(ABS(QMAX - DELQ),.1).GE..01)GO TO 7
NDEC = 1
RETURN
5 NDEC = - 1
  RETURN
7 NDEC = 2
  RETURN
END

```

## APPENDIX E

### USER'S MANUAL FOR THE LINEAR STABILITY PROGRAMS: LINSOL AND LSTB3D

#### General Description

Two auxiliary programs, LINSOL and LSTB3D, calculate the linear stability characteristics of a cylindrical combustion chamber with distributed combustion and a conventional nozzle. For given values of the operating parameters (i.e.,  $n$ ,  $\bar{\tau}$ ,  $\gamma$ ,  $\bar{u}_e$ , and  $L/D$ ) and a given nozzle admittance (i.e.,  $A$  and  $\varphi$ ), Program LINSOL calculates the growth rate,  $\Lambda$ , and the frequency,  $\omega$ , of a given acoustic mode. For given values of  $\bar{\tau}$  Program LSTB3D calculates the corresponding values of  $n$  and  $\omega$  for neutral stability ( $\Lambda = 0$ ). These programs are based on an analytical solution of the linearized version of Eqs. (12). After a discussion of the linear analysis, Programs LINSOL and LSTB3D will be described.

#### Linear Analysis

For a single acoustic mode, dropping the nonlinear terms in Eqs. (12) yields the following linear equation:

$$\frac{d^2 A}{dt^2} + C_1 A + (C_2 - nC_3) \frac{dA}{dt} + nC_3 \frac{d[A(t - \bar{\tau})]}{dt} = 0 \quad (\text{E-1})$$

where  $A(t)$  is the unknown complex amplitude function for the mode under consideration and the coefficients are obtained from Eqs. (C-1) through (C-4) by dividing by  $C_0$ . Thus the coefficients are complex numbers given by:

$$C_1 = S_{mn}^2 + \frac{Z'(z_e)Z^*(z_e) - \int_0^{z_e} Z''Z^* dz}{\int_0^{z_e} ZZ^* dz} \quad (\text{E-2})$$

$$C_2 = \frac{2 \int_0^{z_e} \bar{u}(z) Z' Z^* dz + \gamma \int_0^{z_e} \frac{d\bar{u}}{dz} Z Z^* dz + \gamma Y Z(z_e) Z^*(z_e)}{\int_0^{z_e} Z Z^* dz} \quad (\text{E-3})$$

$$C_3 = \frac{\gamma \int_0^{z_e} \frac{d\bar{u}}{dz} Z Z^* dz}{\int_0^{z_e} Z Z^* dz} \quad (\text{E-4})$$

where the droplet momentum source has been neglected. When the droplet momentum source is included, the  $\gamma$  in the second term of Eq. (E-3) is replaced by  $\gamma + 1$  (see Appendix A).

The linear solutions are determined by substituting a solution of the form:

$$A(t) = ae^{(\Lambda + i\omega)t} \quad (\text{E-5})$$

into Eq. (E-1) and separating real and imaginary parts to obtain:

$$\omega^2 = C_{1r} + \Lambda^2 + (C_{2r} - nC_3)\Lambda - C_{2i}\omega + C_3 ne^{-\Lambda\bar{\tau}} (\Lambda \cos\omega\bar{\tau} + \omega \sin\omega\bar{\tau}) \quad (\text{E-6})$$

$$\Lambda = - \left\{ \frac{C_{1i} + (C_{2r} - nC_3)\omega + nC_3 e^{-\Lambda\bar{\tau}} \omega \cos\omega\bar{\tau}}{2\omega + C_{2i} - nC_3 e^{-\Lambda\bar{\tau}} \sin\omega\bar{\tau}} \right\} \quad (\text{E-7})$$

where  $C_1 = C_{1r} + iC_{1i}$ ,  $C_2 = C_{2r} + iC_{2i}$ , and  $C_3$  is always real. The above equations are solved numerically by Program LINSOL to obtain the growth rate,  $\Lambda$ , and the frequency,  $\omega$ , for given values of  $n$  and  $\bar{\tau}$ .

The equations describing the neutral stability limits are obtained by substituting  $\Lambda = 0$  into Eqs. (E-6) and (E-7). Solving the resulting equations



for  $n$  and  $\omega^2$  gives:

$$n = \frac{C_{2r} + C_{1i}/\omega}{C_3(1 - \cos \omega\bar{\tau})} \quad (\text{E-8})$$

$$\omega^2 = C_{1r} + \omega(nC_3 \sin \omega\bar{\tau} - C_{2i}) \quad (\text{E-9})$$

which are solved numerically by Program LSTB3D.

### Program LINSOL

Program Structure. A flow chart for Program LINSOL is given in Fig. (E-1). This program consists of the following major sections: (1) input, (2) calculation of the coefficients  $C_1$ ,  $C_2$ , and  $C_3$ , (3) iterative solution for  $\Lambda$  and  $\omega$ , and (4) output.

Input. The input data required by Program LINSOL includes: (1) a title for the run, (2) the chamber parameters  $\gamma$ ,  $u_e$ ,  $L/D$ , and  $z_c/z_e$ , (3) several control numbers, (4) the nozzle admittance, (5) the mode under consideration, and (6) the values of  $n$  and  $\bar{\tau}$  for the cases to be run. This data is described in the following table where the location number refers to the columns of the card and the following three formats are used: alphanumeric characters (A), integers (I), and numbers with a decimal point (F). For the "I" formats the values are placed in fields of five locations, while a field of ten locations is used with the "F" formats. In either case the numbers must be placed in the rightmost locations of the allocated field.

<u>No. of Cards</u>	<u>Location</u>	<u>Type</u>	<u>Input Item</u>	<u>Comments</u>
1	1-72	A	TITLE	Title of run.
1	1-10	F	GAMMA	Specific heat ratio, $\gamma$ .
	11-20	F	UE	Steady state Mach number at nozzle entrance, $\bar{u}_e$ .
	21-30	F	RLD	Length-to-diameter ratio, $L/D = z_e/2$ .

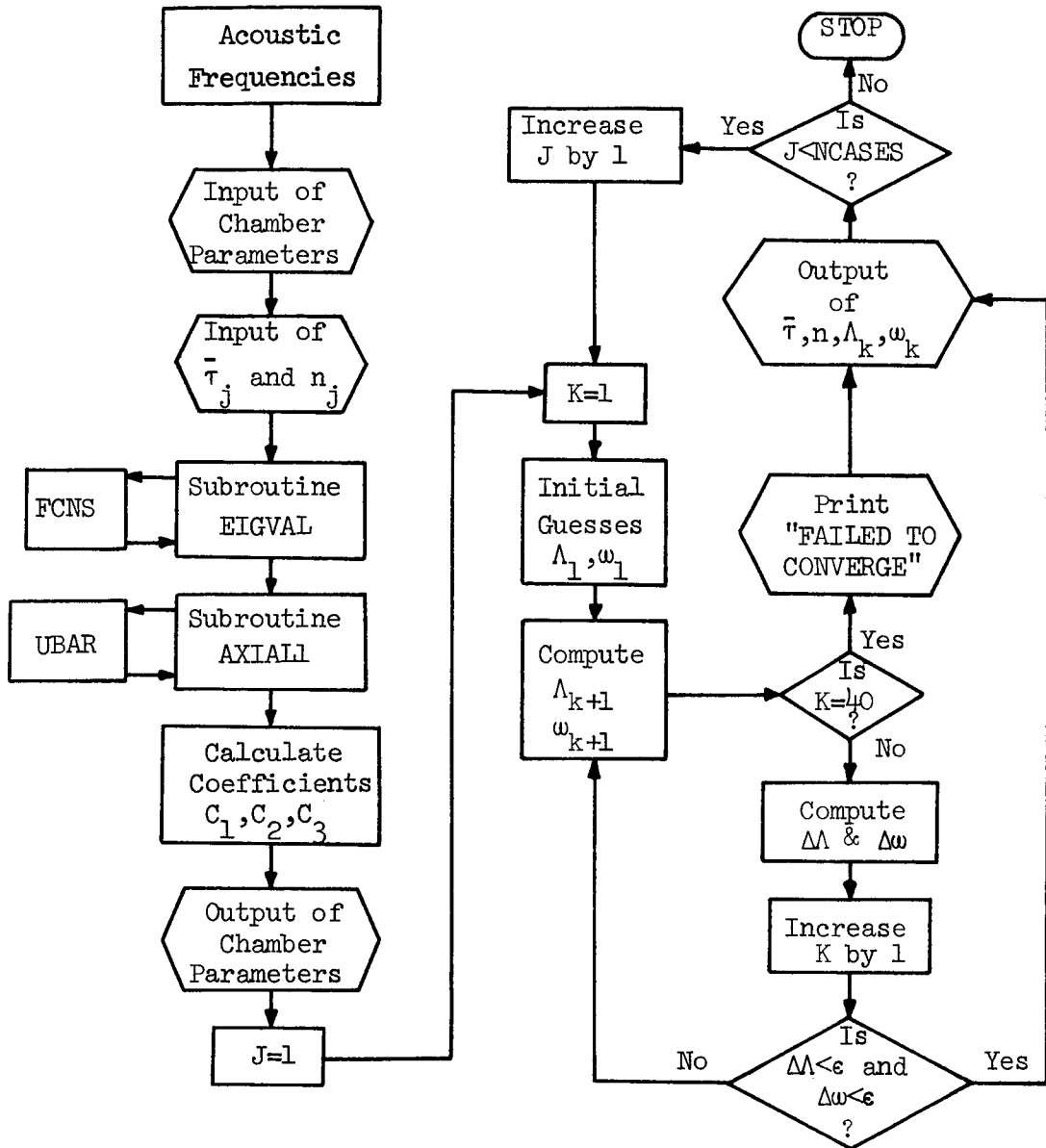


Figure E-1. Flow Chart for Program LINSOL.

<u>No. of Cards</u>	<u>Location</u>	<u>Type</u>	<u>Input Item</u>	<u>Comments</u>
	31-40	F	ZCOMB	Length of combustion zone, $z_c/z_e$ .
	41-45	I	NDROPS	If 0: droplet momentum source neglected. If 1: droplet momentum source included.
	46-50	I	NOZZLE	If 0: quasi-steady nozzle. If 1: conventional nozzle.
	51-55	I	NOPT	If 1: all coefficients included. If 2: imaginary parts neglected.

If NOZZLE = 1 :

1	1-10	F	YAMPL	Amplitude factor of nozzle admittance, <b>A</b> .
	11-20	F	YPHASE	Phase of nozzle admittance, $\varphi$ .

End of input for NOZZLE = 1.

1	1-5	I	L	Axial mode number, $l$ ( $0 \leq L \leq 10$ ).
	6-10	I	M	Tangential mode number, $m$ ( $0 \leq M \leq 8$ ).
	11-15	I	N	Radial mode number, $n$ ( $0 \leq N \leq 5$ ).
	16-20	I	NCASES	Number of cases to be run (NCASES $\leq$ 100).
NCASES	1-10	F	TAU	Time-lag, $\bar{\tau}$ .
	11-20	F	EN	Interaction Index, $n$ .

The title on the first card should identify the mode under consideration. On the second card of input all quantities are the same as those given in the input to COEFFS3D (see Appendix C) except NOPT. NOPT gives the option to neglect the imaginary parts of the coefficients  $C_1$  and  $C_2$  which are an order of magnitude smaller than the corresponding real parts. Neglecting these

imaginary parts (NOPT = 2) yields linear solutions consistent with the non-linear solutions obtained when the small coefficients are neglected (NEGL = 1 in input to COEFFS3D). The values of  $n$  and  $\bar{\tau}$  for the cases to be run are given on a series of NCASES cards. These cards are all read and the values of  $\bar{\tau}$  and  $n$  are stored in the arrays TAU(J) and EN(J) before any computations are made.

In addition to the above card input, the acoustic frequencies  $S_{mn}$  are also needed for these calculations. As in Program COEFFS3D these values are given in a DATA statement, which is an integral part of the program.

Calculation of  $C_1$ ,  $C_2$ , and  $C_3$ . In this section the coefficients  $C_1$ ,  $C_2$ , and  $C_3$  appearing in Eqs. (E-6) and (E-7) are calculated using Eqs. (E-2) through (E-4). As in Program COEFFS3D the axial acoustic eigenvalues necessary for these computations are calculated by Subroutines EIGVAL and FCNS, and the integrals of the products of two axial eigenfunctions appearing in Eqs. (E-2) through (E-4) are computed by Subroutines AXIAL1 and UBAR. Listings of these subroutines are given in Appendix C.

Iterative Solution for  $\Lambda$  and  $\omega$ . Equations (E-6) and (E-7) are of the form:

$$\begin{aligned}\omega^2 &= C_{1r} + f(\Lambda, \omega) \\ \Lambda &= g(\Lambda, \omega)\end{aligned}\tag{E-10}$$

where the quantity  $f(\Lambda, \omega)$  is small compared to  $C_{1r}$  and  $\Lambda$  is small in most cases. Starting with an initial guess of

$$\begin{aligned}\omega_1 &= \sqrt{S_{mn}^2 + \frac{l^2 \pi^2}{z_e^2}} \\ \Lambda_1 &= 0\end{aligned}\tag{E-11}$$

Eqs. (E-10) are solved iteratively using the following recursion formulas:

$$\omega_{k+1}^2 = C_{1r} + f(\Lambda_k, \omega_k) \quad (\text{E-12})$$

$$\Lambda_{k+1} = g(\Lambda_k, \omega_k)$$

At each step of the iteration the quantities  $\Delta\Lambda$  and  $\Delta\omega$  are calculated, where

$$\Delta\Lambda = | \Lambda_{k+1} - \Lambda_k | \quad (\text{E-13})$$

$$\Delta\omega = | \omega_{k+1} - \omega_k |$$

and the computations are terminated when  $k = 40$  or when  $\Delta\Lambda$  and  $\Delta\omega$  are less than  $\epsilon = 10^{-6}$ . The process usually converges in less than 15 iterations.

Output. The output generated by Program LINSOL consists of a restatement of the input data followed by the calculated results in tabular form. For each case the tabulated results give the values of  $\bar{\tau}$  and  $n$  (TAU and EN), the corresponding values of the growth rate  $\Lambda$  and the frequency  $\omega$  (LAMBDA and OMEGA), and the number of iterations (ITER). When ITER is 40 the last values of  $\Lambda$  and  $\omega$  are given followed by the warning message "FAILED TO CONVERGE."

Sample Input and Output. A sample input for the 1T mode is given in Table E-1 followed by the resulting output in Table E-2.

#### Program LSTB3D

Program Structure. A flow chart for Program LSTB3D is given in Figure (E-2). This program consists of the following major sections: (1) input, (2) calculation of the coefficients  $C_1$ ,  $C_2$ , and  $C_3$ , (3) iterative solution for  $n$  and  $\omega$  for neutral stability, and (4) output.



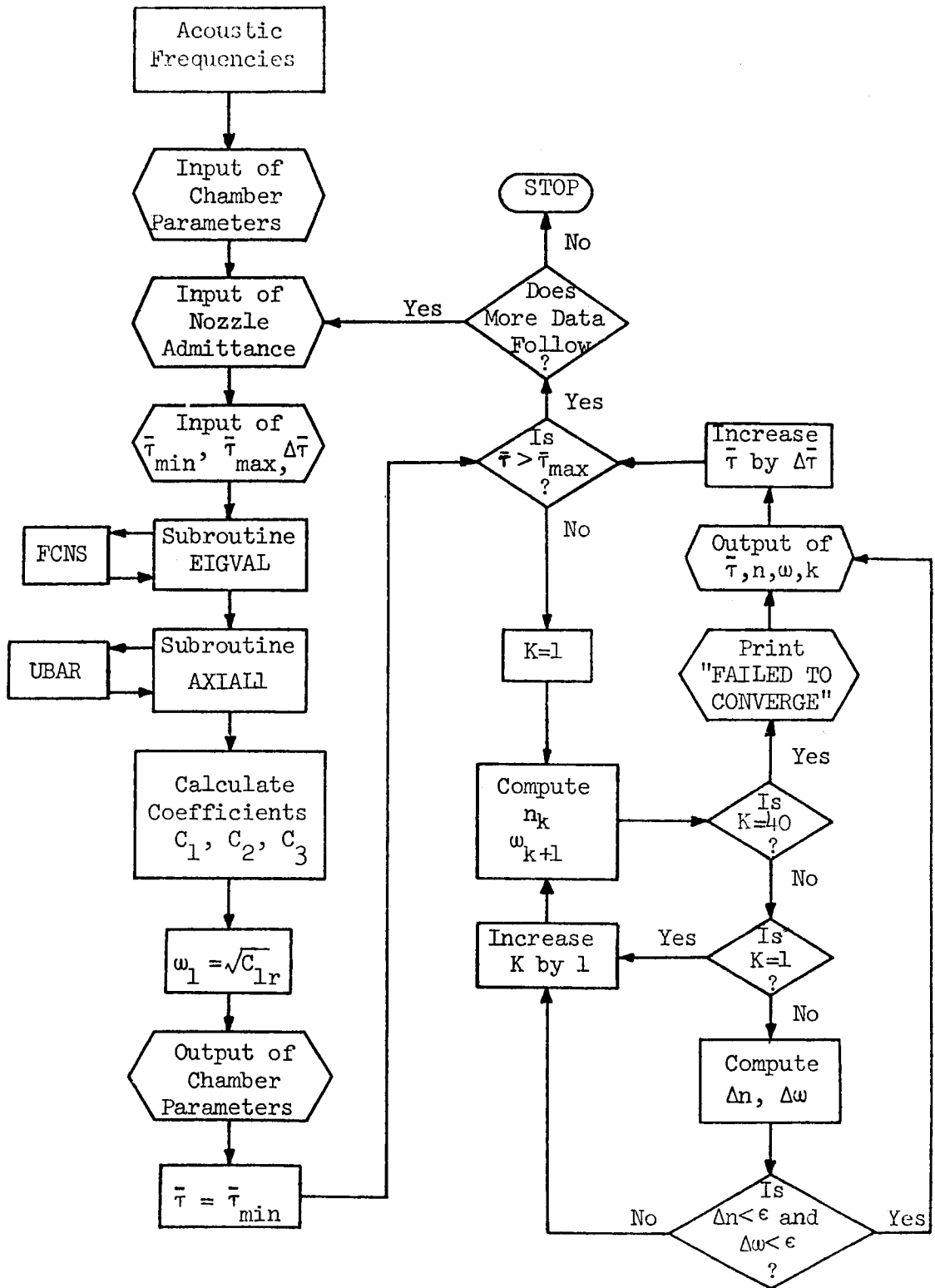


Figure E-2. Flow Chart for Program LSTB3D.

Input. The input data required by Program LSTB3D is basically the same as required by Program LINSOL. The first two cards, which give the title of the case, the chamber parameters, and the control numbers, are identical in content and format to those required by LINSOL. The third card gives the mode numbers  $l$ ,  $m$ , and  $n$  and is followed by a card giving the nozzle admittance if a conventional nozzle is specified. The last card gives the values of  $\bar{\tau}$  for the cases to be run. A detailed description of this input is given below.

<u>No. of Cards</u>	<u>Location</u>	<u>Type</u>	<u>Input Item</u>	<u>Comments</u>
1	1-72	A	TITLE	See input for LINSOL.
1	1-40	F	GAMMA, UE, RLD, ZCOMB	See input for LINSOL.
	41-55	I	NDROPS, NOZZLE, NOPT	See input for LINSOL.
1	1-15	I	L, M, N	See input for LINSOL

If NOZZLE = 1 :

1	1-20	F	YAMPL, YPHASE	See input for LINSOL.
---	------	---	---------------	-----------------------

End of input for NOZZLE = 1.

1	1-10	F	TAUMIN	Smallest value of $\bar{\tau}$ .
	11-20	F	TAUMAX	Largest value of $\bar{\tau}$ .
	21-30	F	DELTAU	Increment in $\bar{\tau}$ .

The last card gives the values of  $\bar{\tau}$  which are used in the computation of the neutral stability limit. Thus computations are begun for  $\bar{\tau} = \text{TAUMIN}$ ,  $\bar{\tau}$  is increased by increments of DELTAU, and computations are terminated when  $\bar{\tau} \geq \text{TAUMAX}$ .

After completion of the computations program control returns to the read statement for the nozzle admittance, thus neutral stability curves can be calculated for several different nozzles for the same set of chamber and mode parameters.

Calculation of  $C_1$ ,  $C_2$ , and  $C_3$ . The calculation of the coefficients  $C_1$ ,  $C_2$ , and  $C_3$  appearing in Eqs. (E-8) and (E-9) is performed in the same manner as





Table E-4. Sample Output for LSTB3D.

1T MODE.

DROPLET MOMENTUM SOURCE NEGLECTED

GAMMA = 1.20      UE = .20      RLD = .50000      ZCOMB = 1.00

AMPL = .02000      PHASE = 45.00

TAU	EN	OMEGA	ITER
.60000	1.66353	2.03102	6
.70000	1.31671	1.99646	6
.80000	1.08482	1.96911	6
.90000	.92333	1.94663	6
1.00000	.80765	1.92753	6
1.10000	.72330	1.91089	6
1.20000	.66137	1.89605	6
1.30000	.61616	1.88255	6
1.40000	.58396	1.87005	6
1.50000	.56230	1.85827	6
1.60000	.54961	1.84702	5
1.70000	.54490	1.83612	5
1.80000	.54769	1.82542	6
1.90000	.55785	1.81479	7
2.00000	.57562	1.80410	8
2.10000	.60157	1.79325	8
2.20000	.63666	1.78210	9
2.30000	.68221	1.77055	10
2.40000	.74006	1.75847	11
2.50000	.81258	1.74575	13
2.60000	.90278	1.73224	14
2.70000	1.01446	1.71783	17
2.80000	1.15226	1.70240	21

```

C
C ***** PROGRAM LINSOL *****
C
C THIS PROGRAM COMPUTES THE DAMPING (LAMBDA) AND FREQUENCY
C (OMEGA) FOR GIVEN VALUES OF THE INTERACTION INDEX (EN) AND
C THE TIME-LAG (TAU). THIS PROGRAM IS BASED ON AN ANALYTICAL
C SOLUTION OF THE COMPLEX DIFFERENTIAL EQUATION.
C
C THE FOLLOWING INPUTS ARE REQUIRED:
C
C FIRST CARD:
C THE TITLE OF THE CASE.
C
C SECOND CARD:
C GAMMA IS THE SPECIFIC HEAT RATIO.
C UE IS THE STEADY STATE MACH NUMBER AT THE NOZZLE ENTRANCE.
C RLD IS THE LENGTH-TO-DIAMETER RATIO.
C ZCOMB IS THE LENGTH OF THE COMBUSTION ZONE, EXPRESSED
C AS A FRACTION OF THE CHAMBER LENGTH.
C NDROPS DETERMINES THE PRESENCE OF DROPLET MOMENTUM SOURCES:
C NDROPS = 0 DROPLET MOMENTUM SOURCE NEGLECTED.
C NDROPS = 1 DROPLET MOMENTUM SOURCE INCLUDED.
C NOZZLE SPECIFIES THE TYPE OF NOZZLE USED:
C NOZZLE = 0 QUASI-STEADY
C NOZZLE = 1 CONVENTIONAL NOZZLE
C NOPT SPECIFIES THE SOLUTIONS DESIRED.
C NOPT = 1 COUPLING COEFFICIENTS INCLUDED.
C NOPT = 2 COUPLING COEFFICIENTS NEGLECTED.
C
C THIRD CARD (FOR CONVENTIONAL NOZZLE ONLY):
C YAMPL IS THE AMPLITUDE OF THE NOZZLE ADMITTANCE.
C YPHASE IS THE PHASE OF THE NOZZLE ADMITTANCE.
C
C FOURTH CARD:
C THE MODE IS SPECIFIED BY THE INDICES L, M, AND N.
C L IS THE AXIAL MODE NUMBER AND MUST NOT EXCEED 10.
C M IS THE AZIMUTHAL MODE NUMBER AND MUST NOT EXCEED 8.
C N IS THE RADIAL MODE NUMBER AND MUST NOT EXCEED 5.
C NCASES IS THE NUMBER OF CASES TO BE RUN.
C
C REMAINING CARDS:
C TAU IS THE TIME LAG.
C EN IS THE INTERACTION INDEX.
C
C *****
C
C COMPLEX YNOZ, RESULT, B(10), BC, AX(4), CI, CZE,
1 CGAM, ZEJ, ZEP1, ZEP2, CC, CD, CE, CSSQ, CAX
C DIMENSION TITLE(72),
1 RJROOT(10,5),
2 D(5), OMEGA(100),
3 EN(100), TAU(100)
C REAL LAMBDA(100)
C COMMON B

```

```

C
C ***** DATA INPUT SECTION *****
C
ERR = 0.000001
PI = 3.1415927
CI = (0.0,1.0)
C
C INPUT ROOTS AND VALUES OF BESSEL FUNCTIONS.
C DATA ((RJROOT(I,J), J = 1,5), I = 1,9)/
1 3.83171, 7.01559, 10.17347, 13.32369, 16.47063,
2 1.84118, 5.33144, 8.53632, 11.70600, 14.86359,
3 3.05424, 6.70613, 9.96947, 13.17037, 16.34752,
4 4.20119, 8.01524, 11.34592, 14.58585, 17.78875,
5 5.31755, 9.28240, 12.68191, 15.96411, 19.19603,
6 6.41562, 10.51986, 13.98719, 17.31284, 20.57551,
7 7.50127, 11.73494, 15.26818, 18.63744, 21.93172,
8 8.57784, 12.93239, 16.52937, 19.94185, 23.26805,
9 9.64742, 14.11552, 17.77401, 21.22906, 24.58720/
C
C INPUT PARAMETERS.
C READ (5,5000) (TITLE(I), I = 1, 72)
C READ (5,5001) GAMMA, UE, RLD, ZCOMB, NDROPS, NOZZLE, NOPT
C IF (NOZZLE .EQ. 1) GO TO 5
C COMPUTE ADMITTANCE FOR QUASI-STEADY NOZZLE.
C YAMPL = (GAMMA - 1.0) * UE/(2.0 * GAMMA)
C YPHASE = 0.0
C GO TO 7
C 5 READ (5,5002) YAMPL, YPHASE
C 7 READ (5,5003) L, M, N, NCASES
C
C THETA = YPHASE * PI/180.0
C YR = YAMPL * COS(THETA)
C YI = YAMPL * SIN(THETA)
C YNOZ = CMPLX(YR,YI)
C
C ZE = 2.0 * RLD
C CZE = CMPLX(ZE,0.0)
C CGAM = CMPLX(GAMMA,0.0)
C CAX = CGAM
C IF (NDROPS .EQ. 1) CAX = CGAM + (1.0,0.0)
C
C DO 10 J = 1, NCASES
C READ (5,5002) TAU(J), EN(J)
C 10 CONTINUE
C
C ***** PRELIMINARY CALCULATIONS *****
C
C ASSIGN ARRAYS FOR ROOTS OF BESSEL FUNCTIONS.
C IF ((M .EQ. 0) .AND. (N .EQ. 0)) GO TO 15
C MM = M + 1
C NN = N
C SMN = RJROOT(MM,NN)

```

```

      GO TO 20
      15 SMN = 0.0
C
      20 SSQ = SMN * SMN
      CSSQ = CMPLX(SSQ,0.0)
C
      CALCULATE AXIAL ACOUSTIC EIGENVALUES.
      CALL EIGVAL(L,SMN,GAMMA,ZE,YAMPL,YPHASE,RESULT)
      B(1) = RESULT
      BC = CONJG(RESULT)
C
      ***** CALCULATE AXIAL INTEGRALS *****
C
      DO 100 NT = 1, 4
      CALL AXIAL1(NT,1,1,UE,ZE,ZCOMB,RESULT)
      AX(NT) = RESULT
      100 CONTINUE
C
      ***** CALCULATE VALUES AT NOZZLE ENTRANCE *****
C
      ZEJ = CCOSH(CI*BC*CZE)
      ZEP1 = CCOSH(CI*B(1)*CZE)
      ZEP2 = CI * B(1) * CSINH(CI*B(1)*CZE)
C
      ***** CALCULATE COEFFICIENTS *****
C
      CC = (CSSQ*AX(1) - AX(2) + ZEP2*ZEJ)/AX(1)
      CD = (CAX*AX(3) + (2.0,0.0)*AX(4)
      1      + CGAM*YNOZ*ZEP1*ZEJ)/AX(1)
      CE = CGAM*AX(3)/AX(1)
C
      D(1) = REAL(CC)
      D(3) = REAL(CD)
      D(5) = REAL(CE)
      IF (NOPT .EQ. 2) GO TO 50
      D(2) = AIMAG(CC)
      D(4) = AIMAG(CD)
      GO TO 55
      50 D(2) = 0.0
      D(4) = 0.0
C
      ***** CALCULATION OF DAMPING AND FREQUENCY *****
C
      55 WRITE (6,6001) (TITLE(I), I = 1, 72)
      IF (NDROPS .EQ. 0) WRITE (6,6020)
      IF (NDROPS .EQ. 1) WRITE (6,6021)
      IF (NOPT .EQ. 2) WRITE (6,6015)
      WRITE (6,6002) GAMMA, UE, RLD, ZCOMB
      IF (NOZZLE .EQ. 0) WRITE (6,6012)
      WRITE (6,6005) YAMPL, YPHASE
      WRITE (6,6011)
      LINE = 14

```

```

C
C   CALCULATE INITIAL GUESSES FOR FREQUENCY.
    RL = L
    AXI = RL * PI/ZE
    AXSQ = AXI * AXI
    SSQ = SMN * SMN
    FRQ = SQRT(SSQ + AXSQ)
C
C
C   DO 200 J = 1, NCASES
C
C     C2R = D(3) - EN(J) * D(5)
C     C3 = EN(J) * D(5)
C
C     LAMBDA(1) = 0.0
C     OMEGA(1) = FRQ
C
C     K = 1
210  X = LAMBDA(K)
    Y = OMEGA(K)
    XT = X * TAU(J)
    YT = Y * TAU(J)
    EX = EXP(-XT)
    SN = SIN(YT)
    CS = COS(YT)
    XSQ = X * X
    WSQ = D(1) + XSQ + C2R*X - D(4)*Y
    1   + C3*EX*(X*CS + Y*SN)
    A = D(2) + C2R*Y + C3*EX*Y*CS
    BB = 2.0*Y + D(4) - C3*EX*SN
C
C     OMEGA(K+1) = SQRT(WSQ)
C     LAMBDA(K+1) = -A/BB
C
C     IF (K .EQ. 40) GO TO 216
C     DX = ABS(LAMBDA(K+1) - LAMBDA(K))
C     DY = ABS(OMEGA(K+1) - OMEGA(K))
C     K = K + 1
C     IF ((DX .LT. ERR) .AND. (DY .LT. ERR)) GO TO 217
C     GO TO 210
C
216  WRITE (6,6009) TAU(J), EN(J), LAMBDA(K), OMEGA(K), K
    GO TO 220
C
217  WRITE (6,6008) TAU(J), EN(J), LAMBDA(K), OMEGA(K), K
C
220  LINE = LINE + 2
    IF (LINE .LT. 54) GO TO 200
    WRITE (6,6007)
    WRITE (6,6011)
    LINE = 4
C
200  CONTINUE

```

```

C
C
C ***** FORMAT SPECIFICATIONS *****
C
C READ FORMATS
5000 FORMAT (72A1)
5001 FORMAT (4F10.0,3I5)
5002 FORMAT (2F10.0)
5003 FORMAT (4I5)
C
C WRITE FORMATS
6001 FORMAT (1H1,1X,72A1/)
6002 FORMAT (2X,8HGAMMA = ,F5.2,5X,5HUE = ,F5.2,5X,6HL/D = ,F8.5,
1      5X,8HZCOMB = ,F5.2/)
6005 FORMAT (2X,7HAMPL = ,F8.5,5X,8HPHASE = ,F6.1/)
6007 FORMAT (1H )
6008 FORMAT (2X,F5.3,F8.5,2F10.5,16/)
6009 FORMAT (2X,F5.3,F8.5,2F10.5,16,5X,18HFAILED TO CONVERGE/)
6011 FORMAT (2X///4X,3HTAU,6X,2HEN,4X,6HLAMBDA,5X,5HOMEGA,
1      2X,4HITER/)
6012 FORMAT (2X,19HQUASI-STEADY NOZZLE/)
6015 FORMAT (2X,24HCOUPLING TERMS NEGLECTED/)
6020 FORMAT (2X,'DROFLET MOMENTUM SOURCE NEGLECTED'/)
6021 FORMAT (2X,'DROFLET MOMENTUM SOURCE INCLUDED'/)
END

```





```

C ***** DATA INPUT SECTION *****
C
ERR = 0.000001
PI = 3.1415927
CI = (0.0,1.0)
C
C INPUT ROOTS AND VALUES OF BESSEL FUNCTIONS.
DATA ((RJROOT(I,J), J = 1,5), I = 1,9)/
1 3.83171, 7.01559, 10.17347, 13.32369, 16.47063,
2 1.84118, 5.33144, 8.53632, 11.70600, 14.86359,
3 3.05424, 6.70613, 9.96947, 13.17037, 16.34752,
4 4.20119, 8.01524, 11.34592, 14.58585, 17.78875,
5 5.31755, 9.28240, 12.68191, 15.96411, 19.19603,
6 6.41562, 10.51986, 13.98719, 17.31284, 20.57551,
7 7.50127, 11.73494, 15.26818, 18.63744, 21.93172,
8 8.57784, 12.93239, 16.52937, 19.94185, 23.26805,
9 9.64742, 14.11552, 17.77401, 21.22906, 24.58720/
C
C INPUT PARAMETERS.
READ (5,5000) (TITLE(I), I = 1, 72)
READ (5,5001) GAMMA, UE, RLD, ZCOMB, NDROPS, NOZZLE, NOPT
READ (5,5002) L, M, N
8 IF (NOZZLE .EQ. 1) GO TO 5
C COMPUTE ADMITTANCE FOR QUASI-STEADY NOZZLE.
YAMPL = (GAMMA - 1.0) * UE / (2.0 * GAMMA)
YPHASE = 0.0
GO TO 7
5 READ (5,5003,END = 300) YAMPL, YPHASE
7 READ (5,5003, END = 300) TAUMIN, TAUMAX, DELTAU
C
C THETA = YPHASE * PI / 180.0
YR = YAMPL * COS(THETA)
YI = YAMPL * SIN(THETA)
YNOZ = CMPLX(YR,YI)
C
C ZE = 2.0 * RLD
CZE = CMPLX(ZE,0.0)
CGAM = CMPLX(GAMMA,0.0)
CAX = CGAM
IF (NDROPS .EQ. 1) CAX = CGAM + (1.0,0.0)
C
C ***** PRELIMINARY CALCULATIONS *****
C
C ASSIGN ARRAYS FOR ROOTS OF BESSEL FUNCTIONS.
IF ((M .EQ. 0) .AND. (N .EQ. 0)) GO TO 15
MM = M + 1
NN = N
SMN = RJROOT(MM,NN)
GO TO 20
15 SMN = 0.0
20 SSQ = SMN * SMN
CSSQ = CMPLX(SSQ,0.0)
C

```

```

C      CALCULATE AXIAL ACOUSTIC EIGENVALUES.
      CALL EIGVAL(L,SMN,GAMMA,ZE,YAMPL,YPHASE,RESULT)
      B(1) = RESULT
      BC = CONJG(RESULT)
C
C      ***** CALCULATE AXIAL INTEGRALS *****
C
      DO 100 NT = 1, 4
      CALL AXIAL1(NT,1,1,UE,ZE,ZCOMB,RESULT)
      AX(NT) = RESULT
100 CONTINUE
C
C      ***** CALCULATE VALUES AT NOZZLE ENTRANCE *****
C
      ZEJ = CCOSH(CI*BC*CZE)
      ZEP1 = CCOSH(CI*B(1)*CZE)
      ZEP2 = CI * B(1) * CSINH(CI*B(1)*CZE)
C
C      ***** CALCULATE COEFFICIENTS *****
C
      CC = (CSSQ*AX(1) - AX(2) + ZEP2*ZEJ)/AX(1)
      CD = (CAX*AX(3) + (2.0,0.0)*AX(4)
1      + CGAM*YNOZ*ZEP1*ZEJ)/AX(1)
      CE = CGAM*AX(3)/AX(1)
C
      C1 = REAL(CC)
      D1 = REAL(CD)
      E = REAL(CE)
      IF (NOPT .EQ. 2) GO TO 50
      C2 = AIMAG(CC)
      D2 = AIMAG(CD)
      GO TO 55
50 C2 = 0.0
      D2 = 0.0
C
C      ***** CALCULATION OF LINEAR STABILITY LIMIT *****
C
55 OMEGA(1) = SQRT(C1)
C
      WRITE (6,6001) (TITLE(J), J = 1,72)
      IF (NDROPS .EQ. 0) WRITE (6,6025)
      IF (NDROPS .EQ. 1) WRITE (6,6026)
      IF (NOPT .EQ. 2) WRITE (6,6022)
      WRITE (6,6002) GAMMA, UE, RLD, ZCOMB
      IF (NOZZLE .EQ. 0) WRITE (6,6012)
      WRITE (6,6005) YAMPL, YPHASE
      WRITE (6,6010)
      LINE = 12
C
      TAU = TAUMIN
370 IF (TAU .GT. TAUMAX) GO TO 8

```

```

C
  K = 1
310 WT = OMEGA(K) * TAU
    BB = (D1 + C2/OMEGA(K))/E
    EN(K) = BB/(1.0 - COS(WT))
    G = (E*EN(K)*SIN(WT) - D2) * OMEGA(K)
    OMEGA(K+1) = SQRT(C1 + G)
    IF (K .EQ. 40) GO TO 316
    IF (K .EQ. 1) GO TO 311
    DN = ABS(EN(K) - EN(K-1))
    DW = ABS(OMEGA(K+1) - OMEGA(K))
    IF ((DN .LT. ERR) .AND. (DW .LT. ERR)) GO TO 317
311 K = K + 1
    GO TO 310

C
316 WRITE (6,6013) TAU, EN(K), OMEGA(K), K
    GO TO 318
317 WRITE (6,6014) TAU, EN(K), OMEGA(K), K

C
318 LINE = LINE + 2
    TAU = TAU + DELTAU
    IF ((LINE .LT. 60) .OR. (TAU .GT. TAU MAX)) GO TO 370
    WRITE (6,6015)
    WRITE (6,6010)
    LINE = 6
    GO TO 370

C
300 CONTINUE

C
C ***** FORMAT SPECIFICATIONS *****
C
C READ FORMATS
5000 FORMAT (72A1)
5001 FORMAT (4F10.0,3I5)
5002 FORMAT (3I5)
5003 FORMAT (3F10.0)

C
C WRITE FORMATS
6001 FORMAT (1H1,1X,72A1/)
6002 FORMAT (2X,8HGAMMA = ,F5.2,5X,5HUE = ,F5.2,5X,6HRLD = ,F8.5,
1      5X,8HZCOMB = ,F5.2/)
6003 FORMAT (2X,A4,5I5,4F10.5/)
6005 FORMAT (2X,7HAMPL = ,F8.5,5X,8HPHASE = ,F7.2/)
6007 FORMAT (1H )
6008 FORMAT (1H0)
6010 FORMAT (2X//8X,3HTAU,8X,2HEN,5X,5HOMEGA,6X,4HITER/)
6012 FORMAT (2X,19HQUASI-STEADY NOZZLE/)
6013 FORMAT (2X,3F10.5,110,5X,19H FAILED TO CONVERGE/)
6014 FORMAT (2X,3F10.5,110/)
6015 FORMAT (1H1)
6022 FORMAT (2X,24HCOUPLING TERMS NEGLECTED/)
6025 FORMAT (2X,'DROPLET MOMENTUM SOURCE NEGLECTED'/)
6026 FORMAT (2X,'DROPLET MOMENTUM SOURCE INCLUDED'/)
    END

```

## REFERENCES

1. Hefner, R. J., "Diagnosis of High Frequency Combustion Stability Characteristics from Pressure Measurements," Third ICRPG Combustion Conference, CPIA Publication No. 138, Vol. I (October 1966).
2. Price, E. W., "Combustion Instability in Rocket Motors with Aluminized Solid Propellants," Naval Weapons Center Report TP 5505 (June 1973).
3. Lores, M. E. and Zinn, B. T., "The Prediction of Nonlinear Longitudinal Combustion Instability in Liquid Propellant Rockets," NASA CR-120904 (April 1972).
4. Lores, M. E. and Zinn, B. T., "Nonlinear Longitudinal Combustion Instability in Rocket Motors," AIAA Paper 73-217, presented at the AIAA 11th Aerospace Sciences Meeting (January 1973) and accepted for publication in Combustion Science and Technology.
5. Zinn, B. T. and Powell, E. A., "Nonlinear Combustion Instability in Liquid-Propellant Rocket Engines," Proceedings of the 13th Symposium (International) on Combustion, The Combustion Institute, 1971, pp. 491-503.
6. Powell, E. A. and Zinn, B. T., "The Prediction of the Nonlinear Behavior of Unstable Liquid Rockets," NASA CR-72902 (July 1971).
7. Crocco, L. and Cheng, S. E., Theory of Combustion Instability in Liquid Propellant Rocket Motors, AGARD Monograph No. 8, 1-24. Butterworths Scientific Pub., Ltd., London (1956).
8. Powell, E. A., "Nonlinear Combustion Instability in Liquid Propellant Rocket Engines," Ph.D. Thesis, Georgia Institute of Technology, GITAER 70-6 (September 1970).
9. Powell, E. A. and Zinn, B. T., "Stable Limit Cycles and Triggering Limits of the First Radial Mode in Unstable Liquid Rockets," Israel Journal of

Technology, March 1971, pp. 177-187.

10. Maslen, S. H. and Moore, F. K., "On Strong Transverse Waves Without Shocks in a Circular Cylinder," Journal of Aeronautical Sciences 23, No. 6, pp. 583-593 (1956).
11. Finlayson, B. A. and Scriven, L. E., "The Method of Weighted Residuals -- a Review," Applied Mechanics Reviews 19, No. 9, pp. 735-744 (September 1966).
12. Ames, W. F., Nonlinear Partial Differential Equations in Engineering, pp. 243-262. Academic Press, New York (1965).
13. Crocco, L. and Sirignano, W. A., "Effect of Transverse Component on the Nonlinear Behavior of Short Nozzles," AIAA J. 4, No. 8, pp. 697-706 (August 1966).
14. Powell, E. A. and Zinn, B. T., "A Single Mode Approximation in the Solution of Nonlinear Combustion Instability Problems," Combustion Science and Technology 3, pp. 121-132 (1971).
15. Mitchell, C. E., "Axial Mode Shock Wave Combustion Instability in Liquid Propellant Rocket Engines," Princeton University AMS Technical Report No. 798, (NASA CR 72259), July 1967, (Ph.D. Thesis).
16. Abramowitz, M. and Stegun, I. A., Handbook of Mathematical Functions, Dover Publications, Inc., New York, 1965, p. 411.
17. Conte, S. D., Elementary Numerical Analysis, McGraw-Hill Book Company, New York, 1965, pp. 45-46.
18. McCracken, D. D., FORTRAN with Engineering Applications, John Wiley and Sons, Inc., New York, 1967, pp. 146-153.
19. Univac 1108 Math-Pack Programmers Reference, UP-7542, Sperry Rand Corporation (Univac Division).

20. Univac 1108 Calcomp Plotter Manual, Georgia Institute of Technology, Office of Computing Services, October 1972.
21. Conte, S. D., Elementary Numerical Analysis, McGraw-Hill Book Company, New York, 1965, pp. 223-224.

REPORT DISTRIBUTION LIST

Dr. R. J. Priem MS 500-209  
 NASA Lewis Research Center  
 21000 Brookpark Road  
 Cleveland, Ohio 44135

Aerospace Corporation  
 Attn: O. W. Dykema  
 Post Office Box 95085  
 Los Angeles, California 90045

NASA-Lewis Research Center  
 Attention: N. T. Musial (M.S. 500-311)  
 21000 Brookpark Road  
 Cleveland, Ohio 44135

Ohio State University  
 Department of Aeronautical and  
 Astronautical Engineering  
 Attn: R. Edse  
 Columbus, Ohio 43210

NASA-Lewis Research Center  
 Attention: Library (M.S. 60-3)  
 21000 Brookpark Road  
 Cleveland, Ohio 44135

TRW Systems  
 Attn: G. W. Elverum  
 One Space Park  
 Redondo Beach, California 90278

NASA-Lewis Research Center  
 Attention: Report Control Office(M.S. 5-5)  
 21000 Brookpark Road  
 Cleveland, Ohio 44135

Bell Aerospace Company  
 Attn: T. F. Fenger  
 Post Office Box 1  
 Mail Zone J-81  
 Buffalo, New York 14205

Brooklyn Polytechnic Institute  
 Attn: V. D. Agosta  
 Long Island Graduate Center  
 Route 110  
 Farmingdale, New York 11735

Pratt & Whitney Aircraft  
 Florida Research & Development  
 Center  
 Attn: G. D. Garrison  
 Post Office Box 710  
 West Palm Beach, Florida 33402

Chemical Propulsion Information Agency  
 Johns Hopkins University/APL  
 Attention: T. W. Christian  
 8621 Georgia Avenue  
 Silver Spring, Maryland 20910

NASA-Lewis Research Center  
 Attn: L. Gordon, MS 500-209  
 21000 Brookpark Road  
 Cleveland, Ohio 44135

NASA-Lewis Research Center  
 Attention: E. W. Conrad (M.S. 500-204)  
 21000 Brookpark Road  
 Cleveland, Ohio 44135

Purdue University  
 School of Mechanical Engineering  
 Attn: R. Goulard  
 Lafayette, Indiana 47907

North American Rockwell Corporation  
 Rocketdyne Division  
 Attention: L. P. Combs, D/991-350  
 Zone 11

Air Force Office of Scientific  
 Research

6633 Canoga Avenue  
 Canoga Park, California 91304

Chief Propulsion Division  
 Attn: Lt. Col. R. W. Haffner (NAE)  
 1400 Wilson Boulevard  
 Arlington, Virginia 22209

NASA Scientific and Technical  
 Information Facility  
 Attention: Acquisitions Branch  
 P. O. Box 33  
 College Park, Maryland 20740

Pennsylvania State University  
 Mechanical Engineering Department  
 Attn: G. M. Faeth  
 207 Mechanical Engineering Bldg.  
 University Park, Pennsylvania 16802

University of Illinois  
Aeronautics/Astronautic Engineering  
Department  
Attn: R. A. Strehlow  
Transportation Building, Room 101  
Urbana, Illinois 61801

NASA  
Manned Spacecraft Center  
Attn: J. C. Thibadaux  
Houston, Texas 77058

Massachusetts Institute of Technology  
Department of Mechanical Engineering  
Attn: T. Y. Toong  
77 Massachusetts Avenue  
Cambridge, Massachusetts 02139

Illinois Institute of Technology  
Attn: T. P. Torda  
Room 200 M. H.  
3300 S. Federal Street  
Chicago, Illinois 60616

U. S. Army Missile Command  
AMSMI-RKL, Attn: W. W. Wharton  
Redstone Arsenal, Alabama 35808

University of California  
Aerospace Engineering Department  
Attn: F. A. Williams  
Post Office Box 109  
LaJolla, California 92037

Georgia Institute of Technology  
School of Aerospace Engineering  
Attn: B. T. Zinn  
Atlanta, Georgia 30332

Marshall Industries  
Dynamic Science Division  
2400 Michelson Drive  
Irvine, California 92664

Mr. Donald H. Dahlene  
U. S. Army Missile Command  
Research, Development, Engineering  
and Missile Systems Laboratory  
Attn: AMSMI-RK  
Redstone Arsenal, Alabama 35809

TISIA  
Defense Documentation Center  
Cameron Station  
Building 5  
5010 Duke Street  
Alexandria, Virginia 22314

Office of Assistant Director  
(Chemical Technician)  
Office of the Director of Defense  
Research and Engineering  
Washington, D. C. 20301

D. E. Mock  
Advanced Research Projects Agency  
Washington, D. C. 20525

Dr. H. K. Doetsch  
Arnold Engineering Development Center  
Air Force Systems Command  
Tullahoma, Tennessee 37389

Library  
Air Force Rocket Propulsion  
Laboratory (RPR)  
Edwards, California 93523

Library  
Bureau of Naval Weapons  
Department of the Navy  
Washington, D. C.

Library  
Director (Code 6180)  
U. S. Naval Research Laboratory  
Washington, D. C. 20390

APRP (Library)  
Air Force Aero Propulsion Laboratory  
Research and Technology Division  
Air Force Systems Command  
United States Air Force  
Wright-Patterson AFB, Ohio 45433

Technical Information Department  
Aeronutronic Division of Philco  
Ford Corporation  
Ford Road  
Newport Beach, California 92663



Library-Documents  
Aerospace Corporation  
2400 E. El Segundo Boulevard  
Los Angeles, California 90045

AFRPL  
Attn: R. R. Weiss  
Edwards, California 93523

Princeton University  
James Forrestal Campus Library  
Attn: D. Harrje  
Post Office Box 710  
Princeton, New Jersey 08540

U. S. Naval Weapons Center  
Attn: T. Inouye, Code 4581  
China Lake, California 93555

Office of Naval Research  
Navy Department  
Attn: R. D. Jackel, 473  
Washington, D. C. 20360

Air Force Aero Propulsion Laboratory  
Attn: APTC Lt. M. Johnson  
Wright Patterson AFB, Ohio 45433

Naval Underwater Systems Center  
Energy Conversion Department  
Attn: Dr. R. S. Lazar, Code TB 131  
Newport, Rhode Island 02840

NASA  
Langley Research Center  
Attn: R. S. Levine, MS 213  
Hampton, Virginia 23365

Aerojet General Corporation  
Attn: David A. Fairchild, Mech. Design  
Post Office Box 15847 (Sect. 9732)  
Sacramento, California 95809

Colorado State University  
Mechanical Engineering Department  
Attn: C. E. Mitchell  
Fort Collins, Colorado 80521

ARL (ARC)  
Attn: K. Scheller  
Wright Patterson AFB, Ohio 45433

University of Wisconsin  
Mechanical Engineering Department  
Attn: P. S. Myers  
1513 University Avenue  
Madison, Wisconsin 53706

North American Rockwell Corporation  
Rocketdyne Division  
Attn: J. A. Nestlerode,  
AC46 D/596-121  
6633 Canoga Avenue  
Canoga Park, California 91304

University of Michigan  
Aerospace Engineering  
Attn: J. A. Nicholls  
Ann Arbor, Michigan 48104

Tulane University  
Attn: J. C. O'Hara  
6823 St. Charles Avenue  
New Orleans, Louisiana 70118

University of California  
Department of Chemical Engineering  
Attn: A. K. Oppenheim  
6161 Etcheverry Hall  
Berkeley, California 94720

Sacramento State College  
School of Engineering  
Attn: F. H. Reardon  
6000 J. Street  
Sacramento, California 95819

Purdue University  
School of Mechanical Engineering  
Attn: B. A. Reese  
Lafayette, Indiana 47907

NASA  
George C. Marshall Space Flight Center  
Attn: R. J. Richmond, SNE-ASTN-PP  
Huntsville, Alabama 35812

Jet Propulsion Laboratory  
California Institute of Technology  
Attn: J. H. Rupe  
4800 Oak Grove Drive  
Pasadena, California 91103

University of California  
Mechanical Engineering Thermal Systems  
Attn: Prof. R. Sawyer  
Berkeley, California 94720

Library  
Bell Aerosystems, Inc.  
Box 1  
Buffalo, New York 14205

Report Library, Room 6A  
Battelle Memorial Institute  
505 King Avenue  
Columbus, Ohio 43201

D. Suichu  
General Electric Company  
Flight Propulsion Laboratory Department  
Cincinnati, Ohio 45215

Library  
Ling-Temco-Vought Corporation  
Post Office Box 5907  
Dallas, Texas 75222

Marquardt Corporation  
16555 Saticoy Street  
Box 2013 - South Annex  
Van Nuys, California 91409

P. F. Winternitz  
New York University  
University Heights  
New York, New York

R. Stiff  
Propulsion Division  
Aerojet-General Corporation  
Post Office Box 15847  
Sacramento, California 95803

Library, Department 596-306  
Rocketdyne Division of Rockwell  
North American Rockwell Inc.  
6633 Canoga Avenue  
Canoga Park, California 91304

Library  
Stanford Research Institute  
333 Ravenswood Avenue  
Menlo Park, California 94025

Library  
Susquehanna Corporation  
Atlantic Research Division  
Shirley Highway and Edsall Road  
Alexandria, Virginia 22314

STL Tech. Lib. Doc. Acquisitions  
TRW System Group  
1 Space Park  
Redondo Beach, California 90278

Dr. David Altman  
United Aircraft Corporation  
United Technology Center  
Post Office Box 358  
Sunnyvale, California 94088

Library  
United Aircraft Corporation  
Pratt and Whitney Division  
Florida Research and Development  
Center  
Post Office Box 2691  
West Palm Beach, Florida 33402

Library  
Air Force Rocket Propulsion  
Laboratory (RPM)  
Edwards, California 93523

Professor Kenneth R. Purdy  
Post Office Box 5014  
Tennessee Technological University  
Cookeville, Tennessee 38501

NASA-Lewis Research Center  
Attn: E. O. Bourke MS 500-209  
21000 Brookpark Road  
Cleveland, Ohio 44135

NASA-Lewis Research Center  
MS 500-313  
Rockets & Spacecraft Procurement  
Section  
21000 Brookpark Road  
Cleveland, Ohio 44135

1. Report No. NASA CR-121279		2. Government Accession No.		3. Recipient's Catalog No.	
4. Title and Subtitle THE PREDICTION OF NONLINEAR THREE-DIMENSIONAL COMBUSTION INSTABILITY IN LIQUID ROCKETS WITH CONVENTIONAL NOZZLES				5. Report Date October 1973	
				6. Performing Organization Code	
7. Author(s) Eugene A. Powell and Ben T. Zinn				8. Performing Organization Report No.	
9. Performing Organization Name and Address Georgia Institute of Technology Atlanta, Georgia 30332				10. Work Unit No.	
				11. Contract or Grant No. NGL 11-002-083	
12. Sponsoring Agency Name and Address National Aeronautics and Space Administration Washington, D. C. 20546				13. Type of Report and Period Covered Contractor Report	
				14. Sponsoring Agency Code	
15. Supplementary Notes Project Manager, Richard J. Priem, Chemical Propulsion Division, NASA Lewis Research Center, Cleveland, Ohio					
16. Abstract <p>An analytical technique is developed to solve nonlinear three-dimensional, transverse and axial combustion instability problems associated with liquid-propellant rocket motors. The Method of Weighted Residuals is used to determine the nonlinear stability characteristics of a cylindrical combustor with uniform injection of propellants at one end and a conventional DeLaval nozzle at the other end. Crocco's pressure sensitive time-lag model is used to describe the unsteady combustion process. The developed model predicts the transient behavior and nonlinear wave shapes as well as limit-cycle amplitudes and frequencies typical of unstable motor operation. The limit-cycle amplitude increases with increasing sensitivity of the combustion process to pressure oscillations. For transverse instabilities, calculated pressure wave-forms exhibit sharp peaks and shallow minima, and the frequency of oscillation is within a few percent of the pure acoustic mode frequency. For axial instabilities, the theory predicts a steep-fronted wave moving back and forth along the combustor.</p>					
17. Key Words (Suggested by Author(s)) Combustion instability Liquid rockets Method of Weighted Residuals			18. Distribution Statement Unclassified - unlimited		
19. Security Classif. (of this report) Unclassified		20. Security Classif. (of this page) Unclassified		21. No. of Pages 173	22. Price* \$3.00